On the Fatigue Life of the Human Anterior Cruciate Ligament: Experimental Studies of the Effects of Limited Internal Femoral Rotation and Microscopic Entheseal Anatomy

by

Mélanie L. Beaulieu

A dissertation submitted in partial fulfillment
of the requirements for the degree of
Doctor of Philosophy
(Kinesiology)
in the University of Michigan
2015

Doctoral Committee:

Professor James A. Ashton-Miller, Chair
Professor Karl J. Jepsen
Associate Professor Riann M. Palmieri-Smith
Professor Edward M. Wojtys

© Mélanie L. Beaulieu 2015

ACKNOWLEDGMENTS

I would like to express my deepest gratitude to everyone who made the completion of this dissertation possible. First and foremost, I would like to sincerely thank my advisor, Dr. James Ashton-Miller, for sharing his enthusiasm and passion for research, for his kindness, patience, and generosity, and for his guidance during this dissertation journey. His investment into research, including the mentorship and support of young scientists, and his ability to stimulate thinking *beyond the box* are unrivaled. I leave his laboratory not only a better researcher, but a better mentor and person. I am also truly indebted and thankful to Dr. Ed Wojtys, who has been a second advisor and mentor to me. His contributions to this dissertation and to my development as a young researcher, as well as his helpful suggestions to the applied aspects of this research, are invaluable. I am grateful to him for always reminding me of the bigger picture, the important reasons why we are doing this work. I am extremely fortunate to have been part of this talented interdisciplinary research team.

I owe sincere and earnest thankfulness to the other members of my dissertation committee, Dr. Karl Jepsen and Dr. Riann Palmieri-Smith, for their generosity in reviewing my dissertation. I would like to extend my appreciation to Dr. Jepsen for his guidance and insightful feedback with regard to the histology portion of this dissertation, as well as for giving me access to histology facilities and tools. This dissertation would not have been possible without his generosity. I am thankful to Dr. Asheesh Bedi who contributed the idea of the restricted hip as a risk factor for ACL injuries. I would also like to show my gratitude to the members of the

Orthopaedic Research Laboratory (ORL), particularly Dr. Stephen Schlecht who has taught me everything I know about histology procedures and entheses and who was always available to answer my numerous questions and to provide valuable feedback. Thank you to Mr. John Baker for his guidance with regard to histology procedures. Thank you to Mrs. Erin Bigelow and Mr. Alex Brunfeldt for sharing and coordinating the dissection facility at the ORL. Thank you to Mr. Charles Roehm for machining the femoral rotation device, for repairing failed parts of the *in vitro* testing apparatus, and for trimming my embedded specimens.

This work would not have been possible without the generosity of the specimen donors and their families. I cannot thank them enough. I would also like to thank Mr. Dean Mueller of the Anatomical Donations Program for his assistance in procuring the donors. I would like to acknowledge Mrs. Suzan Lowe for acquiring the magnetic resonance images used in this dissertation. I would like to pay tribute to all the generous individuals who assisted me with specimen preparation and/or data collection, in particular, Ms. Kathryn van Ham, Ms. Kayla Curtis, Ms. Grace Curtis, and Ms. Sasha Kapshai.

I am obliged to many of my colleagues who supported me, including the former and current members of the Biomechanics Research Laboratory. I would like to show distinct gratitude to Dr. David Lipps for teaching me how to prepare and test knee specimens, to Dr. Youkeun Oh for his assistance in the design of the femoral rotation device and for always lending a helping hand when needed, and to both of them for the invaluable research discussions.

I am also thankful to my funding sources: the National Sciences and Engineering Research Council of Canada, the Bone and Joint Injury Prevention & Rehabilitation Center and Rackham Graduate School at the University of Michigan, and the National Institutes of Health. Without these sources, I would not have been able to pursue a doctoral degree.

Finally, I would like to thank my family and friends for their infinite support. Thank you to Sasha for her wonderful friendship over the past five years. Thank you to my parents, Michel and Louise, for believing in me and for their continuous encouragement and interest in my research. And an enormous thank you to John, my fiancé, for his patience and devotion, for sharing in my excitement and listening to my frustrations, and most importantly, for making me laugh every day and reminding me of the important things in life. Merci ! Je vous aime beaucoup !

PREFACE

Chapters 2-5 have been written as separate manuscripts. For this reason, there may be some repetition of material, particularly in the Materials and Methods sections, between Chapters 2 and 3, as well as between Chapters 4 and 5.

TABLE OF CONTENTS

ACKNOWLEDGMENTS ..... **ii**

PREFACE ..... **v**

LIST OF FIGURES ..... **viii**

LIST OF TABLES ..... **xiv**

LIST OF APPENDICES ..... **xvii**

ABSTRACT ..... **xviii**

CHAPTER 1: INTRODUCTION **1**

1.1 Overview of the Problem 1
1.2 Background and Knowledge Gaps 2
1.3 Overall Objective and Working Hypothesis 6
1.4 Dissertation Structure including Specific Aims, Hypotheses, and Significance 6
1.5 References 9

CHAPTER 2: DOES LIMITED INTERNAL FEMORAL ROTATION INCREASE PEAK ANTERIOR CRUCIATE LIGAMENT STRAIN DURING A SIMULATED PIVOT LANDING? **17**

2.1 Abstract 17
2.2 Introduction 18
2.3 Materials and Methods 20
2.4 Results 27
2.5 Discussion 33
2.6 Conclusion 38
2.7 References 38

CHAPTER 3: RISK OF ACL FATIGUE FAILURE IS INCREASED BY LIMITED INTERNAL FEMORAL ROTATION DURING IN VITRO REPEATED PIVOT LANDINGS **43**

3.1 Abstract 43
3.2 Introduction 44
3.3 Materials and Methods 46
3.4 Results 54
3.5 Discussion 57
3.6 Conclusion 63
3.7 References 63

CHAPTER 4: A QUANTITATIVE COMPARISON OF THE MICROSCOPIC ANATOMY OF THE HUMAN ACL FEMORAL AND TIBIAL ENTHESES 67

4.1 Abstract 67
4.2 Introduction 68
4.3 Materials and Methods 69
4.4 Results 74
4.5 Discussion 77
4.6 Conclusion 80
4.7 References 80

CHAPTER 5: A QUANTITATIVE ANALYSIS OF THE REGIONAL AND BILATERAL VARIATIONS IN THE MICROSCOPIC ANATOMY OF THE HUMAN ACL FEMORAL ENTHESIS 84

5.1 Abstract 84
5.2 Introduction 85
5.3 Materials and Methods 86
5.4 Results 89
5.5 Discussion 92
5.6 Conclusion 96
5.7 References 97

CHAPTER 6: GENERAL DISCUSSION 100

6.1 Restriction in Hip Internal Rotation 100
6.2 Microscopic Anatomy of the ACL Entheses 104
6.3 Limitations 108
6.4 References 112

CHAPTER 7: CONCLUSIONS 118

CHAPTER 8: RECOMMENDATIONS FOR FUTURE RESEARCH 121

8.1 Restriction in Hip Internal Rotation 121
8.2 Microscopic Anatomy of the ACL Entheses 123
8.3 References 124

APPENDICES 127

LIST OF FIGURES

CHAPTER 2

Figure

2.1 Sagittal-plane diagram (left) of the *in vitro* testing apparatus that simulated a single-leg pivot landing, with a top view (right) of the femoral rotation device, *R*. The solid portions represent the starting position of the specimen and device; meanwhile, the transparent portions represent their end position during a trial for which terminal internal femoral rotation was set to ~7° (block C of the testing protocol). *B*, position of steel stop for block B of the repeated-measures protocol (locked); *C*, position of steel stop for block C of the repeated-measures protocol (hard stop at ~11°); *G*, gastrocnemii tendons; *H*, hamstring tendons; *L*, 6-axis load cell; *Q*, quadriceps tendon; *R*, femoral rotation device; *T*, tibial torsion device; *W*, weight dropped. Note: positions of steel stops are not to scale to allow better visualization..... 24

2.2 Sample temporal plots of a representative trial for each axial femoral rotation condition: (A) femoral rotation locked; (B) hard stop at ~7° of rotation; (C) hard stop at ~11° of rotation; and (D) free femoral rotation. Subplots display (1) compressive force (CF), internal femoral torque (IFT), quadriceps force (QF), and knee flexion angle (KFA) and (2) anterior tibial translation (ATT), internal femoral rotation (IFR), internal tibial rotation (ITR), and relative strain of the anteromedial bundle of the anterior cruciate ligament during a cadaver-simulated single-leg pivot landing. Insets in B-1 and C-1 indicate portions of the internal femoral torque curve showing the bilinear stiffness response because of the hard stop. All data are from one knee specimen (ID No. 20686R). Data are normalized to their peak values (values in parentheses)..... 28

2.3 Scatter plot of peak relative strain of the anteromedial bundle of the anterior cruciate ligament (AM-ACL) versus range of internal femoral rotation quantified for 20 knees under four axial femoral rotation conditions (rotation locked, hard stop at ~7° of rotation, hard stop at ~11° of rotation, no sudden stop in rotation) during the pivot landings. Data points from the same knee specimen are connected with a dashed line. The solid line represents the line of best fit of the full linear mixed model, with a slope (β_{IFRot}) of –0.132, which explained 91% of the variance in the peak AM-ACL relative strain data. This model predicted peak ACL relative strain with range of hip internal rotation, sex, and age of knee donor as fixed effects and with knee specimen and knee donor as random effects. IFRot, internal femoral rotation 29

2.4 Scatter plots of peak relative strain of the anteromedial bundle of the anterior cruciate ligament (AM-ACL) versus (A) femoral rotational stiffness (B) range of anterior tibial translation, (C) range of internal tibial rotation, (D) peak internal tibial deceleration, and (E) difference between time-to-peak internal tibial and femoral rotations quantified for 20 knees under four axial femoral rotation conditions (rotation locked, hard stop at ~7° of rotation, hard stop at ~11° of rotation, no hard stop in rotation) during the pivot landings. In plot E, a negative value indicates that peak internal tibial rotation is occurring before peak internal femoral rotation, and vice versa. Data points from the same knee specimen are connected with a dashed line. The solid lines represent the lines of best fit of the full linear mixed models, including their corresponding R^2 values. IR, internal rotation 30

2.5 Simulation of axial impulsive torque applied distally to a simple lower limb model, including resulting mechanics. (A) The lower limb was modeled with three rigid bodies (femur, tibia, foot) attached to each other by springs (k_{Knee}, k_{Ankle}). The end of a third spring (k_{Hip}) was attached to the femur, with its other end fixed. The torsional stiffness of k_{Hip} was systematically varied, while that of k_{Knee} and k_{Ankle} remained constant. An axial torque of 10 Nm was applied to the foot. (B) With a compliant spring (i.e., low k_{Hip} stiffness), larger peak femoral rotation and smaller peak tibial rotation were observed. Femoral rotation peaked shortly after tibial rotation, as shown in D (dark gray shaded area). In comparison, a stiff spring (i.e., high k_{Hip} stiffness) resulted in smaller peak femoral rotation and larger tibial rotation. Femoral rotation peaked much longer after tibial rotation, as shown in D (light gray shaded area). This difference in time-to-peak tibial and femoral rotation is shown in D as the gray shaded areas between the vertical lines, which represent time of peak rotation for each segment and condition. (C) As peak femoral rotation increased, peak tibial rotation decreased. Note: femoral rotation is defined as the absolute angle of the femur, whereas tibial rotation is defined as the angle of the tibia relative to the femur 32

CHAPTER 3

Figure

3.1 (A) Example of the femoral-ACL attachment angle measurement. Left: oblique-sagittal MR image showing the location of the oblique-frontal slice (red line, at mid-portion of the ACL) that was used to measure the angle. Right: oblique-frontal MR image showing the definition of the femur-ACL attachment angle (α). (B) Example of the tibial eminence (TE) measurement. Frontal plane MR image showing the outlined area of the TE, which was multiplied by the sum of the slice thickness and slice spacing to obtain each slice's TE volume. Total TE volume was calculated by taking the sum of the TE volume of all slices..... 50

3.2 Sagittal plane diagram of the *in vitro* testing apparatus used to simulate single-leg pivot landings (left) and a top view of the femoral rotation device (right). The position of the specimen and device at peak relative internal femoral rotation during

the trials with limited and free femoral rotation is represented by the solid and transparent portions of the diagram, respectively. *L*: 6-axis load cell 52

3.3 Scatterplot of the range of internal femoral rotation versus the maximum number of loading cycles of the knee specimens. A failed ACL is represented by a circle; whereas an intact ACL (at the end of the experiment) is represented by a square. The red and blue markers identify female and male knee specimens, respectively, with data from each donor connected with a solid line. A: tibial avulsion; D: did not fail; E permanent elongation; P: partial ACL tear; T: complete ACL tear..... 57

CHAPTER 4

Figure

4.1 Location of tissue sections (black lines) prepared for histological analysis on the femoral and tibial tissue blocks of a right knee specimen. White lines indicate the edges of the entheses. a: 20%; b: 40%; c: 60%; d: 80% of the width of the enthesis..... 72

4.2 Example of the (A) outline of CF area, (B) UF depth measured at 500-µm intervals, and (C) ligament entheseal attachment angle measurement. (D) Definition of the enthesis regions for which the dependent variables were quantified. cf: calcified fibrocartilage; uf: uncalcified fibrocartilage; tm: tidemark; b: bone; l: ligament. Toluidine blue strain 73

4.3 Histology of the four tissue sections of the ACL femoral (A: 20%; B: 40%; C: 60%; D: 80% of the width of the enthesis) and tibial (E: 20%; F: 40%; G: 60%; H: 80% of the width of the enthesis) entheses in a representative specimen in terms of fibrocartilage quantity, entheseal tidemark profile, and ligament entheseal attachment angle. The large voids in the tibia may be fat deposits. (I) Femoral entheses had four zones of tissue: ligamentous tissue (l), uncalcified fibrocartilage (uf), calcified fibrocartilage (cf), and bone (b). Note how the ligamentous tissue transitions into uncalcified fibrocartilage and curves to insert into the calcified tissue at a less acute angle. *Inset*: High power view of tissue outlined in white showing uncalcified fibrocartilage with its fibrocartilage cells (arrow heads). (J) The femoral enthesis often extended to, and blended into, the posterior articular cartilage (ac). (K) Tibial entheses also had four zones of tissue, but with less fibrocartilage. Toluidine blue stain 76

4.4 Mean and standard deviation of (A) relative area of calcified fibrocartilage and (B) depth of uncalcified fibrocartilage of all tissue sections for the entire enthesis and by region, as well as (C) ligament entheseal attachment angle of all tissue sections for the entire enthesis presented for the femoral and tibial entheses. *significantly different, $p < 0.001$; **significantly different, $p < 0.010$ 77

CHAPTER 5

Figure

5.1 Excised femoral attachment site from a right distal femur showing the location of the tissue sections (black lines) processed and prepared, as well as the location of the regions of interest defined for histological analysis. a: 20%; b: 40%; c: 60%; d: 80% of the width of the enthesis. 1: antero-superior; 2: antero-inferior; 3: postero-superior; 4: postero-inferior regions. Regions 1-2 corresponded to the origin of the anteromedial (AM) fibers; meanwhile regions 3-4 corresponded to the origin of the posterolateral (PL) fibers 87

5.2 Mean and standard deviation of (A) relative area of calcified fibrocartilage and (B) depth of uncalcified fibrocartilage for each entheseal region of interest (1-4), as well as (C) ligament entheseal attachment angle of the anterior (a-b) and posterior (c-d) tissue sections presented for the femoral entheses. Example of (D) anterior (section b in Fig. 1) and (E) posterior (section c in Fig. 1) tissue sections of the ACL femoral enthesis of a representative specimen. *Insets*: High power views of tissue outlined in black showing four zones of tissue: ligamentous tissue (l), uncalcified fibrocartilage (uf), calcified fibrocartilage (cf), and bone (b). *significantly greater than region 1 ($p = 0.041$), region 3 ($p < 0.001$), and region 4 ($p = 0.020$); **significantly greater than all other regions ($p < 0.001$); ***significantly greater than region 3 ($p = 0.032$) 90

5.3 Examples of the six types of entheseal tidemark profiles: A: convex; B: concave; C: convex with a single re-entrant; D: concave with a single re-entrant; E: half concave, half convex; F: half convex, half concave. The portion of sections classified as being of a given tidemark profile is shown in the lower corner of each image 91

5.4 Examples of bilateral correlation in entheseal tidemark profiles. Sections from the right and left ACL femoral entheses from (A) specimen #34578 and (B) specimen #34593 92

5.5 Histological images of (A) anterior sections (Fig. 1, b) and (B) posterior sections (Fig. 1, c) showing local concentrations in calcification (top) and the corresponding sections in the paired enthesis (bottom) from specimen #34602 96

CHAPTER 6

Figure

6.1 An ACL injury and prevention conceptual model. This dissertation was aimed at identifying contributing factors to ACL injury risk, as well as the magnitude of the associated risk (items highlighted by dashed box). Adapted from the Physical Activity Injury Reduction tool 101

APPENDIX B

Figure

B.1 Location of tissue sections (black lines) whose digital images are presented in this appendix. White lines indicate the edges of the entheses. Letters correspond to the various parts of the following figures. A: 20%; B: 40%; C: 60%; D: 80% of the width of the femoral enthesis. E: 20%; F: 40%; G: 60%; H: 80% of the width of the tibial enthesis 131

B.2 Histology of the four tissue sections of the left ACL femoral (A: 20%; B: 40%; C: 60%; D: 80% of the width of the enthesis) and tibial (E: 20%; F: 40%; G: 60%; H: 80% of the width of the enthesis) entheses in specimen #34372 132

B.3 Histology of the four tissue sections of the left ACL femoral (A: 20%; B: 40%; C: 60%; D: 80% of the width of the enthesis) and tibial (E: 20%; F: 40%; G: 60%; H: 80% of the width of the enthesis) entheses in specimen #34563. 133

B.4 Histology of the four tissue sections of the right ACL femoral (A: 20%; B: 40%; C: 60%; D: 80% of the width of the enthesis) and tibial (E: 20%; F: 40%; G: 60%; H: 80% of the width of the enthesis) entheses in specimen #34563 134

B.5 Histology of the four tissue sections of the left ACL femoral (A: 20%; B: 40%; C: 60%; D: 80% of the width of the enthesis) and tibial (E: 20%; F: 40%; G: 60%; H: 80% of the width of the enthesis) entheses in specimen #34571 135

B.6 Histology of the four tissue sections of the right ACL femoral (A: 20%; B: 40%; C: 60%; D: 80% of the width of the enthesis) and tibial (E: 20%; F: 40%; G: 60%; H: 80% of the width of the enthesis) entheses in specimen #34571 136

B.7 Histology of the four tissue sections of the left ACL femoral (A: 20%; B: 40%; C: 60%; D: 80% of the width of the enthesis) and tibial (E: 20%; F: 40%; G: 60%; H: 80% of the width of the enthesis) entheses in specimen #34578 137

B.8 Histology of the four tissue sections of the right ACL femoral (A: 20%; B: 40%; C: 60%; D: 80% of the width of the enthesis) and tibial (E: 20%; F: 40%; G: 60%; H: 80% of the width of the enthesis) entheses in specimen #34578 138

B.9 Histology of the four tissue sections of the left ACL femoral (A: 20%; B: 40%; C: 60%; D: 80% of the width of the enthesis) and tibial (E: 20%; F: 40%; G: 60%; H: 80% of the width of the enthesis) entheses in specimen #34593 139

B.10 Histology of the four tissue sections of the right ACL femoral (A: 20%; B: 40%; C: 60%; D: 80% of the width of the enthesis) and tibial (E: 20%; F: 40%; G: 60%; H: 80% of the width of the enthesis) entheses in specimen #34593 140

B.11 Histology of the four tissue sections of the left ACL femoral (A: 20%; B: 40%; C: 60%; D: 80% of the width of the enthesis) and tibial (E: 20%; F: 40%; G: 60%; H: 80% of the width of the enthesis) entheses in specimen #34602 141

B.12 Histology of the four tissue sections of the right ACL femoral (A: 20%; B: 40%; C: 60%; D: 80% of the width of the enthesis) and tibial (E: 20%; F: 40%; G: 60%; H: 80% of the width of the enthesis) entheses in specimen #34602 142

B.13 Histology of the four tissue sections of the left ACL femoral (A: 20%; B: 40%; C: 60%; D: 80% of the width of the enthesis) and tibial (E: 20%; F: 40%; G: 60%; H: 80% of the width of the enthesis) entheses in specimen #34626 143

B.14 Histology of the four tissue sections of the right ACL femoral (A: 20%; B: 40%; C: 60%; D: 80% of the width of the enthesis) and tibial (E: 20%; F: 40%; G: 60%; H: 80% of the width of the enthesis) entheses in specimen #34626 144

B.15 Histology of the four tissue sections of the left ACL femoral (A: 20%; B: 40%; C: 60%; D: 80% of the width of the enthesis) and tibial (E: 20%; F: 40%; G: 60%; H: 80% of the width of the enthesis) entheses in specimen #34630 145

B.16 Histology of the four tissue sections of the right ACL femoral (A: 20%; B: 40%; C: 60%; D: 80% of the width of the enthesis) and tibial (E: 20%; F: 40%; G: 60%; H: 80% of the width of the enthesis) entheses in specimen #34630 146

LIST OF TABLES

CHAPTER 2

Table

2.1 Demographic data of the donors of knee specimens tested 21

2.2 Testing protocol for each block of trials 22

CHAPTER 3

Table

3.1 Testing protocol for each block of trials 48

3.2 List of the specimens tested, status of internal femoral rotation, number of cycles to failure, description of the failure pattern, and morphological data 54

3.3 Results of Cox regression models with shared frailty..... 56

CHAPTER 4

Table

4.1 Tissue processing protocol for histological analysis..... 71

CHAPTER 5

Table

5.1 Mean (standard deviation) coefficients of fifth-order polynomial fit to entheseal surfaces of the left and right ACLs, including correlation coefficient and p values 92

APPENDIX A

Table

A.1 Lower limb model parameters. 129

APPENDIX C

Table

C.1 Demographic data of the donors of the knee specimens tested in Chapter 2..... 148

C.2 Chapter 2 dataset: Non-pivot baseline trials (knee compression force and flexion moment) performed before the trials of the main testing sequence..... 149

C.3 Chapter 2 dataset: Pivot trials (knee compression force, flexion moment, and internal tibial torque) with locked internal femoral rotation (block B)..... 150

C.4 Chapter 2 dataset: Pivot trials (knee compression force, flexion moment, and internal tibial torque) with internal femoral rotation limited by a hard stop to ~7° (block C) 151

C.5 Chapter 2 dataset: Pivot trials (knee compression force, flexion moment, and internal tibial torque) with internal femoral rotation limited by a hard stop to ~11° (block D) 152

C.6 Chapter 2 dataset: Pivot trials (knee compression force, flexion moment, and internal tibial torque) with unrestricted internal femoral rotation limited (block E)..... 153

C.7 Chapter 2 dataset: Non-pivot baseline trials (knee compression force and flexion moment) performed after the trials of the main testing sequence..... 154

C.8 Demographic and morphological data of the donors of the knee specimens tested in Chapter 3..... 155

C.9 Chapter 3 dataset: Kinematic and kinetic data for the last non-pivot trial (knee compression force and flexion moment) of all 32 knee specimens..... 157

C.10 Chapter 3 dataset: Kinematic and kinetic data for the first pivot trial (knee compression force, flexion moment, and internal tibial torque) of all 32 knee specimens..... 159

C.11 Chapter 3 dataset: Kinematic and kinetic data for the last pivot trial (knee compression force, flexion moment, and internal tibial torque), including the trial during which ACL failure occurred in the 8 failed knee specimens..... 161

C.12 Demographic data of the donors of the knee specimens tested in Chapters 4-5..... 163

C.13 Chapter 4 dataset: Microscopic anatomy of the ACL femoral and tibial entheses.. 164

C.14 Chapter 5 dataset: Regional microscopic anatomy of the ACL femoral enthesis ... 166

C.15 Chapter 5 dataset: Coefficient of fifth-order polynomial fit to femoral entheseal surface 167

LIST OF APPENDICES

APPENDIX

A. Detailed Methods Used for the Lower Limb Computational Model in Chapter 2. . 128

B. Collection of Histological Images of All Femoral and Tibial Entheses of 15 Human Anterior Cruciate Ligaments 131

C. Comprehensive Datasets for the Dissertation 147

ABSTRACT

On the Fatigue Life of the Human Anterior Cruciate Ligament:
Experimental Studies of the Effects of Limited Internal Femoral Rotation
and Microscopic Entheseal Anatomy

by

Mélanie L. Beaulieu

Chair: James A. Ashton-Miller

Anterior cruciate ligament (ACL) injuries pose significant health and financial burdens, such as the early development of knee osteoarthritis. It is imperative to better prevent these injuries, but several knowledge gaps exist, including: (1) why athletes with a restricted range of hip internal rotation are more prone to ACL injuries; (2) whether this restriction can increase the ACL's susceptibility to a fatigue failure; and (3) why the ACL ruptures more frequently near its femoral enthesis, especially the posterolateral fibers during pivot landings. This dissertation addresses these gaps.

I hypothesized that limiting range of internal femoral rotation would increase peak ACL strain and risk of ACL fatigue failure during *in vitro* single-leg pivot landings. A custom-built testing apparatus applied an impulsive load, which induced knee compression, flexion moment, and internal tibial torque to human male and female knee specimens. A novel femoral rotation device controlled internal femoral rotation. As the range of internal femoral rotation was

decreased, peak ACL strain increased 1.3% per 10° decrease and ACL fatigue failure risk increased 17-fold, when accounting for sex of specimen donor. These results suggest that screening for a limited range of hip internal rotation should become a component of ACL injury prevention programs and evaluation protocols for those with ACL injuries and/or reconstructions.

I also hypothesized that micro-anatomical differences would exist between ACL entheses, as well as regionally within the femoral enthesis. The microscopic appearance of the ACL entheses was quantified in unembalmed human knee specimens using standard histological methods. The femoral enthesis had more fibrocartilage and a more acute ligament entheseal attachment angle than the tibial enthesis. The profiles of the femoral entheseal tidemarks varied within an enthesis and between donors, with six profiles predominating, but bilateral similarities existed. Within the femoral enthesis, there was more fibrocartilage in the inferior region of the origin of the anteromedial fibers. These fibers originated from the femur at a more acute angle than the posterolateral fibers. Perhaps these differences can induce a strain concentration at the inferior margin of the posterolateral fibers femoral enthesis, thus making this region susceptible to damage accumulation, during pivot landings.

CHAPTER 1

INTRODUCTION

1.1 Overview of the Problem

Injuries to the anterior cruciate ligament (ACL) continue to occur at a rate of more than 250,000 per year in the United States.[20] Occurring as early as the age of 5 years,[59] they are especially common in females.[1,75] In fact, females are two to five times more likely to sustain an ACL injury than their male counterparts, especially in sports such as soccer and basketball.[69,75] They are also getting injured at a younger age than males (on average, 20 vs. 25 years).[8,56,74] Of particular concern is the increased susceptibility to the development of knee osteoarthritis within 10 years of injury.[38,44] These otherwise healthy women will suffer premature aging of their knees, thus limiting physical activity. This poses an enormous health and financial burden for the future.[20,24] For example, ACL-injured soccer players exhibit greater knee pain and other symptoms, reduced knee function in general and in sports and recreation, and a reduced knee-related quality of life 12 years after injury in comparison with healthy soccer players and the general female population.[39]

There is an urgent need, therefore, to prevent ACL injuries to eliminate the costly consequences of these injuries. Currently, effective preventive strategies continue to elude us mostly due to a lack of understanding of the pathomechanics of injury. It is difficult to prevent something that is not fully understood. Most ACL injuries occur during athletic maneuvers that are performed repeatedly during a sporting career (e.g., landing from a jump, running and

changing direction).[9,28,30,48] They also occur more frequently near the femoral origin of the ACL.[36,80] We do not understand, however, how and why injury occurs during a particular maneuver but not during another, apparently similar maneuver, or why the femoral origin, or enthesis, of the ACL is vulnerable to injury. Hence, it is of importance to elucidate how and why ACL injuries occur.

1.2 Background and Knowledge Gaps

The ACL is one of four major ligaments of the knee joint that connects the distal femur to the proximal tibia.[2] It originates on the posterior-superior-medial facet of the lateral femoral condyle and inserts on the anterior-lateral portion of the medial tibial plateau.[15,18,21] Oriented in the anterior-posterior and medial-lateral directions, the ACL plays a primary role in limiting anterior translation and internal rotation of the tibia relative to the femur.[12,34,45,81] It is often described as a 'two-bundle' structure comprising the fibers of the anteromedial (AM) and the posterolateral (PL) bundles whose contributions to resisting such translation and rotation differ.[13,40,81] Although they function in a complementary manner, the AM fibers play a primary role in resisting anterior tibial translation;[13,40] whereas the PL fibers play a primary role in resisting internal tibial rotation.[81] The fiber contributions are also dependent on knee flexion angle, with a gradual transition from the anteriorly positioned fibers resisting peak loads at moderate (i.e., 30°-60°) knee flexion angles to the posteriorly positioned fibers resisting peak loads near full extension (i.e., 0°-15°).[19,25,26,43,57] This is because the location where the PL fibers attach to the femur rotates toward the attachment site on the tibia as the knee flexes, thus causing shortening of the fibers. Also, the bundle of PL fibers, which is narrower and shorter,[27] elongates more than the AM fibers during weight bearing with a knee near full extension.[25]

Most ACL injuries occur during 'noncontact' situations, in which no direct contact between the injured individual and another individual or an object (other than the ground) occurs.[9,30,48] Typically, injury occurs upon landing on one leg after a jump and/or during a change of direction.[9,28,30,48] Such injuries have been described numerous times by athletes via questionnaires[9,48] and interviews[9,28] and by medical experts and researchers with video analyses, both qualitatively[48] and quantitatively.[10,29,30] For example, Koga et al.[29] analyzed video sequences from 10 ACL injuries in women's basketball and handball. By using model-based image matching, they were able to quantify three-dimension (3D) knee rotations during the injurious maneuvers. Though the accuracy of this imaging analysis method is questionable, since it has not been validated against the gold standard (bone-pin markers[6,53,54]), it provides useful information.[31] For instance, all injuries occurred without direct contact to the knee during single-leg landings or changes of direction. Also, knee flexion, abduction, and internal rotation occurred, with injury time estimated at 40 milliseconds after initial ground contact.

Similar descriptions have been published of other noncontact ACL injury scenarios.[10,30,48] A common theme among studies investigating actual ACL injury scenarios is their focus on the single event when ligament failure appears to occur.[9,10,29,30,48] They do not account for the history of landing and cutting events of the injured individual, whether earlier in the game/practice or earlier in the season, when ligament failure did not occur. Recent evidence supports the importance of the ACL's loading history in the failure risk of the ligament.[36] The ACL has been shown to be susceptible to a material fatigue failure mechanism whereby the ACL tissue failed after being loaded repetitively by a series of single-leg pivot landings.[36] The most common mode of ACL failure was a partial tear of the PL fibers near its femoral 'enthesis'.[36] Similar ACL rupture pattern have been reported both *in vitro*[42] and *in vivo*.[63,68,80] Although most research

efforts have focused on the single event when ACL failure appears to occur, recent research from our laboratory suggests that the ACL's loading history may also be a significant contributor to injury risk.[36] Further research is therefore needed to understand the mechanism of the ACL fatigue failure, the factors influencing the fatigue life of the ACL (Chapter 3), and the reasons for the vulnerability of the ACL's femoral enthesis to failure, especially that of the PL fibers during pivot landings (Chapters 4-5).

Numerous contributing factors to ACL injury risk exist, including extrinsic and intrinsic factors. *Extrinsic* factors include factors that relate to the environment in which an individual sustains the injury, such as type of shoe and/or playing surface. For example, ACL injury rates in the NFL were found to be 67% higher on artificial surfaces (FieldTurf) than on natural grass surface.[23] This may be due to greater shoe-turf frictional torques developed on artificial surfaces that apply larger torques to the knee, and thus lead to ACL injuries. For example, during a controlled axial rotation of the lower leg, greater axial torques were produced on artificial grass with sand/rubber infill in comparison with natural grass, as well as in soccer shoes with blade-type cleats in comparison with stud-type cleats.[66]

More frequently investigated are *intrinsic* factors which are factors that relate to the individual sustaining the injury, as opposed to risk factors in the environment. Scientists and clinicians have examined such intrinsic factors as joint anatomy,[41] genetics,[52] hormones,[76] and neuromechanics of athletic maneuvers.[41] Anatomical factors include knee joint morphology, which has been found to be different between healthy and ACL-injured knees. Specifically, ACL-injured knees have a larger posterior-directed slope of the tibial plateau,[11,58,67,70,71,73,82] a shallower medial tibial plateau,[22] and a smaller femoral intercondylar notch.[64,67,72,83] In fact, a greater slope of the lateral tibia and a smaller ACL cross-sectional area have been found to

increase ACL strain *in vitro*,[35] which appears to explain, in part, the role of anatomical factors in ACL injury risk. Genetic factors include the gene (COL1A1) that encodes for a major chain that makes up type I collagen (the ACL's main structural component), which is associated with ACL injury risk.[51,52] Hormonal factors include estrogen levels, which are known to affect the metabolic[32,33,37,62,78,79] and structural[65,77] properties of the ACL and muscle stiffness.[4,5,49,50,61] Lastly, neuromechanical factors include both neuromuscular and biomechanical components, such as muscle activation patterns and joint rotations, translations, forces, and torques during injurious, noninjurious, and cadaver-modeled athletic maneuvers (e.g., single-leg pivot landings). A combination of knee axial compression force, knee flexion moment, internal tibial torque, and knee abduction moment is the 'worst-case' loading scenario for the ACL, as tested *in vitro* and *in silico*.[14,45,47,55,60] These kinetic variables and muscle activation patterns, however, have not been measured *in vivo* during injurious scenarios due to methodological and ethical constraints. Only kinematic variables have been measured in actual *in vivo* injury events (from video sequences), with knee abduction and internal tibial rotation identified as important elements of injury.[7,29,48] As stated earlier, the reliability of such video-based image analyses is questionable, and therefore must be interpreted with caution.

While many factors contributing to injury risk have been investigated, attention has mostly focused on the knee joint. The mechanics of the hip joint, however, may also contribute to injury risk. For example, a limited passive range of internal rotation at the hip, as seen in some femoroacetabular impingement (FAI) patients, has been correlated with ACL ruptures in soccer and football players.[3,16,17] It is unknown, however, how limited hip internal rotation increases ACL injury risk (Chapter 2).

Although advances have been made in understanding the mechanism of ACL injuries in the last few decades, many questions remain unanswered. We do not know (1) why athletes with a restricted range of hip internal rotation are more prone to ACL injuries (Chapter 2); (2) whether such a limitation in hip internal rotation can increase the ACL's susceptibility to a fatigue failure via repetitive loading (Chapter 3); (3) why the ACL ruptures more frequently near its femoral enthesis (Chapter 4); and (4) and why the PL fibers appear to be more susceptible to injury than the AM fibers during pivot landings (Chapter 5). A better understanding of why and how ACL injuries occur is needed before screening and prevention strategies can improve, and thus before injury rates can decrease.

1.3 Overall Objective and Working Hypothesis

The overall objective of this dissertation is to elucidate the noncontact ACL injury mechanism for which ACL loading history, limited range of hip internal rotation, and the geometry and microscopic anatomy of the ACL's entheses are contributing factors to peak ACL strain and/or injury risk. The central hypothesis is that the ACL fails under repeated loading, with limited range of hip internal rotation reducing ACL fatigue life. Decreased terminal hip internal rotation is compensated by greater axial motion at the knee (i.e., internal tibial rotation), thereby increasing ACL strain. Internal tibial rotation is known to strain the ACL during pivot landings.[46,47] Outcomes of this work should help explain the ACL fatigue mechanism, including the role of limited range of hip internal rotation and the microscopic anatomy of the ACL entheses, and therefore guide the improvement of injury prevention efforts.

1.4 Dissertation Structure including Specific Aims, Hypotheses, and Significance

To accomplish the overall objective of this work, four sets of hypotheses were tested in Chapters 2-5.

Chapter 2. Using an *in vitro* knee loading model, we determined the effect of limited range of internal femoral rotation and sex on peak ACL strain during a simulated single-leg pivot landing. We hypothesized that as the available range of internal femoral rotation decreased, the magnitude of peak ACL strain would significantly increase. It was also hypothesized that the female knee specimens would exhibit greater peak ACL strain, in comparison with the male knee specimens, regardless of the range of internal femoral rotation. The significance is that establishing an inverse relationship between the available range of internal femoral rotation and peak ACL strain during cadaver-simulated pivot landings will help explain why athletes with limited range of hip internal rotation are at greater risk of sustaining an ACL injury. As such, athletes could be screened for such a restriction in axial hip rotation, as part of ACL injury prevention programs, and possibly treated. This would reduce their risk of ACL injury by reducing ACL strain during athletic maneuvers like the pivot landing. ACL-injured individuals could also be evaluated to help prevent subsequent injuries to the reconstructed ACL and the contralateral ACL. Results of this aim will also help explain why women sustain more ACL injuries than their male counterparts.

Chapter 3. Using the *in vitro* model presented in Chapter 2, we determined the effect of limited range of internal femoral rotation, sex, and knee morphology on ACL fatigue life during repetitive simulated single-leg pivot landings. We hypothesized that the risk of ACL failure would be significantly greater with limited range of internal femoral rotation than with unrestricted rotation. It was also hypothesized that the female knee specimens would have a higher risk of ACL failure than the male specimens. The significance is that showing that the number of loading cycles required to fail the ACL is greater in a cadaver model with unrestricted internal femoral rotation than in a model with limited rotation would strongly suggest that the

ACL can fail due to repetitive loading (fatigue). Furthermore, it would suggest that limited axial hip rotation can significantly reduce the fatigue life of the ACL, and thus increase risk of ACL injury. Findings of this chapter should also help explain why women are at a greater risk of ACL injury than men if the number of loading cycles required to fail the male ACL is found to be greater than that of the female ACL. Hence, it should lead to improved injury prevention programs.

Chapter 4. To understand why the majority of ACL ruptures occur near the femoral origin of the ACL, we investigated the microscopic anatomy of the human ACL femoral and tibial entheses by means of quantitative histological analyses. We tested the null hypothesis that there would be no difference in the amount of fibrocartilage (calcified and uncalcified) or the ligament entheseal attachment angle between the femoral and tibial entheses. The significance is that determining whether histological and morphologic differences exist between the femoral and tibial entheses will help explain why the ACL ruptures more frequently near its femoral enthesis. If no differences are found, for instance, differences in other factors, such as tissue material properties, may be responsible for the susceptibility of the ACL femoral enthesis to injury.

Chapter 5. To understand why the PL fibers of the ACL appear to be more susceptible to injury than the AM fibers during pivot landings, we performed a secondary analysis of the femoral enthesis data presented in Chapter 4 and also compared the profile of the femoral entheseal tidemark between paired specimens (i.e., specimens from the same donor). We tested the null hypotheses that there would be no regional differences in the amount of fibrocartilage or in the ligament entheseal attachment angle within the femoral enthesis. We tested the secondary hypotheses that all entheses would have the same general tidemark surface shape and that tidemark shape would be correlated between paired specimens. The significance is that

determining regional differences in the microscopic anatomy within the femoral enthesis should provide the first insights into the mechanism underlying isolated tears of the PL fibers. It will help explain why the ACL tends to rupture near the femoral enthesis of the PL fibers, as opposed to that of the AM fibers, during pivot landings. Furthermore, a bilateral comparison of the shape of the femoral entheseal tidemark surfaces will provide a baseline measure of intra-subject variability, which will provide a basis for future research aimed at investigating histological evidence of entheseal injury. When assessing the histology of an ACL femoral enthesis loaded in an *in vitro* knee loading model, for example, it would be beneficial to know whether bilateral differences are normal or reflect entheseal injury incurred during growth or later in life.

Chapters 6-8. A general discussion that draws together the findings from Chapters 2-5 and interprets them within the context of what is known in the literature is presented in Chapter 6. Novel insights are also described within the context of the methodological limitations. In Chapter 7, the main conclusions from the dissertation are drawn in a concise format. Existing knowledge gaps are identified in Chapter 8, along with suggestions for further research for students interested in these topics.

Appendices. Appendix A presents the detailed methods used for the lower limb computational model in Chapter 2. Appendix B comprises a collection of the histological images of all femoral and tibial entheses of the 15 human ACLs. Lastly, the comprehensive datasets from Chapters 2-5 are gathered in Appendix C for use by future investigators.

1.5 References

1. Agel J, Arendt EA, Bershadsky B. (2005) Anterior cruciate ligament injury in national collegiate athletic association basketball and soccer: a 13-year review. *Am J Sports Med*, 33(4): 524-30.

2. Arnoczky SP. (1983) Anatomy of the anterior cruciate ligament. *Clin Orthop Relat Res*,(172): 19-25.

3. Bedi A, Warren RF, Wojtys EM, Oh YK, Ashton-Miller JA, Oltean H, Kelly BT. (2014) Restriction in hip internal rotation is associated with an increased risk of ACL injury. *Knee Surg Sports Traumatol Arthrosc*, Sept 12. [Epub ahead of print].

4. Bell DR, Blackburn JT, Norcorss MF, Ondrak KS, Hudson JD, Hackney AC, Padua DA. (2012) Estrogen and muscle stiffness have a negative relationship in females. *Knee Surg Sports Traumatol Arthrosc*, 20(2): 361-7.

5. Bell DR, Troy Blackburn J, Ondrak KS, Hackney AC, Hudson JD, Norcross MF, Padua DA. (2011) The effects of oral contraceptive use on muscle stiffness across the menstrual cycle. *Clin J Sport Med*, 21(6): 467-473.

6. Benoit DL, Ramsey DK, Lamontagne M, Xu L, Wretenberg P, Renstrom P. (2006) Effect of skin movement artifact on knee kinematics during gait and cutting motions measured in vivo. *Gait Posture*, 24(2): 152-64.

7. Bere T, Mok KM, Koga H, Krosshaug T, Nordsletten L, Bahr R. (2013) Kinematics of anterior cruciate ligament ruptures in World Cup alpine skiing: 2 case reports of the slip-catch mechanism. *Am J Sports Med*, 41(5): 1067-73.

8. Bjordal JM, Arnly F, Hannestad B, Strand T. (1997) Epidemiology of anterior cruciate ligament injuries in soccer. *Am J Sports Med*, 25(3): 341-5.

9. Boden BP, Dean GS, Feagin JA, Jr., Garrett WE, Jr. (2000) Mechanisms of anterior cruciate ligament injury. *Orthopedics*, 23(6): 573-8.

10. Boden BP, Torg JS, Knowles SB, Hewett TE. (2009) Video analysis of anterior cruciate ligament injury. *Am J Sports Med*, 37(2): 252-259.

11. Brandon ML, Haynes PT, Bonamo JR, Flynn MI, Barrett GR, Sherman MF. (2006) The association between posterior-inferior tibial slope and anterior cruciate ligament insufficiency. *Arthroscopy*, 22(8): 894-9.

12. Butler DL, Noyes FR, Grood ES. (1980) Ligamentous restraints to anterior-posterior drawer in the human knee. A biomechanical study. *J Bone Joint Surg Am*, 62(2): 259-70.

13. Christel PS, Akgun U, Yasar T, Karahan M, Demirel B. (2012) The contribution of each anterior cruciate ligament bundle to the Lachman test: a cadaver investigation. *J Bone Joint Surg Br*, 94(1): 68-74.

14. Durselen L, Claes L, Kiefer H. (1995) The influence of muscle forces and external loads on cruciate ligament strain. *Am J Sports Med*, 23(1): 129-36.

15. Duthon VB, Barea C, Abrassart S, Fasel JH, Fritschy D, Menetrey J. (2006) Anatomy of the anterior cruciate ligament. *Knee Surg Sports Traumatol Arthrosc*, 14(3): 204-13.

16. Ellera Gomes JL, de Castro JV, Becker R. (2008) Decreased hip range of motion and noncontact injuries of the anterior cruciate ligament. *Arthroscopy*, 24(9): 1034-7.

17. Ellera Gomes JL, Palma HM, Ruthner R. (2014) Influence of hip restriction on noncontact ACL rerupture. *Knee Surg Sports Traumatol Arthrosc*, 22(1): 188-91.

18. Ferretti M, Doca D, Ingham SM, Cohen M, Fu FH. (2012) Bony and soft tissue landmarks of the ACL tibial insertion site: an anatomical study. *Knee Surg Sports Traumatol Arthrosc*, 20(1): 62-8.

19. Gabriel MT, Wong EK, Woo SL, Yagi M, Debski RE. (2004) Distribution of in situ forces in the anterior cruciate ligament in response to rotatory loads. *J Orthop Res*, 22(1): 85-9.

20. Griffin LY, Albohm MJ, Arendt EA, Bahr R, Beynnon BD, Demaio M, Dick RW, Engebretsen L, Garrett WE, Jr., Hannafin JA, Hewett TE, Huston LJ, Ireland ML, Johnson RJ, Lephart S, Mandelbaum BR, Mann BJ, Marks PH, Marshall SW, Myklebust G, Noyes FR, Powers C, Shields C, Jr., Shultz SJ, Silvers H, Slauterbeck J, Taylor DC, Teitz CC, Wojtys EM, Yu B. (2006) Understanding and preventing noncontact anterior cruciate ligament injuries: a review of the Hunt Valley II meeting, January 2005. *Am J Sports Med*, 34(9): 1512-32.

21. Han Y, Kurzencwyg D, Hart A, Powell T, Martineau PA. (2012) Measuring the anterior cruciate ligament's footprints by three-dimensional magnetic resonance imaging. *Knee Surg Sports Traumatol Arthrosc*, 20(5): 986-95.

22. Hashemi J, Chandrashekar N, Mansouri H, Gill B, Slauterbeck JR, Schutt RC, Jr., Dabezies E, Beynnon BD. (2010) Shallow medial tibial plateau and steep medial and lateral tibial slopes: new risk factors for anterior cruciate ligament injuries. *Am J Sports Med*, 38(1): 54-62.

23. Hershman EB, Anderson R, Bergfeld JA, Bradley JP, Coughlin MJ, Johnson RJ, Spindler KP, Wojtys E, Powell JW. (2012) An analysis of specific lower extremity injury rates on grass and FieldTurf playing surfaces in National Football League games: 2000-2009 seasons. *Am J Sports Med*, 40(10): 2200-5.

24. Hewett TE, Myer GD, Ford KR. (2006) Anterior cruciate ligament injuries in female athletes: Part 1, mechanisms and risk factors. *Am J Sports Med*, 34(2): 299-311.

25. Hosseini A, Gill TJ, Li G. (2009) In vivo anterior cruciate ligament elongation in response to axial tibial loads. *J Orthop Sci*, 14(3): 298-306.

26. Jordan SS, DeFrate LE, Nha KW, Papannagari R, Gill TJ, Li G. (2007) The in vivo kinematics of the anteromedial and posterolateral bundles of the anterior cruciate ligament during weightbearing knee flexion. *Am J Sports Med*, 35(4): 547-54.

27. Katouda M, Soejima T, Kanazawa T, Tabuchi K, Yamaki K, Nagata K. (2011) Relationship between thickness of the anteromedial bundle and thickness of the posterolateral bundle in the normal ACL. *Knee Surg Sports Traumatol Arthrosc*, 19(8): 1293-8.

28. Kimura Y, Ishibashi Y, Tsuda E, Yamamoto Y, Tsukada H, Toh S. (2010) Mechanisms for anterior cruciate ligament injuries in badminton. *Br J Sports Med*, 44(15): 1124-7.

29. Koga H, Nakamae A, Shima Y, Iwasa J, Myklebust G, Engebretsen L, Bahr R, Krosshaug T. (2010) Mechanisms for noncontact anterior cruciate ligament injuries: knee joint kinematics in 10 injury situations from female team handball and basketball. *Am J Sports Med*, 38(11): 2218-25.

30. Krosshaug T, Nakamae A, Boden BP, Engebretsen L, Smith G, Slauterbeck JR, Hewett TE, Bahr R. (2007) Mechanisms of anterior cruciate ligament injury in basketball: video analysis of 39 cases. *Am J Sports Med*, 35(3): 359-67.

31. Krosshaug T, Slauterbeck JR, Engebretsen L, Bahr R. (2007) Biomechanical analysis of anterior cruciate ligament injury mechanisms: three-dimensional motion reconstruction from video sequences. *Scand J Med Sci Sports*, 17(5): 508-19.

32. Lee CY, Liu X, Smith CL, Zhang X, Hsu HC, Wang DY, Luo ZP. (2004) The combined regulation of estrogen and cyclic tension on fibroblast biosynthesis derived from anterior cruciate ligament. *Matrix Biol*, 23(5): 323-9.

33. Lee CY, Smith CL, Zhang X, Hsu HC, Wang DY, Luo ZP. (2004) Tensile forces attenuate estrogen-stimulated collagen synthesis in the ACL. *Biochem Biophys Res Commun*, 317(4): 1221-5.

34. Lipke JM, Janecki CJ, Nelson CL, McLeod P, Thompson C, Thompson J, Haynes DW. (1981) The role of incompetence of the anterior cruciate and lateral ligaments in anterolateral and anteromedial instability. A biomechanical study of cadaver knees. *J Bone Joint Surg Am*, 63(6): 954-60.

35. Lipps DB, Oh YK, Ashton-Miller JA, Wojtys EM. (2012) Morphologic characteristics help explain the gender difference in peak anterior cruciate ligament strain during a simulated pivot landing. *Am J Sports Med*, 40(1): 32-40.

36. Lipps DB, Wojtys EM, Ashton-Miller JA. (2013) Anterior cruciate ligament fatigue failures in knees subjected to repeated simulated pivot landings. *Am J Sports Med*, 41(5): 1058-66.

37. Liu SH, Al-Shaikh RA, Panossian V, Finerman GA, Lane JM. (1997) Estrogen affects the cellular metabolism of the anterior cruciate ligament. A potential explanation for female athletic injury. *Am J Sports Med*, 25(5): 704-9.

38. Lohmander LS, Englund PM, Dahl LL, Roos EM. (2007) The long-term consequence of anterior cruciate ligament and meniscus injuries: osteoarthritis. *Am J Sports Med*, 35(10): 1756-69.

39. Lohmander LS, Ostenberg A, Englund M, Roos H. (2004) High prevalence of knee osteoarthritis, pain, and functional limitations in female soccer players twelve years after anterior cruciate ligament injury. *Arthritis Rheum*, 50(10): 3145-52.

40. Markolf KL, Park S, Jackson SR, McAllister DR. (2008) Contributions of the posterolateral bundle of the anterior cruciate ligament to anterior-posterior knee laxity and ligament forces. *Arthroscopy*, 24(7): 805-9.

41. McLean SG, Beaulieu ML. (2010) Complex integrative morphological and mechanical contributions to ACL injury risk. *Exerc Sport Sci Rev*, 38(4): 192-200.

42. Meyer EG, Baumer TG, Slade JM, Smith WE, Haut RC. (2008) Tibiofemoral contact pressures and osteochondral microtrauma during anterior cruciate ligament rupture due to excessive compressive loading and internal torque of the human knee. *Am J Sports Med*, 36(10): 1966-77.

43. Mommersteeg TJ, Huiskes R, Blankevoort L, Kooloos JG, Kauer JM. (1997) An inverse dynamics modeling approach to determine the restraining function of human knee ligament bundles. *J Biomech*, 30(2): 139-46.

44. Neuman P, Englund M, Kostogiannis I, Friden T, Roos H, Dahlberg LE. (2008) Prevalence of tibiofemoral osteoarthritis 15 years after nonoperative treatment of anterior cruciate ligament injury: a prospective cohort study. *Am J Sports Med*, 36(9): 1717-25.

45. Nielsen S, Ovesen J, Rasmussen O. (1984) The anterior cruciate ligament of the knee: an experimental study of its importance in rotatory knee instability. *Arch Orthop Trauma Surg*, 103(3): 170-4.

46. Oh YK, Kreinbrink JL, Wojtys EM, Ashton-Miller JA. (2012) Effect of axial tibial torque direction on ACL relative strain and strain rate in an in vitro simulated pivot landing. *J Orthop Res*, 30(4): 528-34.

47. Oh YK, Lipps DB, Ashton-Miller JA, Wojtys EM. (2012) What strains the anterior cruciate ligament during a pivot landing? *Am J Sports Med*, 40(3): 574-83.

48. Olsen OE, Myklebust G, Engebretsen L, Bahr R. (2004) Injury mechanisms for anterior cruciate ligament injuries in team handball: a systematic video analysis. *Am J Sports Med*, 32(4): 1002-12.

49. Park SK, Stefanyshyn DJ, Loitz-Ramage B, Hart DA, Ronsky JL. (2009) Changing hormone levels during the menstrual cycle affect knee laxity and stiffness in healthy female subjects. *Am J Sports Med*, 37(3): 588-98.

50. Park SK, Stefanyshyn DJ, Ramage B, Hart DA, Ronsky JL. (2009) Alterations in knee joint laxity during the menstrual cycle in healthy women leads to increases in joint loads during selected athletic movements. *Am J Sports Med*, 37(6): 1169-77.

51. Posthumus M, September AV, Keegan M, O'Cuinneagain D, Van der Merwe W, Schwellnus MP, Collins M. (2009) Genetic risk factors for anterior cruciate ligament ruptures: COL1A1 gene variant. *Br J Sports Med*, 43(5): 352-6.

52. Posthumus M, September AV, O'Cuinneagain D, van der Merwe W, Schwellnus MP, Collins M. (2009) The COL5A1 gene is associated with increased risk of anterior cruciate ligament ruptures in female participants. *Am J Sports Med*, 37(11): 2234-40

53. Reinschmidt C, van den Bogert AJ, Lundberg A, Nigg BM, Murphy N, Stacoff A, Stano A. (1997) Tibiofemoral and tibiocalcaneal motion during walking: external vs. skeletal markers. *Gait Posture*, 6(2): 98-109.

54. Reinschmidt C, van den Bogert AJ, Nigg BM, Lundberg A, Murphy N. (1997) Effect of skin movement on the analysis of skeletal knee joint motion during running. *J Biomech*, 30(7): 729-32.

55. Ren Y, Jacobs BJ, Nuber GW, Koh JL, Zhang LQ. (2010) Developing a 6-DOF robot to investigate multi-axis ACL injuries under valgus loading coupled with tibia internal rotation. *Conf Proc IEEE Eng Med Biol Soc*, 2010: 3942-5.

56. Roos H, Ornell M, Gardsell P, Lohmander LS, Lindstrand A. (1995) Soccer after anterior cruciate ligament injury--an incompatible combination? A national survey of incidence and risk factors and a 7-year follow-up of 310 players. *Acta Orthop Scand*, 66(2): 107-12.

57. Sakane M, Fox RJ, Woo SL, Livesay GA, Li G, Fu FH. (1997) In situ forces in the anterior cruciate ligament and its bundles in response to anterior tibial loads. *J Orthop Res*, 15(2): 285-93.

58. Senisik S, Özgürbüz C, Ergün M, Yüksel O, Taskiran E, Islegen C, Ertat A. (2011) Posterior tibial slope as a risk factor for anterior cruciate ligament rupture in soccer players. *J Sports Sci Med*, 10(4): 763-767.

59. Shea KG, Pfeiffer R, Wang JH, Curtin M, Apel PJ. (2004) Anterior cruciate ligament injury in pediatric and adolescent soccer players: an analysis of insurance data. *J Pediatr Orthop*, 24(6): 623-8.

60. Shin CS, Chaudhari AM, Andriacchi TP. (2011) Valgus plus internal rotation moments increase ACL strain more than either alone. *Med Sci Sports Exerc*, 43(8): 1484-91.

61. Shultz SJ, Schmitz RJ, Nguyen AD, Levine B, Kim H, Montgomery MM, Shimokochi Y, Beynnon BD, Perrin DH. (2011) Knee joint laxity and its cyclic variation influence tibiofemoral motion during weight acceptance. *Med Sci Sports Exerc*, 43(2): 287-95.

62. Shultz SJ, Wideman L, Montgomery MM, Beasley KN, Nindl BC. (2012) Changes in serum collagen markers, IGF-I, and knee joint laxity across the menstrual cycle. *J Orthop Res*, 30(9): 1405-12.

63. Siebold R, Fu FH. (2008) Assessment and augmentation of symptomatic anteromedial or posterolateral bundle tears of the anterior cruciate ligament. *Arthroscopy*, 24(11): 1289-98.

64. Simon RA, Everhart JS, Nagaraja HN, Chaudhari AM. (2010) A case-control study of anterior cruciate ligament volume, tibial plateau slopes and intercondylar notch dimensions in ACL-injured knees. *J Biomech*, 43(9): 1702-7.

65. Slauterbeck J, Clevenger C, Lundberg W, Burchfield DM. (1999) Estrogen level alters the failure load of the rabbit anterior cruciate ligament. *J Orthop Res*, 17(3): 405-8.

66. Smeets K, Jacobs P, Hertogs R, Luyckx JP, Innocenti B, Corten K, Ekstrand J, Bellemans J. (2012) Torsional injuries of the lower limb: an analysis of the frictional torque between different types of football turf and the shoe outsole. *Br J Sports Med*, 46(15): 1078-83.

67. Sonnery-Cottet B, Archbold P, Cucurulo T, Fayard JM, Bortolletto J, Thaunat M, Prost T, Chambat P. (2011) The influence of the tibial slope and the size of the intercondylar notch on rupture of the anterior cruciate ligament. *J Bone Joint Surg Br*, 93(11): 1475-8.

68. Sonnery-Cottet B, Barth J, Graveleau N, Fournier Y, Hager JP, Chambat P. (2009) Arthroscopic identification of isolated tear of the posterolateral bundle of the anterior cruciate ligament. *Arthroscopy*, 25(7): 728-32.

69. Swenson DM, Collins CL, Best TM, Flanigan DC, Fields SK, Comstock RD. (2013) Epidemiology of knee injuries among US high school athletes, 2005/06-2010/11. *Med Sci Sports Exerc*, 45(3): 462-9.

70. Terauchi M, Hatayama K, Yanagisawa S, Saito K, Takagishi K. (2011) Sagittal alignment of the knee and its relationship to noncontact anterior cruciate ligament injuries. *Am J Sports Med*, 39(5): 1090-4.

71. Todd MS, Lalliss S, Garcia E, DeBerardino TM, Cameron KL. (2010) The relationship between posterior tibial slope and anterior cruciate ligament injuries. *Am J Sports Med*, 38(1): 63-7.

72. Uhorchak JM, Scoville CR, Williams GN, Arciero RA, St Pierre P, Taylor DC. (2003) Risk factors associated with noncontact injury of the anterior cruciate ligament: a prospective four-year evaluation of 859 West Point cadets. *Am J Sports Med*, 31(6): 831-42.

73. Vyas S, van Eck CF, Vyas N, Fu FH, Otsuka NY. (2011) Increased medial tibial slope in teenage pediatric population with open physes and anterior cruciate ligament injuries. *Knee Surg Sports Traumatol Arthrosc*, 19(3): 372-7.

74. Walden M, Hagglund M, Magnusson H, Ekstrand J. (2011) Anterior cruciate ligament injury in elite football: a prospective three-cohort study. *Knee Surg Sports Traumatol Arthrosc*, 19(1): 11-9.

75. Walden M, Hagglund M, Werner J, Ekstrand J. (2011) The epidemiology of anterior cruciate ligament injury in football (soccer): a review of the literature from a gender-related perspective. *Knee Surg Sports Traumatol Arthrosc*, 19(1): 3-10.

76. Wild CY, Steele JR, Munro BJ. (2012) Why do girls sustain more anterior cruciate ligament injuries than boys?: A review of the changes in estrogen and musculoskeletal structure and function during puberty. *Sports Med*, 42(9): 733-49.

77. Woodhouse E, Schmale GA, Simonian P, Tencer A, Huber P, Seidel K. (2007) Reproductive hormone effects on strength of the rat anterior cruciate ligament. *Knee Surg Sports Traumatol Arthrosc*, 15(4): 453-60.

78. Yoshida A, Morihara T, Kajikawa Y, Arai Y, Oshima Y, Kubo T, Matsuda K, Sakamoto H, Kawata M. (2009) In vivo effects of ovarian steroid hormones on the expressions of estrogen receptors and the composition of extracellular matrix in the anterior cruciate ligament in rats. *Connect Tissue Res*, 50(2): 121-31.

79. Yu WD, Liu SH, Hatch JD, Panossian V, Finerman GA. (1999) Effect of estrogen on cellular metabolism of the human anterior cruciate ligament. *Clin Orthop Relat Res*,(366): 229-38.

80. Zantop T, Brucker PU, Vidal A, Zelle BA, Fu FH. (2007) Intraarticular rupture pattern of the ACL. *Clin Orthop Relat Res*, 454: 48-53.

81. Zantop T, Herbort M, Raschke MJ, Fu FH, Petersen W. (2007) The role of the anteromedial and posterolateral bundles of the anterior cruciate ligament in anterior tibial translation and internal rotation. *Am J Sports Med*, 35(2): 223-7.

82. Zeng C, Cheng L, Wei J, Gao SG, Yang TB, Luo W, Li YS, Xu M, Lei GH. (2014) The influence of the tibial plateau slopes on injury of the anterior cruciate ligament: a meta-analysis. *Knee Surg Sports Traumatol Arthrosc*, 22(1): 53-65.

83. Zeng C, Gao SG, Wei J, Yang TB, Cheng L, Luo W, Tu M, Xie Q, Hu Z, Liu PF, Li H, Yang T, Zhou B, Lei GH. (2013) The influence of the intercondylar notch dimensions on injury of the anterior cruciate ligament: a meta-analysis. *Knee Surg Sports Traumatol Arthrosc*, 21(4): 804-15.

CHAPTER 2

DOES LIMITED INTERNAL FEMORAL ROTATION INCREASE PEAK ANTERIOR CRUCIATE LIGAMENT STRAIN DURING A SIMULATED PIVOT LANDING?

This chapter is published and should be referred as:

Beaulieu ML, Oh YK, Bedi A, Ashton-Miller JA, Wojtys EM. (2014) Does limited internal femoral rotation increase peak anterior cruciate ligament strain during a simulated pivot landing? *Am J Sports Med*, 42(12), 2955-63.

2.1 Abstract

Many factors contributing to anterior cruciate ligament (ACL) injury risk have been investigated. Recently, some ACL-injured individuals have presented with a decreased range of hip internal rotation compared with controls. The pathomechanics of why decreased hip range of motion increases risk of ACL injury have not yet been studied. We hypothesized that peak relative strain of the anteromedial bundle of the ACL (AM-ACL) during a simulated single-leg pivot landing is inversely related to the available range of internal femoral rotation.

A series of pivot landings were simulated in 10 female and 10 male human knee specimens with a testing apparatus that applied a two-bodyweight impulsive load, inducing knee compression, flexion moment, and internal tibial torque. The range of internal femoral rotation was (1) locked at ~0°, (2) limited with a hard stop to ~7°, (3) limited with a hard stop to ~11°, or (4) free, with rotation resisted by two springs to simulate the resistance of the active hip rotator muscles to stretch. The AM-ACL strain was quantified with a differential variable reluctance

transducer. A linear mixed model was used to determine whether a significant linear relation existed between peak AM-ACL relative strain and range of internal femoral rotation.

Peak AM-ACL relative strain was inversely related to the available range of internal femoral rotation ($R^2 = 0.91$; $p < 0.001$), with strain increasing 1.3% for every 10° decrease in rotation; this represented a 20% increase in peak relative strain, given an average range of femoral rotation of 15° upon landing in healthy athletes.

Peak AM-ACL relative strain was inversely proportional to the available range of internal femoral rotation during simulated single-leg pivot landings. Decreased range of internal femoral rotation results in greater ACL strain and may therefore increase the susceptibility to ACL rupture with athletic cutting and pivoting activities. Screening for a limited range of hip internal rotation should therefore become a component of not only ACL injury prevention programs but also evaluation protocols for those with ACL injuries and/or reconstructions.

2.2 Introduction

Injuries to the anterior cruciate ligament (ACL) continue to occur at significant rates,[21,39] especially in younger females.[41] Given that knee osteoarthritis is an expensive sequela of ACL injuries,[29,30,33] in terms of both financial and health costs, insights are needed to better prevent ACL injuries.

While many factors contributing to injury risk have been investigated,[38] attention has focused on the knee joint.[15,37,40,46] The mechanics of the hip, however, may also contribute to injury risk. For example, a restricted passive range of internal rotation at the hip, mostly associated with abnormal proximal femoral or acetabular anatomy,[7] has been correlated with ACL ruptures and reruptures in soccer players.[6,8] Restricted hip internal rotation was defined as being less than 30-35°, with ACL-injured and ACL-reinjured soccer players having an average

range of 26° and 18°, respectively, compared with 39° in the control group.[6,8] A similar restriction in range of hip internal rotation has been identified as a contributing factor to ACL injury risk in professional American football athletes.[2] Specifically, players at the 2012 National Football League Combine with a restricted range of internal rotation at the hip were more likely to have had sustained an ACL injury that required surgical reconstruction.[2] Also, as compared to uninjured controls, a group of ACL-injured individuals were found to have a larger cam-type femoroacetabular deformity of the femoral head, as measured by the alpha angle,[31] as well as a greater prevalence of acetabular dysplasia.[47] Abnormal hip anatomy therefore may play a critical role in increasing ACL injury risk given its prevalence in healthy and pathologic populations. For example, femoroacetabular impingement (FAI) is present in 6% to 24% of asymptomatic individuals,[10,14,16,23,32] in addition to 63% of patients with an intra-articular hip disorders.[1]

The underlying mechanism for an increased risk of ACL injury with restricted terminal hip range of motion, however, remains unexplored. We theorized that limiting the available range of hip internal rotation will cause an increase in peak ACL strain during athletic maneuvers via compensatory axial tibial rotation at the knee joint.[27] If hip internal rotation is limited by a bony impingement between the acetabular rim and the femoral head-neck junction, then rotation at an adjacent joint may have to increase to achieve the desired athletic outcome. Hence, the purpose of this study was to quantify the effect of limiting the range of internal femoral rotation on peak ACL strain during a simulated single-leg pivot landing. We also examined whether sex modulated this peak strain.

We used a custom-built *in vitro* knee testing apparatus[17,18,26-28,42-44] to simulate a single-leg pivot landing under a two-bodyweight (2×BW) impulsive load. To titrate the available range of internal femoral rotation, a new femoral rotation device was added to the apparatus whereby

the experimenter could set the range of available internal femoral rotation to restrict axial hip motion. Such a restriction can occur because of bony contact in hips with abnormal anatomy, such as FAI, as well as axial hip motion resisted by pretensed muscles. We used the apparatus to test the primary hypothesis that peak strain in the anteromedial bundle of the ACL (AM-ACL) would be inversely related to the available range of internal femoral rotation during the landing. We also tested the secondary hypothesis that female knee specimens would exhibit greater peak AM-ACL strain, in comparison with male knee specimens, regardless of the range of internal femoral rotation.

2.3 Materials and Methods

Specimen Procurement and Preparation. To determine the sample size needed to reveal statistically significant differences in peak AM-ACL strain among femoral rotation conditions as well as between sexes, two-sided paired and unpaired two-sample *t*-test models ($\alpha = 0.05$; $1\text{-}\beta = 0.80$)[34] were applied to pilot data. These a priori power analyses revealed required total sample sizes between 6 and 18 knee specimens. A total of 20 unembalmed knee specimens (10 female, 10 male specimens) were therefore harvested from 6 female and 6 male human donors (Table 2.1) acquired from the University of Michigan Anatomical Donations Program, Anatomy Gifts Registry and Research for Life. All knee specimens were free of scars indicative of knee surgery, free of evidence of joint degeneration, and free of joint deformity. Knee specimens were stored in a freezer at –20°C, and each specimen was thawed at room temperature 48 hours before dissection. The specimens were dissected until only the joint capsule remained, including the ligaments and the tendons of the quadriceps, hamstrings (medial and lateral), and gastrocnemii (medial and lateral). The dissected knee was stored in a freezer (–20°C) until testing. Each specimen was removed from the freezer and thawed at room temperature 24 hours before testing.

Immediately before testing, the femur and tibia were cut 20 cm proximal and distal of the joint line, respectively, to standardize the length of the specimen. Then, each bone extremity was potted in polymethylmethacrylate as previously described.[18]

Table 2.1 Demographic data of the donors of knee specimens tested[a]

Sex	Age (yrs)	Height (m)	Mass (kg)	BMI (kg/m^2)
Female (n=10[b])	55.2 ± 10.5	1.67 ± 0.06	60.5 ± 8.3	21.6 ± 3.1
Male (n=10[b])	59.9 ± 6.6	1.77 ± 0.05	81.3 ± 8.2	25.9 ± 2.3

[a]Values are represented as average ± 1 SD. BMI, body mass index.
[b]There were 10 knee specimens harvested from 6 donors.

Experimental Design and Protocol. A cross-sectional repeated-measures design (block order, A-B-C-D-E-A) (Table 2.2) was used to test the hypotheses. Each testing session began with five trials for which only an impulsive compression force and knee flexion moment were applied (i.e., no axial tibial torque) to precondition the knee specimen. After these preconditioning trials, the repeated-measures design, which consisted of six blocks of six trials, was executed. The first trial of each block served to precondition the knee, while the subsequent five trials were used for analysis. In block B, the femoral rotation device was locked, allowing minimal axial femoral rotation. In blocks C and D, the range of internal femoral rotation was limited by a hard stop to ~7° and ~11°, respectively. In block E, internal femoral rotation was not limited and achieved ~15°. The rationale for the selection of these particular ranges of rotation is given in the Discussion. A block of non-pivot trials (block A) was included both before and after the main testing sequence (blocks B-C-D-E) (Table 2.2), the data from which were used to ensure that the integrity of the knee specimens was not compromised during the testing protocol. The sequence of the main testing blocks (B-C-D-E) was randomized.

Table 2.2 Testing protocol for each block of trials[a]

Protocol Block	Loading Condition	Femoral Rotation
A	comp + flex m	N/A
B[b]	comp + flex m + int tib trq	locked
C[b]	comp + flex m + int tib trq	hard stop at ~7°
D[b]	comp + flex m + int tib trq	hard stop at ~11°
E[b]	comp + flex m + int tib trq	free
A	comp + flex m	N/A

[a]comp, compression force; flex m, flexion moment; int tib trq, internal tibial torque; N/A : not applicable.
[b]Randomized sequence.

Knee Testing Apparatus. The single-leg pivot landings were simulated with a modified Withrow-Oh apparatus,[26] which impacted the distal end of the tibia of an inverted knee specimen (Figure 2.1). Specifically, a weight (Figure 2.1, *W*) was dropped onto the distal end of the knee specimen in 15° of flexion from a height that would simulate an impulsive ground-reaction force of 2×BW (±10%). This height was determined by trial and error during the preconditioning trials. The impact of the weight on the distal end of the knee specimen induced an impulsive compression force and knee flexion moment, with and without internal tibial torque (pivot and non-pivot trials, respectively), that were measured by the proximal and distal 6-axis load cells (Figure 2.1, *L*). Internal tibial torque was developed by means of a tibial torsion device (Figure 2.1, *T*), which could be locked (without tibial torque) or unlocked (with tibial torque). When the tibial torsion device was unlocked, the apparatus applied a compressive force, flexion moment, and axial torque to the knee via the distal tibia. A novel addition to the apparatus was a proximal femoral rotation device (Figure 2.1, *R*) able to limit the range of axial femoral rotation. This device comprised a circular plate that rotated in the transverse plane on a tapered-roller bearing. Two pretensioned springs were attached tangentially to the perimeter of the plate via aircraft

cables to represent the tensile resistance of active external hip rotator muscles to rapid stretch during a pivot landing. To limit internal femoral rotation, a steel stop was inserted into a hole on the femoral rotation device to lock it (Table 2.2, block B) or abruptly halt rotation after ~7° (Table 2.2, block C) or ~11° (Table 2.2, block D) of internal femoral rotation. The goal of the stop was to mimic the bone-on-bone restriction in terminal hip motion secondary to FAI. The stop was removed from the device for the trials in block E (Table 2.2), during which femoral rotation was resisted by only the springs of the femoral device to represent the resistance of active pretensed hip muscles to axial femoral rotation without any bone-on-bone contact; hence, no hard stop was present. To simulate dynamic muscle tension and tensile resistance to stretch during the landing, tendons of the quadriceps (Figure 2.1, *Q*), medial and lateral hamstrings (Figure 2.1, *H*), and gastrocnemii (Figure 2.1, *G*) were attached via cryoclamps to elastic structures made of woven nylon cord. The tendon-muscle unit of the quadriceps was pretensioned to 180 N, while those of the hamstrings and gastrocnemii were pretensioned to 70 N before every trial.[26] Individual muscle tensions were measured at 2 kHz with five uniaxial load cells (Transducer Techniques) attached, in series, to the woven nylon cord and cryoclamps.

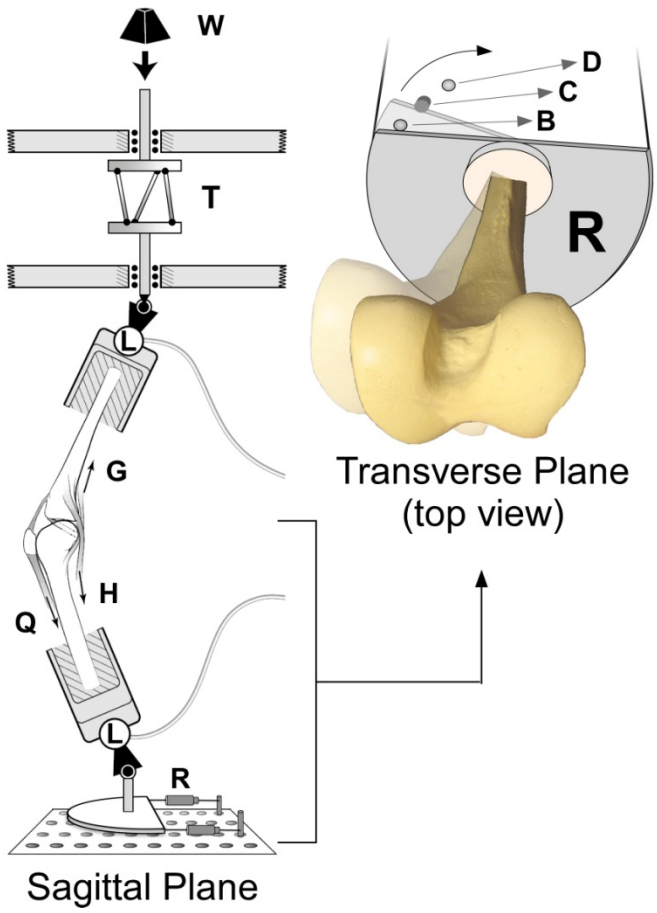

Figure 2.1 Sagittal-plane diagram (left) of the *in vitro* testing apparatus that simulated a single-leg pivot landing, with a top view (right) of the femoral rotation device, *R*. The solid portions represent the starting position of the specimen and device; meanwhile, the transparent portions represent their end position during a trial for which terminal internal femoral rotation was set to ~7° (block C of the testing protocol). *B*, position of steel stop for block B of the repeated-measures protocol (locked); *C*, position of steel stop for block C of the repeated-measures protocol (hard stop at ~11°); *G*, gastrocnemii tendons; *H*, hamstring tendons; *L*, 6-axis load cell; *Q*, quadriceps tendon; *R*, femoral rotation device; *T*, tibial torsion device; *W*, weight dropped. Note: positions of steel stops are not to scale to allow better visualization.

The 3-dimensional (3D) motions of the femur and tibia were quantified via infrared-emitting diodes tracked by an optoelectric imaging system (Optotrak Certus; Northern Digital) at 400 Hz. Three diodes were affixed to the femur segment and to the tibia segment such that they defined the three anatomic planes of the knee (sagittal, coronal, and transverse). The 3D coordinates of the diodes were used to calculate 3D angles and translations of the knee joint during each landing trials. Three-dimensional forces and moments produced at the distal tibia

and proximal femur were quantified via two 6-axis force sensors (Advanced Manufacturing Technology Inc) (Figure 2.1, *L*) at 2 kHz. Finally, a 3-mm differential variable reluctance transducer (DVRT; MicroStrain Sensing Systems) was affixed to the distal third portion of the AM bundle of the ACL to measure ligament elongation. Displacement data were recorded at 2 kHz.

Data Processing. Three-dimensional marker coordinates acquired from the motion capture system were low-pass filtered with a Butterworth filter (4th order, 20-Hz cutoff frequency). From the 3D coordinates of the six markers as well as those of the knee's origin (roof of the femoral notch digitized before the landing trials), 3D angles and translations were calculated via the method established by Grood and Suntay.[9] Femoral rotation was defined as rotation of the femur relative to the testing apparatus, whereas tibial rotation was defined as rotation of the tibia relative to the femur. Data acquired from all load cells, as well as the elongation data acquired from the DVRT, were also low-pass filtered with a Butterworth filter (4th order, 70-Hz cutoff frequency). The AM-ACL relative strain (ε) was quantified as $\varepsilon = (L - L_0) / L_0 \times 100$, where L_0 is the reference interbarb distance of the DVRT and L is the instantaneous interbarb distance of the DVRT. The reference length (L_0) was defined as the interbarb distance of the DVRT at the beginning of each trial.

From each trial, peak AM-ACL relative strain was extracted as the main dependent variable of interest. Range of internal femoral rotation was set as the independent variable. Last, femoral rotational stiffness, range of anterior tibial translation, range of internal tibial rotation, peak internal tibial deceleration, and difference between time-to-peak internal tibial and femoral rotations were obtained to gain further insight into differences in peak AM-ACL relative strain between femoral rotation conditions. A positive value for difference between time-to-peak

rotations indicated that peak internal femoral rotation occurred before peak internal tibial rotation, whereas a negative value indicated that peak internal tibial rotation occurred first.

Statistical Analysis. The hypotheses were tested with a linear mixed model, with *range of internal femoral rotation*, *sex of donor*, and *age* treated as fixed effects and *knee specimen* and *knee donor* as random effects. Age was included in the model to account for differences in this variable between the male and female donors given that the tensile properties of the ACL (e.g., linear stiffness) have been reported to decrease significantly with age.[45] Knee donor was included in the model to account for the correlation between paired specimens. The model determined whether a significant inverse (linear) relation existed between peak AM-ACL relative strain and range of internal femoral rotation. The proportion of variance explained by the full model, R^2, was quantified with a method recommended by Nakagawa and Schielzeth.[24] The model also compared peak AM-ACL relative strain between the female and male knee specimens. An alpha level below 0.05 indicated statistical significance.

Lower Limb Computational Model. To help interpret our findings from a biomechanical perspective, we developed a simple computer simulation of an axial impulsive torque applied distally to a lower extremity having segmental inertias (see Appendix A). Briefly, the lower limb, consisting of a foot, tibia, and femur, was represented by three rigid bodies connected by torsional springs to represent the axial rotational stiffnesses of the ankle, knee, and hip passive structures and active muscles. To represent the transverse-plane mechanics of a pivot landing, an axial impulsive torque of 10 N·m was applied in the transverse plane, over 80 milliseconds, orthogonal to the longitudinal axis of the foot to create foot angular momentum (see Results). The stiffness of the spring representing the hip was then systematically increased from 0.9 to 9.4 N·m/deg in separate trials to cause a systematic decrease in femoral rotation. For each trial, the

magnitude and timing of peak intersegmental rotations were then calculated over the first 200 milliseconds. Tibial rotation, relative to the femur, in the transverse plane was then calculated as an outcome measure.

2.4 Results

The temporal behavior of the variables from a representative trial for each axial femoral rotation condition is presented in Figure 2.2. For the axial femoral rotation conditions where rotation was abruptly limited to ~7° and ~11°, the slope of the axial femoral torque curves revealed that the femoral rotation device adequately modeled a hard stop with a bilinear stiffness response (Figure 2.2, B-1 and C-1). Specifically, there was low rotational stiffness within the available range of motion, with a sudden increase in stiffness at the limit of motion (i.e., when the femoral rotation device hit the stop). In contrast, the conditions during which axial femoral rotation was either locked or free, a linear stiffness response was observed, with the free rotation condition presenting with a more compliant response (Figure 2.2, A-1 and D-1).

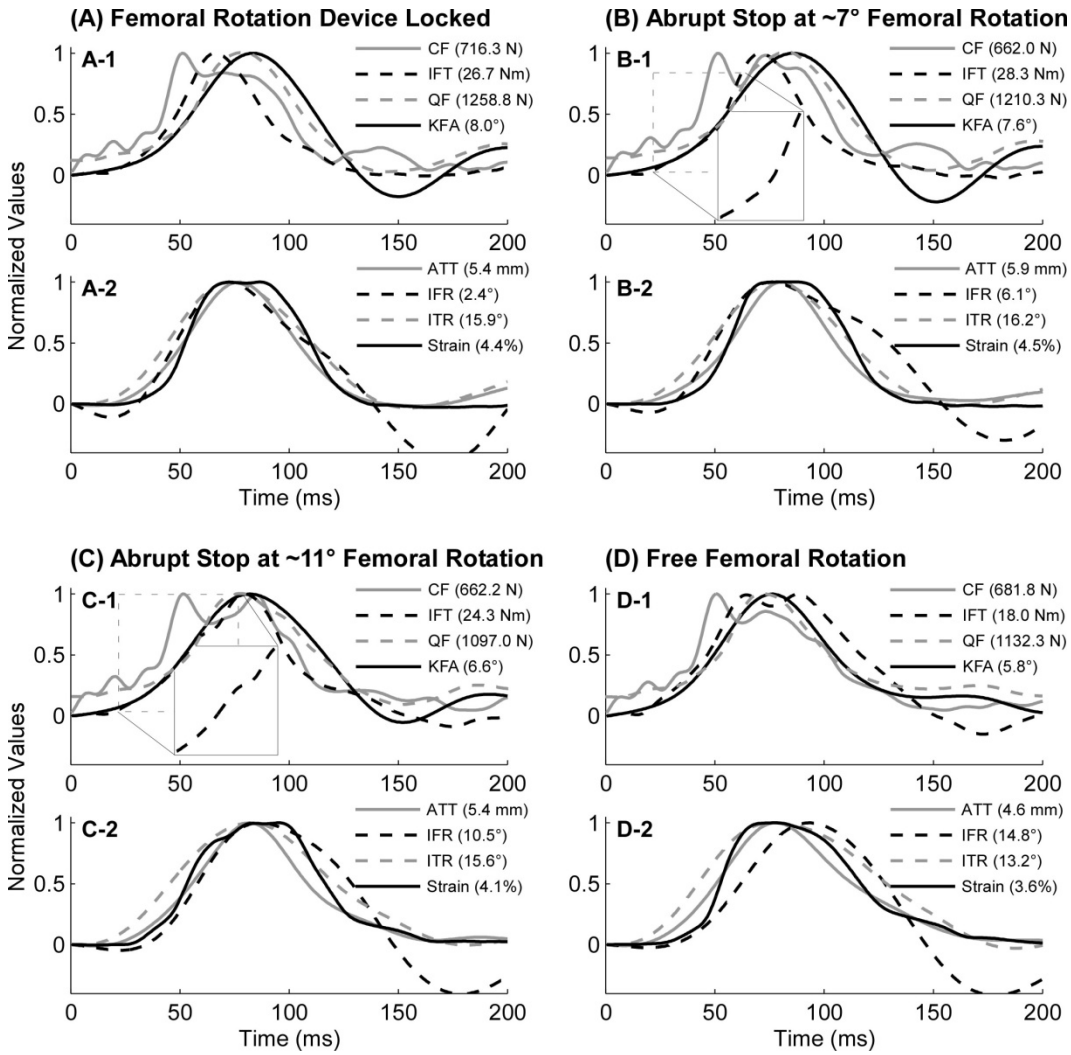

Figure 2.2 Sample temporal plots of a representative trial for each axial femoral rotation condition: (**A**) femoral rotation locked; (**B**) hard stop at ~7° of rotation; (**C**) hard stop at ~11° of rotation; and (**D**) free femoral rotation. Subplots display (1) compressive force (CF), internal femoral torque (IFT), quadriceps force (QF), and knee flexion angle (KFA) and (2) anterior tibial translation (ATT), internal femoral rotation (IFR), internal tibial rotation (ITR), and relative strain of the anteromedial bundle of the anterior cruciate ligament during a cadaver-simulated single-leg pivot landing. Insets in B-1 and C-1 indicate portions of the internal femoral torque curve showing the bilinear stiffness response because of the hard stop. All data are from one knee specimen (ID No. 20686R). Data are normalized to their peak values (values in parentheses).

Peak AM-ACL relative strain was inversely proportional to internal femoral rotation during the simulated single-leg pivot landings ($p < 0.001$) (Figure 2.3). Peak AM-ACL relative strain was generally largest when the range of internal femoral rotation was abruptly arrested

after ~7° and 28.4% larger when femoral rotation was locked than when it was free. Furthermore, strong positive relations were also found between peak ACL relative strain and femoral rotational stiffness ($p < 0.001$) (Figure 2.4A), range of anterior tibial translation ($p < 0.001$) (Figure 2.4B), range of internal tibial rotation ($p < 0.001$) (Figure 2.4C), peak internal tibial deceleration ($p < 0.001$) (Figure 2.4D), and the difference between time-to-peak internal tibial and femoral rotations ($p < 0.001$) (Figure 2.4E). Peak ACL relative strain increased as each of these variables increased with decreasing femoral internal rotation.

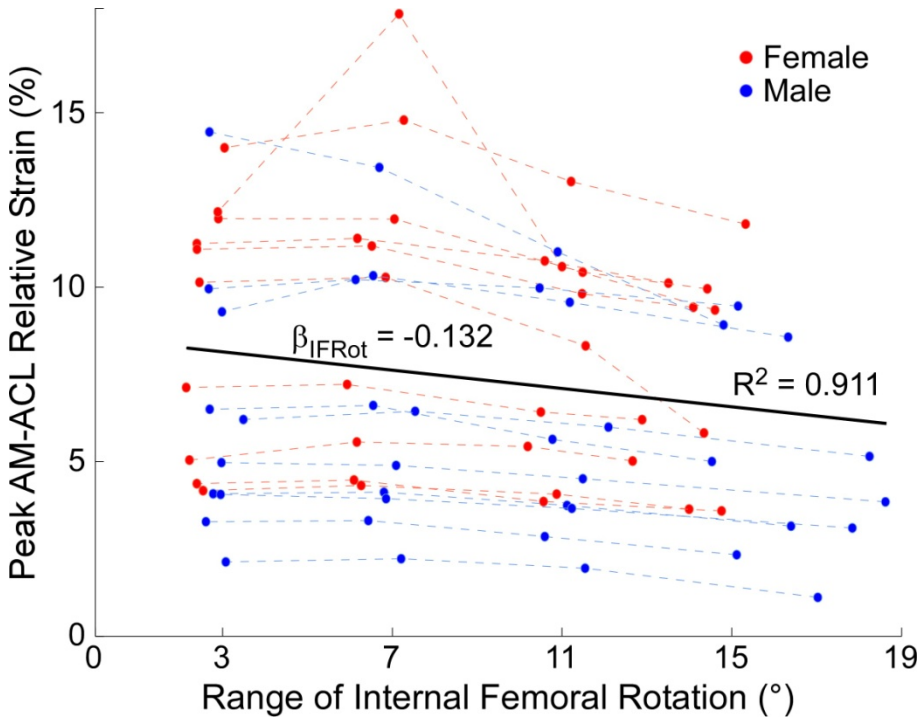

Figure 2.3 Scatter plot of peak relative strain of the anteromedial bundle of the anterior cruciate ligament (AM-ACL) versus range of internal femoral rotation quantified for 20 knees under four axial femoral rotation conditions (rotation locked, hard stop at ~7° of rotation, hard stop at ~11° of rotation, no sudden stop in rotation) during the pivot landings. Data points from the same knee specimen are connected with a dashed line. The solid line represents the line of best fit of the full linear mixed model, with a slope (β_{IFRot}) of –0.132, which explained 91% of the variance in the peak AM-ACL relative strain data. This model predicted peak ACL relative strain with range of hip internal rotation, sex, and age of knee donor as fixed effects and with knee specimen and knee donor as random effects. IFRot, internal femoral rotation.

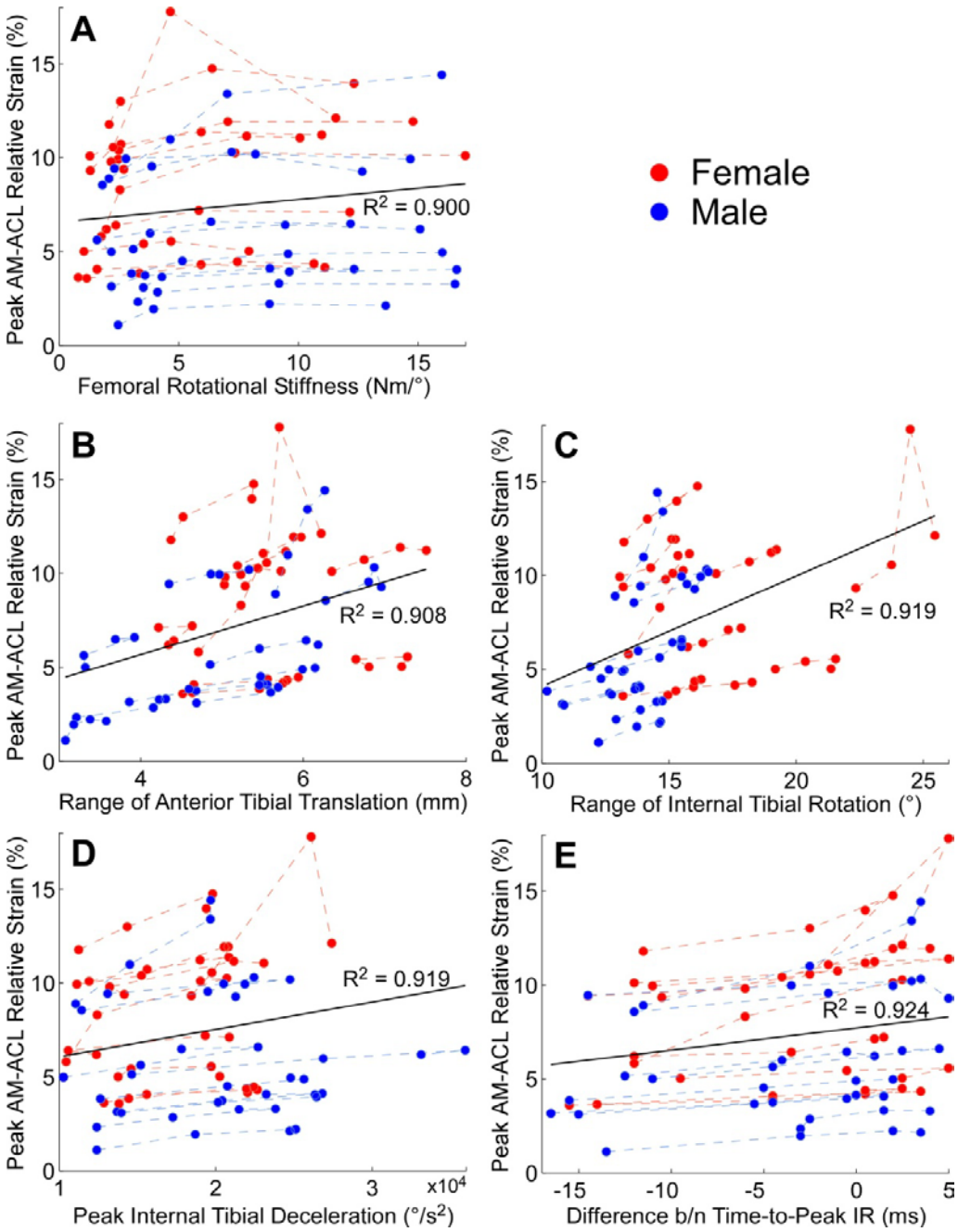

Figure 2.4 Scatter plots of peak relative strain of the anteromedial bundle of the anterior cruciate ligament (AM-ACL) versus (**A**) femoral rotational stiffness (**B**) range of anterior tibial translation, (**C**) range of internal tibial rotation, (**D**) peak internal tibial deceleration, and (**E**) difference between time-to-peak internal tibial and femoral rotations quantified for 20 knees under four axial femoral rotation conditions (rotation locked, hard stop at ~7° of rotation, hard stop at ~11° of rotation, no hard stop in rotation) during the pivot landings. In plot E, a negative value indicates that peak internal tibial rotation is occurring before peak internal femoral rotation, and vice versa. Data points from the same knee specimen are connected with a dashed line. The solid lines represent the lines of best fit of the full linear mixed models, including their corresponding R^2 values. IR, internal rotation.

The transverse-plane mechanics of the lower limb computational model revealed that as femoral rotation decreased, tibial rotation and torque (relative to the femur) increased (Figure 2.5C). The model also showed an increase in the difference in time-to-peak tibial rotation (relative to the femur) and time-to-peak femoral rotation with decreasing hip resistance (k_{Hip}), as found in the *in vitro* data (Figure 2.5D).

The female ACL experienced greater peak strain, in comparison to the male ACL, during the pivot landings. On average, peak AM-ACL relative strain was 45% larger in the female knee specimens than the male specimens, regardless of axial femoral rotation condition (8.69% ± 3.46% vs. 6.00% ± 3.35%; $p = 0.003$) (Figure 2.3). However, restricting femoral range of rotation did not appear to differentially affect the female knee specimens more than the male knee specimens (Figure 2.3).

Last, no differences in peak AM-ACL relative strain were found between the two non-pivot blocks of trials (Table 2.2, block A), which occurred before and after the experimental blocks (before: 3.78 ± 2.03% vs. after: 3.52 ± 1.90%; $p = 0.106$). That result confirmed that the integrity of the knee specimens was not compromised during the testing protocol.

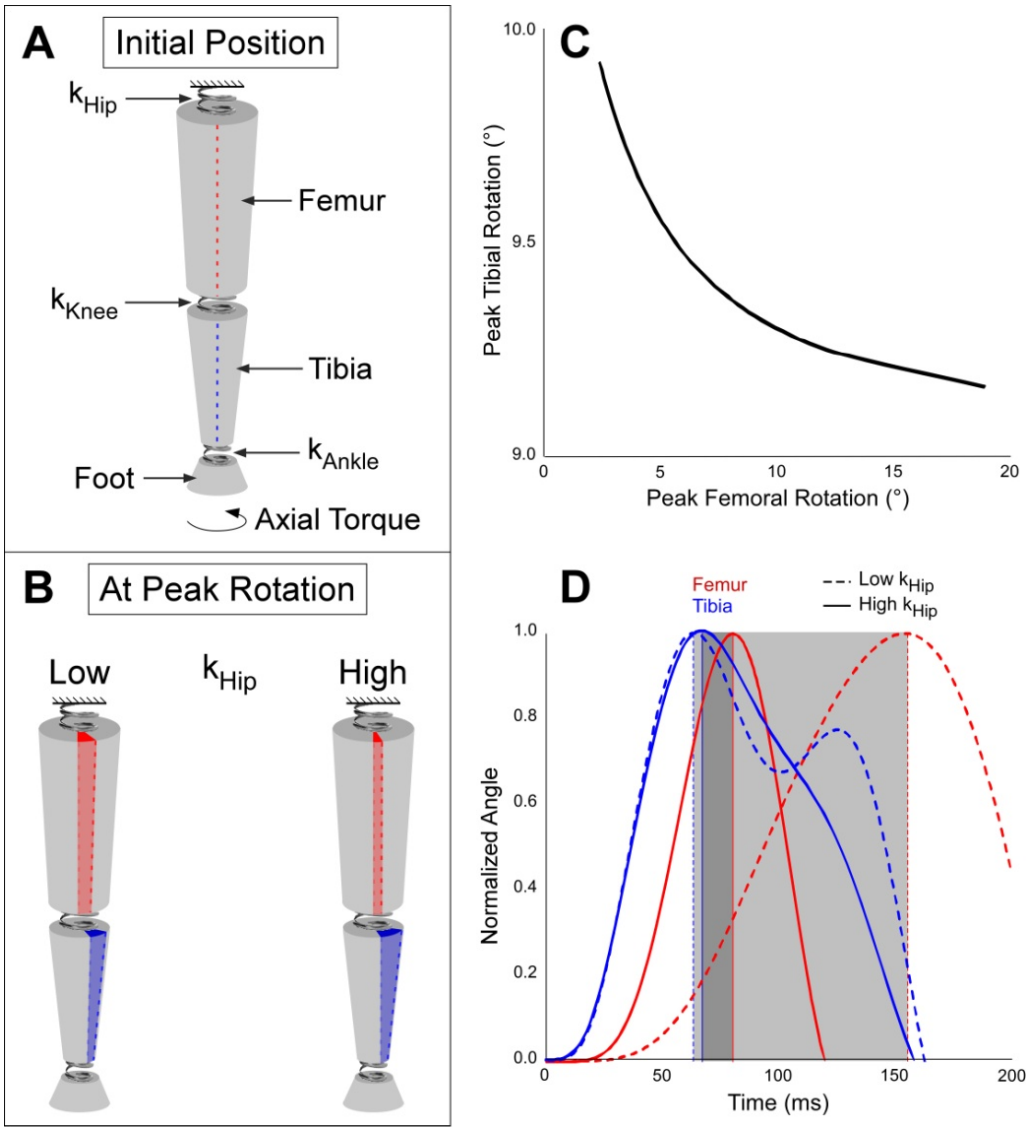

Figure 2.5 Simulation of axial impulsive torque applied distally to a simple lower limb model, including resulting mechanics. (A) The lower limb was modeled with three rigid bodies (femur, tibia, foot) attached to each other by springs (k_{Knee}, k_{Ankle}). The end of a third spring (k_{Hip}) was attached to the femur, with its other end fixed. The torsional stiffness of k_{Hip} was systematically varied, while that of k_{Knee} and k_{Ankle} remained constant. An axial torque of 10 Nm was applied to the foot. (B) With a compliant spring (i.e., low k_{Hip} stiffness), larger peak femoral rotation and smaller peak tibial rotation were observed. Femoral rotation peaked shortly after tibial rotation, as shown in D (dark gray shaded area). In comparison, a stiff spring (i.e., high k_{Hip} stiffness) resulted in smaller peak femoral rotation and larger tibial rotation. Femoral rotation peaked much longer after tibial rotation, as shown in D (light gray shaded area). This difference in time-to-peak tibial and femoral rotation is shown in D as the gray shaded areas between the vertical lines, which represent time of peak rotation for each segment and condition. (C) As peak femoral rotation increased, peak tibial rotation decreased. Note: femoral rotation is defined as the absolute angle of the femur, whereas tibial rotation is defined as the angle of the tibia relative to the femur.

2.5 Discussion

This study presents a cause-and-effect relation between limiting internal femoral rotation and ACL strain during dynamic 3D knee loading. The literature reveals a relation between range of passive axial hip motion and ACL injury risk.[2,6] It is not clear, however, whether a lack of range of hip motion leads to an increase in risk of ACL injury or whether an ACL injury leads to a decrease in range of hip motion.[6] Furthermore, previous work did not show, or even speculate, how decreased hip internal rotation may increase ACL injury risk. Our results suggest that when the range of hip rotation is abruptly limited by a hard stop (modeling FAI), peak ACL strain increases and thus ACL injury risk during athletic maneuvers such as single-leg pivot landings.

Our primary hypothesis—that peak AM-ACL relative strain would increase as the range of internal femoral rotation decreased—was supported. According to our statistical model, peak ACL relative strain increased 1.3% with every 10° decrease in femoral rotation with a hard stop. Given an average range of internal femoral rotation of 15° upon landing,[11] this amounts to a 20% relative increase in peak ACL strain. For example, an athlete presenting with FAI with a 10° deficiency in internal femoral rotation would systematically experience 20% more peak ACL strain during a landing than a healthy athlete.

Because we limited the range of internal femoral rotation by adding a hard stop to our *in vitro* landing to simulate the most commonly observed scenario of FAI or femoral retroversion, we believe that it is the result of the increase in femoral rotation stiffness (via the stop, which abruptly decreased axial femoral rotation), the increase in peak internal tibial deceleration, and the increase in the timing difference between peak internal tibial and femoral rotations that caused the increase in peak ACL strain. As illustrated in Figure 2.4A, peak ACL relative strain increased as femoral rotational stiffness increased. Also, abruptly arresting internal femoral

rotation appears to cause internal femoral rotation to reach its terminal range of motion sooner in relation to internal tibial rotation and peak internal tibial deceleration to increase, thereby increasing internal tibia rotation and coupled anterior tibial translation, and thus peak ACL relative strain (Figure 2.4, B-E). This explains why peak AM-ACL relative strain was generally largest when the range of internal femoral rotation was abruptly arrested after ~7°, not when it was locked. When femoral rotation was limited to ~7°, peak internal tibial deceleration and the difference in time-to-peak internal tibial and femoral rotations had, on average, the greatest values.

The increase in anterior tibial translation with decreasing internal femoral rotation was most likely due to coupled tibial motion of this translation with axial tibial rotation,[20,28] as well as an increase in peak quadriceps force. In part because of the geometry of the tibial plateau, including the larger posteriorly directed slope of the lateral plateau in comparison with the medial plateau,[12] the center of axial rotation is located in the knee's medial compartment.[22,25] As the tibia rotates internally in relation to the femur under a compressive load and an internal tibial torque, the lateral plateau and geometric center of the plateau translate anteriorly, thus producing both internal tibial rotation and anterior tibial translation. In addition to this coupled tibial motion, the quadriceps force, whose peak increased 148 N, or 12% on average from the free to the locked femoral internal rotation condition, may have played a role in the increase in anterior tibial translation via the patellofemoral reaction force. Given that anterior tibial translation and internal tibial rotation are known to strain the ACL, it is likely that this increase in axial rotation and translation at the knee joint caused the increase in measured peak ACL strain. We acknowledge that, *in vivo*, various combinations of forces and torques can contribute to an

increase in peak ACL strain and to ACL injury and that the mechanism simulated herein represents one sequence of events.

Our interpretation of the *in vitro* knee mechanics during the pivot landings was supported by the lower limb model simulations (Figure 2.5 and Appendix A). The 3–rigid body computational model clearly illustrates how decreasing axial femoral rotation, by increasing the torsional spring stiffness representing the hip joint, increased peak tibial rotation in relation to the femoral segment. With a compliant spring, the femur reached the terminal range of motion long after the tibia did in relation to the femur. As spring stiffness was increased, time to terminal range of axial motion of the femur approached that of the tibia, thereby producing greater rotation at the torsional spring representing the knee.

Our secondary hypothesis that the female ACL would exhibit greater peak strain than the male ACL, regardless of the range of internal femoral rotation, was also accepted. Differences in peak ACL relative strain under similar relative loads (i.e., %BW) between sexes are likely a contributing factor to the higher ACL injury rate in women.[41] These sex-based differences in ACL strain were likely attributed to sexual dimorphism in ACL size and/or knee joint structure given that the initial knee kinematics and knee loading conditions, including muscle preloads, were not simulated differently for the female and male knee specimens. In a recent study, Lipps et al.[17] found the smaller cross-sectional area of the female ACL and the steeper posteriorly directed slope of the female lateral tibial plateau to be mainly responsible for sex differences in peak AM-ACL relative strain in knee specimens subjected to a similar impulsive loading scenario. In addition to its smaller size, the female ACL has a lower strain to failure, stress at failure, and modulus of elasticity,[5] which are most likely due to ultrastructural differences.[13]

Without accounting for sex differences in neuromuscular control, it appears that the female ACL is at greater risk of injury owing, in part, to greater peak ACL strain than the male ACL.

The four conditions of internal femoral rotation were selected to include values ranging from minimal femoral rotation (Table 2.2, block B) to free femoral rotation (Table 2.2, block E). The range of internal femoral rotation of this latter condition was based on Hart et al.,[11] who reported an average of 14.9° of hip internal rotation in female and male collegiate soccer players during a single-leg landing. The values selected for blocks B through D allowed for a relation between range of internal femoral rotation and peak AM-ACL strain to be established without compromising the integrity of the ACL by executing too many loading trials. The values were selected to provide a spectrum of limited ranges of rotation.

Several limitations of the present study are acknowledged. First, knee specimens from older donors were tested. Results therefore cannot necessarily be generalized to younger populations, in which ACL injuries occur most frequently.[36] We believe, however, that similar qualitative results would be found in younger specimens, even if the quantitative results would most likely differ owing to changes in structural and mechanical properties of the ACL with age.[45] Second, relative strain was measured only in the distal third of the AM bundle of the ACL. It was not possible to attach an additional DVRT to the posterolateral bundle without compromising the integrity of the knee joint, especially the posterior joint capsule, or causing measurement error because of contact between the strain transducer and the knee structures. Previous work has demonstrated, however, that strain measured in the AM bundle of the ACL is representative of that in the entire ligament.[3,4,19] Third, absolute ACL strain could not be measured, but rather relative strain was quantified and compared between conditions. Given that the preloading condition and initial knee specimen position were the same for all internal femoral

rotation conditions, we believe that peak AM-ACL relative strain did indeed allow for valid intra-condition peak strain comparison. In addition, the sequence of the internal femoral rotation conditions was randomized, which eliminated any effect that previous conditions may have had on the reference interbarb distance of the DVRT. Fourth, an ankle joint was not included in our cadaveric model. The loads induced at the distal tibia by the simulated landing may therefore be overestimated because the ankle joint can absorb energy during the landing.[35] In our opinion, the lack of an ankle joint actually strengthens this study because it allows one to minimize confounding variables in the cadaveric model. Fifth, although tension of the major knee muscles and their tensile resistance to stretch during the landing were represented in the *in vitro* model, only their monoarticular actions were simulated (along with the monoarticular actions of the hip external rotator muscles). Sixth, this work addresses only the effect of limited range of internal femoral rotation because of a sudden stop, as someone with FAI may experience because of bone-on-bone contact. It does not simulate limited rotation because of a volitional increase in muscle tension during the rotation, for example, which may cause a smaller peak internal tibial deceleration as the femur encounters increasing resistance to internal rotation. Last, an interaction term was not included in our statistical model to evaluate whether the effect of the range of femoral internal rotation on peak AM-ACL strain was dependent on sex of the donor. We did not want to decrease the statistical power of our model by including such a term, because this was beyond the scope of this study. Also, data presented in Figure 2.3 provide no qualitative evidence that such an interaction exists.

There are two clinical implications from our study. First, it matters where the femur is in its range of internal femoral rotation when ground contact occurs during a landing or cut maneuver. The closer the femur is to its terminal range of internal rotation, the more likely it is

that bone-on-bone contact will occur between the femur and the acetabular rim, thereby decreasing femoral rotation and increasing peak ACL strain. This may offer justification for physical therapy for FAI and rehabilitation to improve the functional range of motion available at the hip even in the absence of surgical correction of the deformity. Second, screening for restricted internal rotation at the hip is advisable for ACL injury prevention programs, as well as for evaluation protocols in individuals with ACL injuries and/or reconstructions. With a simple examination of passive internal hip range of motion before preseason training, at-risk athletes could be identified and targeted for injury prevention interventions. Future research might translate our *in vitro* findings *in vivo* by prospectively confirming limited hip internal rotation as a risk factor for ACL injury.

2.6 Conclusion

Peak AM-ACL relative strain during *in vitro* pivot landings was inversely related to the available range of internal femoral rotation.

2.7 References

1. Beck M, Kalhor M, Leunig M, Ganz R. (2005) Hip morphology influences the pattern of damage to the acetabular cartilage: femoroacetabular impingement as a cause of early osteoarthritis of the hip. *J Bone Joint Surg Br*, 87(7): 1012-8.

2. Bedi A, Warren RF, Wojtys EM, Oh YK, Ashton-Miller JA, Oltean H, Kelly BT. (2014) Restriction in hip internal rotation is associated with an increased risk of ACL injury. *Knee Surg Sports Traumatol Arthrosc*, Sept 12. [Epub ahead of print].

3. Beynnon BD, Fleming BC. (1998) Anterior cruciate ligament strain in-vivo: a review of previous work. *J Biomech*, 31(6): 519-25.

4. Butler DL, Kay MD, Stouffer DC. (1986) Comparison of material properties in fascicle-bone units from human patellar tendon and knee ligaments. *J Biomech*, 19(6): 425-32.

5. Chandrashekar N, Mansouri H, Slauterbeck J, Hashemi J. (2006) Sex-based differences in the tensile properties of the human anterior cruciate ligament. *J Biomech*, 39(16): 2943-50.

6. Ellera Gomes JL, de Castro JV, Becker R. (2008) Decreased hip range of motion and noncontact injuries of the anterior cruciate ligament. *Arthroscopy*, 24(9): 1034-7.

7. Ellera Gomes JL, Palma HM, Becker R. (2010) Radiographic findings in restrained hip joints associated with ACL rupture. *Knee Surg Sports Traumatol Arthrosc*, 18(11): 1562-7.

8. Ellera Gomes JL, Palma HM, Ruthner R. (2014) Influence of hip restriction on noncontact ACL rerupture. *Knee Surg Sports Traumatol Arthrosc*, 22(1): 188-91.

9. Grood ES, Suntay WJ. (1983) A joint coordinate system for the clinical description of three-dimensional motions: application to the knee. *J Biomech Eng*, 105(2): 136-44.

10. Hack K, Di Primio G, Rakhra K, Beaule PE. (2010) Prevalence of cam-type femoroacetabular impingement morphology in asymptomatic volunteers. *J Bone Joint Surg Am*, 92(14): 2436-44.

11. Hart JM, Garrison JC, Palmieri-Smith R, Kerrigan DC, Ingersoll CD. (2008) Lower extremity joint moments of collegiate soccer players differ between genders during a forward jump. *J Sport Rehabil*, 17(2): 137-47.

12. Hashemi J, Chandrashekar N, Mansouri H, Gill B, Slauterbeck JR, Schutt RC, Jr., Dabezies E, Beynnon BD. (2010) Shallow medial tibial plateau and steep medial and lateral tibial slopes: new risk factors for anterior cruciate ligament injuries. *Am J Sports Med*, 38(1): 54-62.

13. Hashemi J, Chandrashekar N, Mansouri H, Slauterbeck JR, Hardy DM. (2008) The human anterior cruciate ligament: sex differences in ultrastructure and correlation with biomechanical properties. *J Orthop Res*, 26(7): 945-50.

14. Jung KA, Restrepo C, Hellman M, AbdelSalam H, Morrison W, Parvizi J. (2011) The prevalence of cam-type femoroacetabular deformity in asymptomatic adults. *J Bone Joint Surg Br*, 93(10): 1303-7.

15. Kristianslund E, Krosshaug T. (2013) Comparison of drop jumps and sport-specific sidestep cutting: implications for anterior cruciate ligament injury risk screening. *Am J Sports Med*, 41(3): 684-688.

16. Laborie LB, Lehmann TG, Engesaeter IO, Eastwood DM, Engesaeter LB, Rosendahl K. (2011) Prevalence of radiographic findings thought to be associated with femoroacetabular impingement in a population-based cohort of 2081 healthy young adults. *Radiology*, 260(2): 494-502.

17. Lipps DB, Oh YK, Ashton-Miller JA, Wojtys EM. (2012) Morphologic characteristics help explain the gender difference in peak anterior cruciate ligament strain during a simulated pivot landing. *Am J Sports Med*, 40(1): 32-40.

18. Lipps DB, Wojtys EM, Ashton-Miller JA. (2013) Anterior cruciate ligament fatigue failures in knees subjected to repeated simulated pivot landings. *Am J Sports Med*, 41(5): 1058-66.

19. Markolf KL, Gorek JF, Kabo JM, Shapiro MS. (1990) Direct measurement of resultant forces in the anterior cruciate ligament. An in vitro study performed with a new experimental technique. *J Bone Joint Surg Am*, 72(4): 557-67.

20. Markolf KL, Jackson SR, Foster B, McAllister DR. (2014) ACL forces and knee kinematics produced by axial tibial compression during a passive flexion-extension cycle. *J Orthop Res*, 32(1): 89-95.

21. McCarthy MM, Voos JE, Nguyen JT, Callahan L, Hannafin JA. (2013) Injury profile in elite female basketball athletes at the Women's National Basketball Association combine. *Am J Sports Med*, 41(3): 645-651.

22. Meyer EG, Haut RC. (2008) Anterior cruciate ligament injury induced by internal tibial torsion or tibiofemoral compression. *J Biomech*, 41(16): 3377-83.

23. Monazzam S, Bomar JD, Dwek JR, Hosalkar HS, Pennock AT. (2013) Development and prevalence of femoroacetabular impingement-associated morphology in a paediatric and adolescent population: a CT study of 225 patients. *Bone Joint J*, 95-B(5): 598-604.

24. Nakagawa S, Schielzeth H. (2013) A general and simple method for obtaining R2 from generalized linear mixed-effects models. *Methods Ecol Evol*, 4(2): 133-142.

25. Noyes FR. (2009) The function of the human anterior cruciate ligament and analysis of single- and double-bundle graft reconstructions. *Sports Health*, 1(1): 66-75.

26. Oh YK, Kreinbrink JL, Ashton-Miller JA, Wojtys EM. (2011) Effect of ACL transection on internal tibial rotation in an in vitro simulated pivot landing. *J Bone Joint Surg Am*, 93(4): 372-80.

27. Oh YK, Kreinbrink JL, Wojtys EM, Ashton-Miller JA. (2012) Effect of axial tibial torque direction on ACL relative strain and strain rate in an in vitro simulated pivot landing. *J Orthop Res*, 30(4): 528-34.

28. Oh YK, Lipps DB, Ashton-Miller JA, Wojtys EM. (2012) What strains the anterior cruciate ligament during a pivot landing? *Am J Sports Med*, 40(3): 574-83.

29. Oiestad BE, Holm I, Aune AK, Gunderson R, Myklebust G, Engebretsen L, Fosdahl MA, Risberg MA. (2010) Knee function and prevalence of knee osteoarthritis after anterior cruciate ligament reconstruction: a prospective study with 10 to 15 years of follow-up. *Am J Sports Med*, 38(11): 2201-10.

30. Oiestad BE, Holm I, Engebretsen L, Aune AK, Gunderson R, Risberg MA. (2013) The prevalence of patellofemoral osteoarthritis 12 years after anterior cruciate ligament reconstruction. *Knee Surg Sports Traumatol Arthrosc*, 21(4): 942-9.

31. Philippon M, Dewing C, Briggs K, Steadman JR. (2012) Decreased femoral head-neck offset: a possible risk factor for ACL injury. *Knee Surg Sports Traumatol Arthrosc*, 20(12): 2585-9.

32. Reichenbach S, Juni P, Werlen S, Nuesch E, Pfirrmann CW, Trelle S, Odermatt A, Hofstetter W, Ganz R, Leunig M. (2010) Prevalence of cam-type deformity on hip magnetic resonance imaging in young males: a cross-sectional study. *Arthritis Care Res (Hoboken)*, 62(9): 1319-27.

33. Riordan EA, Frobell RB, Roemer FW, Hunter DJ. (2013) The health and structural consequences of acute knee injuries involving rupture of the anterior cruciate ligament. *Rheum Dis Clin North Am*, 39(1): 107-22.

34. Schambra HM, Abe M, Luckenbaugh DA, Reis J, Krakauer JW, Cohen LG. (2011) Probing for hemispheric specialization for motor skill learning: a transcranial direct current stimulation study. *J Neurophysiol*, 106(2): 652-61.

35. Self BP, Paine D. (2001) Ankle biomechanics during four landing techniques. *Med Sci Sports Exerc*, 33(8): 1338-44.

36. Shea KG, Pfeiffer R, Wang JH, Curtin M, Apel PJ. (2004) Anterior cruciate ligament injury in pediatric and adolescent soccer players: an analysis of insurance data. *J Pediatr Orthop*, 24(6): 623-8.

37. Shin CS, Chaudhari AM, Andriacchi TP. (2011) Valgus plus internal rotation moments increase ACL strain more than either alone. *Med Sci Sports Exerc*, 43(8): 1484-91.

38. Shultz SJ, Schmitz RJ, Benjaminse A, Chaudhari AM, Collins M, Padua DA. (2012) ACL Research Retreat VI: an update on ACL injury risk and prevention. *J Athl Train*, 47(5): 591-603.

39. Swenson DM, Collins CL, Best TM, Flanigan DC, Fields SK, Comstock RD. (2013) Epidemiology of knee injuries among US high school athletes, 2005/06-2010/11. *Med Sci Sports Exerc*, 45(3): 462-9.

40. Torry MR, Shelburne KB, Myers C, Giphart JE, Pennington WW, Krong JP, Peterson DS, Steadman JR, Woo SL. (2013) High knee valgus in female subjects does not yield higher knee translations during drop landings: A biplane fluoroscopic study. *J Orthop Res*, 31(2): 257-67.

41. Walden M, Hagglund M, Werner J, Ekstrand J. (2011) The epidemiology of anterior cruciate ligament injury in football (soccer): a review of the literature from a gender-related perspective. *Knee Surg Sports Traumatol Arthrosc*, 19(1): 3-10.

42. Withrow TJ, Huston LJ, Wojtys EM, Ashton-Miller JA. (2006) The effect of an impulsive knee valgus moment on in vitro relative ACL strain during a simulated jump landing. *Clin Biomech (Bristol, Avon)*, 21(9): 977-83.

43. Withrow TJ, Huston LJ, Wojtys EM, Ashton-Miller JA. (2006) The relationship between quadriceps muscle force, knee flexion, and anterior cruciate ligament strain in an in vitro simulated jump landing. *Am J Sports Med*, 34(2): 269-74.

44. Withrow TJ, Huston LJ, Wojtys EM, Ashton-Miller JA. (2008) Effect of varying hamstring tension on anterior cruciate ligament strain during in vitro impulsive knee flexion and compression loading. *J Bone Joint Surg Am*, 90(4): 815-23.

45. Woo SL, Hollis JM, Adams DJ, Lyon RM, Takai S. (1991) Tensile properties of the human femur-anterior cruciate ligament-tibia complex. The effects of specimen age and orientation. *Am J Sports Med*, 19(3): 217-25.

46. Wordeman SC, Quatman CE, Kaeding CC, Hewett TE. (2012) In vivo evidence for tibial plateau slope as a risk factor for anterior cruciate ligament injury: a systematic review and meta-analysis. *Am J Sports Med*, 40(7): 1673-81.

47. Yamazaki J, Muneta T, Ju YJ, Morito T, Okuwaki T, Sekiya I. (2011) Hip acetabular dysplasia and joint laxity of female anterior cruciate ligament-injured patients. *Am J Sports Med*, 39(2): 410-4.

CHAPTER 3

RISK OF ACL FATIGUE FAILURE IS INCREASED BY LIMTIED INTERNAL FEMORAL ROTATION DURING IN VITRO REPEATED PIVOT LANDINGS

This chapter has been submitted for consideration of publication:

Beaulieu ML, Wojtys EM, Ashton-Miller JA. *Am J Sports Med*. [In review]

3.1 Abstract

A reduced range of hip internal rotation is associated with increased peak ACL strain and risk for injury. It is unknown, however, whether limiting the available range of internal femoral rotation increases the susceptibility of the ACL to fatigue failure. The purpose of this study was to determine the effect of limited range of internal femoral rotation, sex, femoral-ACL attachment angle, and tibial eminence volume on *in vitro* ACL fatigue life during repeated simulated single-leg pivot landings.

A custom-built testing apparatus was used to simulate repeated single-leg pivot landings with a 4-bodyweight impulsive load that induces knee compression, knee flexion and internal tibial torque in 32 paired human knee specimens (16 females). These test loads were applied to each pair of specimens, with one knee with limited internal femoral rotation and the contralateral knee with femoral rotation only resisted by two springs to simulate the active hip rotator muscles' resistance to stretch. The landings were repeated until ACL failure occurred or until a minimum of 100 trials were executed. The angle at which the ACL originates from the femur and the tibial eminence volume were measured on magnetic resonance images.

The final Cox regression model ($p = 0.024$) revealed that range of internal femoral rotation and sex of donor were important factors in determining risk of an ACL fatigue failure. The specimens with limited range of internal femoral rotation had a failure risk 17.1 times higher than the specimens with free rotation ($p = 0.016$). The female knee specimens had a risk of ACL failure 26.9 times higher than the male specimens ($p = 0.055$).

Knee specimens with limited range of internal femoral rotation during repetitive *in vitro* pivot landings had a risk of ACL fatigue failure much greater than those with free rotation. Screening for restricted internal rotation at the hip in ACL injury prevention programs as well as in individuals with ACL injuries and/or reconstructions is warranted.

3.2 Introduction

Injuries to the anterior cruciate ligament (ACL) continue to pose significant health and financial burdens due to their short- and long-term consequences,[25] especially in young females who are at greater risk of ACL injury.[34] Although research has long been directed at elucidating noncontact ACL injury mechanism(s), the role of repetitive loading has received little attention.[28] Many joints in the human body are susceptible to repetitive loading injuries, including the wrist,[10] shoulder,[3] elbow,[9] intervertebral disc,[33], and the hip.[5] As for the knee and the ACL, the current dogma is that injury results from a single loading rather than repetitive loading. However, athletes appear to rupture their ACL during maneuvers that they have performed thousands, if not millions of times before—maneuvers such as jump landings and plant-and-cut movements.[16,23] Only recently has evidence emerged of tissue fatigue as an ACL failure mechanism: ACL rupture occurred with cyclic loading of a magnitude that if repeated only a few times would not injure the ACL.[19] Greater impact load and smaller ligament cross-sectional area were identified as contributing factors to ACL fatigue injury risk.[19] Similar failures due to tissue

fatigue have been reported in the leporine medial collateral ligament[37] and the human extensor digitorum longus tendon.[26]

It appears that deterioration of the mechanical properties due to tissue microdamage is the mechanism by which ligaments and tendons fail under cyclic loading. For example, stiffness of the medial collateral ligament decreased both *in vivo* in humans and *in vitro* in rats, which was found to correlate with a reduction in strength of the ligament, following cyclic loading.[35] Although tendons can repair and adapt to loading, their ability to do so deteriorates when tissue damage is too severe.[1] This may also be true for ligaments given their similar collagen composition to tendons.[2] Consequently, loading the ACL at a magnitude and frequency that exceed its ability to repair and adapt can result in damage accumulation, and thence failure.

Even if one accepts the concept that the ACL can fail via a fatigue mechanism, many questions remain. For example, the factors that increase ACL loading magnitude and reduce ACL fatigue life remain unknown. Firstly, limited range of internal rotation at the hip has been shown to be a contributing factor to ACL injury risk;[6,8] might this be due to it reducing the ACL's fatigue life? Restrictions in internal femoral rotation have been shown to increase ACL strain during cadaver-simulated single-leg pivot landings.[4] Hence, limited hip internal rotation might be expected to decrease ACL fatigue life by increasing ligament loading. Secondly, ACL injuries frequently occur near the femoral enthesis, especially of the PL bundle,[19,29] however the reason for this is unknown. It has been posited that the acute angle at which the ACL originates from the femur induces a stress concentration at the femoral enthesis, as shown *in silico*.[21] Thirdly, the size of the tibial eminence could also contribute to injury risk by reducing ACL fatigue life because the volume and height of this bony structure were found to be smaller in ACL-injured individuals than healthy, uninjured controls.[13] Hence, these three factors may

contribute to ACL injury risk because they decrease the fatigue life of the ACL by increasing ACL load during each loading cycle.

The purpose of the study, therefore, was to determine the effect of limited range of internal femoral rotation, sex, femoral-ACL attachment angle, and tibial eminence volume on *in vitro* ACL fatigue life during repetitive simulated single-leg pivot landings. This landing model is representative of the period *in vivo* before any accumulated microdamage can be repaired. A custom-built *in vitro* knee testing apparatus[4,19,22] was used to simulate single-leg pivot landings in paired knees, with one knee from each pair loaded with limited internal femoral rotation and the other knee with free femoral rotation. We tested the primary hypothesis that the risk of ACL failure would be significantly greater with limited range of internal femoral rotation than with free rotation. We also tested the secondary hypothesis that the female knee specimens, as well as the specimens with a smaller femoral-ACL attachment angle and a smaller tibial eminence volume, would have a higher risk of ACL failure than the male specimens.

3.3 Materials and Methods

Specimen Procurement and Preparation. To determine the sample size required to test our hypotheses, two-sided two-group survival analyses based on exponential survival ($\alpha = 0.05$; $1-\beta = 0.80$) were performed with pilot data. Because power analyses available for survival data are limited to dichotomized data, only range of internal femoral rotation and sex were included as independent variables to predict risk of ACL failure. This power analysis provided a conservative estimate because it could not account for the presence of paired knees, which have greater correlation than unpaired knees. These *a priori* power analyses revealed a total sample size of between 4-17 knee specimens. Given the conservative nature of these power analyses and the fact that an equal number of female and male knee specimens was preferred, 16 pairs of

fresh-frozen knee specimens, for a total of 32 specimens from 8 male (age = 42.4 ± 16.6 years; height = 1.75 ± 0.06 m; mass = 71.3 ± 8.5 kg) and 8 female (age = 47.6 ± 11.1 years; height = 1.65 ± 0.08 m; mass = 53.5 ± 8.4 kg) donors, were procured for this study. They were procured from the University of Michigan Anatomical Donations Program, Anatomy Gifts Registry, MedCure, Research for Life, and Science Care. No scars indicative of knee surgery, no evidence of joint degeneration, and no joint deformity were present in the procured knee specimens.

The knee specimens were stored in a freezer at -20°C until dissection, magnetic resonance (MR) imaging, and testing. The specimens were removed from the freezer 48 hours prior to dissection and thawed at room temperature. They were dissected down to the knee joint capsule, leaving intact its ligaments, as well as the tendons of the quadriceps (rectus femoris), medial hamstrings (semitendinosus, semimembranosus, gracilis), lateral hamstrings (biceps femoris), medial gastrocnemius, and lateral gastrocnemius. Following dissection, each knee specimen was MR imaged, and then mechanically tested on a later day. Immediately prior to testing, the proximal femur and the distal tibia and fibula were cut to a length of 20 cm each, from the joint line. Then, each bone extremity was potted in polymethylmethacrylate.

Experimental Design and Protocol. A cross-sectional, matched-pair design (Table 3.1) was used to test the hypotheses. From each donor, one knee specimen was randomly assigned to a pivot landing with a limited range of internal femoral rotation and the paired knee specimen to a pivot landing with free range of femoral rotation. Each session began with five non-pivot trials that served two purposes: (1) precondition the knee specimen; and (2) determine the height from which the weight needed to be dropped from the top of the testing apparatus to simulate a jump landing with a ground reaction force approximating four times bodyweight (xBW), ± 10%. During these preconditioning trials, only an impulsive compression force and knee flexion

moment were produced (no axial tibial torque). After this set of trials, pivot trials were executed (with internal tibial torque), approximately one minute apart, until ACL failure occurred or until a minimum of 100 trials was achieved. For the knees with limited range of femoral rotation, the femoral rotation device was locked. For the knees with free range of femoral rotation, the femoral rotation device was unlocked. ACL failure was defined as either a macroscopic failure of the ligament or a 3-mm increase in cumulative anterior tibial translation, as previously defined[19] and accepted clinically.[7] The presence of macroscopic failure was assessed when a sudden increase in the range of anterior tibial translation occurred (≥ 10%, based on pilot work), and confirmed, along with injury location, by visual inspection.

Table 3.1 Testing protocol for each block of trials

Landing Type	Knee Loading Condition	Femoral Rotation	Number of Trials
non-pivot	compression + flexion moment	N/A	5
pivot	compression + flexion moment + internal tibial torque	locked or free[a]	until ACL failure[b] or a minimum of 100

[a]From each paired knee specimens, one specimen was randomly assigned to limited femoral rotation (locked femoral rotation device) and the other specimen to unrestricted femoral rotation (free femoral rotation device).
[b]Defined as either a macroscopic failure or a 3-mm increase in cumulative anterior tibial.

Magnetic Resonance Imaging. Prior to testing, each knee specimen was placed in a coil in full extension and scanned with a 3.0-Tesla MR imaging system (Ingenia model, Philips Medical Systems), using a three-dimensional T2-weighted, proton-density sequence with the following parameters: repetition time = 1,000 ms; echo time = 35 ms; slice thickness = 0.7 mm; pixel spacing = 0.49 x 0.49 mm; spacing between slices = 0.35 mm; field of view = 330 x 200 x 96 mm (inferior-superior, anterior-posterior, medial-lateral, respectively).

From the MR images, the angle at which the ACL originates from the femur, termed here the “femoral-ACL attachment angle”, and the volume of the tibial eminence were measured

using OsiriX software (version 4.1.2, www.osirix-viewer.com). For the femoral-ACL attachment angle, the images were reconstructed to create oblique-sagittal and oblique-frontal planes, which ran parallel to the longitudinal axis of the ACL. In the oblique-sagittal view, the oblique-frontal slice running through the mid-portion of the ACL was identified (red line, Figure 3.1A). From that oblique-frontal slice, the femoral-ACL attachment angle was measured. Specifically, the angle between (1) a line drawn along the edge of the lateral femoral condyle where the ACL inserts and (2) a line along the longitudinal axis of the proximal 25% of the ACL was calculated (α, Figure 3.1A). For the tibial eminence volume, all frontal-plane slices in which this structure was present were identified. From these slices, the area of the tibial eminence that was proximal of a line connecting the most superior points of the medial and lateral tibial plateau was outlined (Figure 3.1B). Tibial eminence volume was calculated by OsiriX, which multiplied, for each slice, the outlined area by the sum of slice thickness and slice spacing and then added each slice volume to obtain total volume. The intraclass correlation coefficients for the MRI measurements were excellent, with 0.78 for the femoral-ACL attachment angle and 0.88 for the tibial eminence volume.

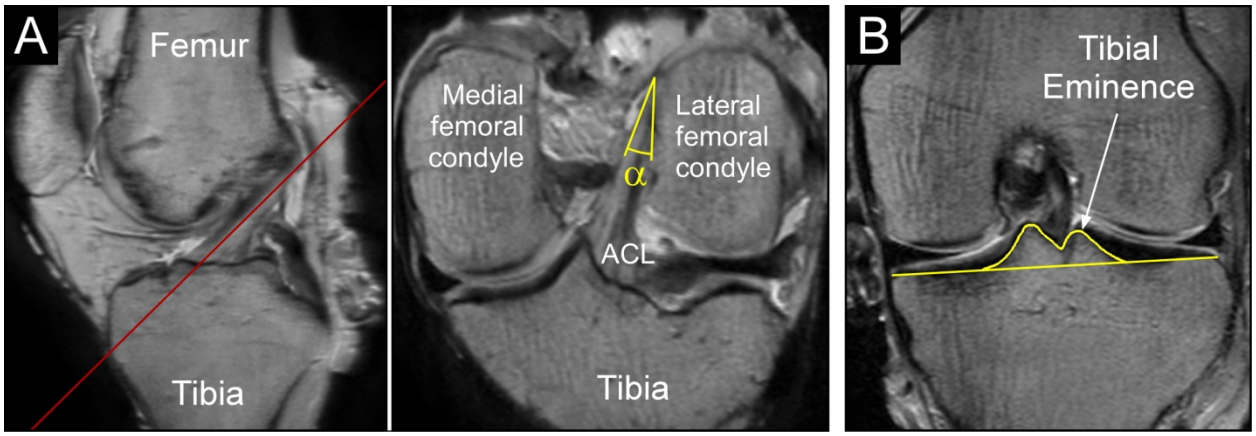

Figure 3.1 (**A**) Example of the femoral-ACL attachment angle measurement. Left: oblique-sagittal MR image showing the location of the oblique-frontal slice (red line, at mid-portion of the ACL) that was used to measure the angle. Right: oblique-frontal MR image showing the definition of the femur-ACL attachment angle (α). (**B**) Example of the tibial eminence (TE) measurement. Frontal plane MR image showing the outlined area of the TE, which was multiplied by the sum of the slice thickness and slice spacing to obtain each slice's TE volume. Total TE volume was calculated by taking the sum of the TE volume of all slices.

Knee Testing Apparatus. The dissected and imaged knee specimens were inverted and mounted in a modified Withrow-Oh testing apparatus[22] in 15° of knee flexion. This apparatus simulated a single-leg pivot jump landing with a ground reaction force approximating 4x bodyweight by impacting the distal end of the tibia and producing an impulsive compression force, knee flexion moment, with and without internal tibial torque (pivot and non-pivot trials, respectively, Table 3.1). Specifically, a weight (Figure 3.2) was dropped onto the tibia from a height that was determined by trial-and-error during the non-pivot trials. Loading forces and moments were measured by two 6-axis load cells located at the distal tibia and the proximal femur (Figure 3.2, *L*). Internal tibial torque was produced with a tibial torsion device (Figure 3.2), which was either locked to simulate a non-pivot landing or unlocked to simulate a pivot landing.[4] Axial femoral rotation was controlled by a novel femoral rotation device (Figure 3.2) at the proximal end of the femur. As previously described,[4] it consisted of a circular plate, which rotated in the transverse plane, and two pre-tensioned springs to resist axial rotation. To model

limited internal femoral rotation, the femoral rotation device was locked with a steel stop. To model unrestricted rotation, the steel stop was removed from the device to allow free femoral rotation. In this condition, rotation was only resisted by the femoral rotation device's springs, which simulated the tensile resistance of the hip rotator muscles to stretch. Knee muscle tension and tensile resistance to stretch were modeled by means of pretensioned elastic structures (i.e., woven nylon cord) connected to the tendons of the quadriceps and medial and lateral hamstrings and gastrocnemii with cryoclamps (Figure 3.2). Before every trial, the quadriceps muscle-tendon unit and the hamstrings and gastrocnemii muscle-tendon units were pretensioned to ~180 N and ~70 N, respectively. Tension of the muscle-tendon units were measured at 2 kHz by five uni-axial load cells (Transducer Techniques) attached, in series, to the woven nylon cords and cryoclamps.

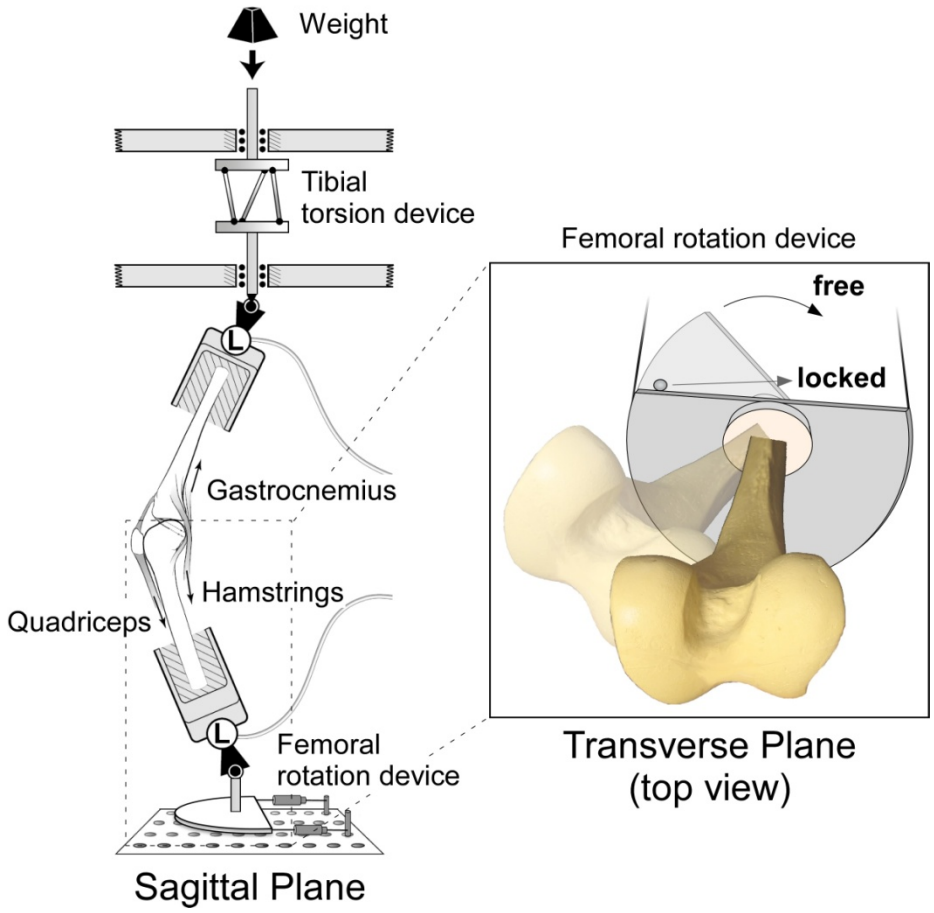

Figure 3.2 Sagittal plane diagram of the *in vitro* testing apparatus used to simulate single-leg pivot landings (left) and a top view of the femoral rotation device (right). The position of the specimen and device at peak relative internal femoral rotation during the trials with limited and free femoral rotation is represented by the solid and transparent portions of the diagram, respectively. *L*: 6-axis load cell.

Tibiofemoral kinematics were recorded at 400 Hz via an optoelectronic imaging system (Optotrak Certus, Northern Digital) that tracked the three-dimensional (3D) location of six infrared-emitting diodes. Three diodes were affixed to the femur segment, with three other diodes affixed to the tibia segment, in a configuration that defined the sagittal, coronal, and transverse planes of each segment. The 3D coordinates of the femoral and tibial diodes were used to quantify the knee rotations and translations. Meanwhile, 3D forces and moments produced at the distal tibia and proximal femur were recorded at 2 kHz via two 6-axis force sensors (Figure 3.2, *L*) (Advanced Manufacturing Technology Inc).

Data Processing. The 3D coordinates of the infrared-emitting markers, as acquired by the motion capture system, were low-pass filtered using a Butterworth filter (4th order, 20 Hz cutoff frequency). From the markers' 3D coordinates, in addition to the coordinates of the knee's origin—defined as the roof of the femoral notch and digitized prior to the landing trials, 3D rotations and translations were calculated using the method described by Grood and Suntay.[12] Femoral rotation was defined with respect to the testing apparatus; whereas tibial rotations and translations were defined with respect to the femur. Kinematic data were calculated as relative and/or cumulative changes in rotations and translations. A "relative" measurement was defined relative to the data point at time 0 (initial contact) of the trial of interest. A "cumulative" measurement was defined relative to the data point at time 0 of the first pivot trial. All load cell data were also low-pass filtered with a Butterworth filter (4th order, 70 Hz cutoff frequency).

The main outcome measure was the number of trials executed until ACL failure occurred or until a minimum of 100 pivot trials was reached. From each trial, peak relative internal femoral rotation was extracted as the main independent variable. Peak relative and cumulative anterior tibial translations were also extracted to assist in determining ACL failure.

Statistical Analysis. The hypotheses were statistically tested by means of Cox regression models with shared frailty (to account for paired knee specimens). Specifically, the primary hypothesis was tested with a model that predicted ACL failure risk with *internal femoral rotation* (dichotomized and coded as 1 = free and 2 = locked) as the predictor variable. The secondary hypothesis was tested with the full model, which included *internal femoral rotation*, *sex of donor*, *femoral-ACL attachment angle*, and *tibial eminence volume* as the predictor variables. Lastly, a final model was selected based on the variables that best predicted risk of ACL failure. An alpha level below 0.05 indicated statistical significance.

3.4 Results

Eight of the 32 knee specimens that were tested failed during the repetitive pivot landings: 7 specimens loaded with limited internal femoral rotation ("locked" condition) and merely 1 specimen loaded with free rotation. The failed specimens included 5 female knees, which failed in 15 ± 13 loading cycles and 3 male knees, which failed in 84 ± 41 cycles. There was 1 complete ACL tear, 2 partial ACL tears, 2 permanent elongation failures, and 3 tibial avulsions (Table 3.2). On average, 3.3 ± 0.6° and 14.1 ± 2.5° of internal femoral rotation occurred during the pivot landings with limited and free rotation, respectively. During the non-pivot trials, the mean landing force was approximately 4xBW for both groups (locked: 4.2 ± 0.4xBW, free: 4.2 ± 0.2xBW). During the pivot trials, the mean landing force and internal tibial torque were 5.0 ± 0.7xBW and 31.3 ± 5.9 Nm, respectively, for the specimens loaded with limited internal femoral rotation and 4.5 ± 0.5xBW and 27.8 ± 5.5 Nm, respectively, for those loaded with free rotation.

Table 3.2 List of the specimens tested, status of internal femoral rotation, number of cycles to failure, description of the failure pattern, and morphological data

Specimen[a]	Internal Femoral Rotation	Cycles to Failure[b]	Failure Pattern[c]	Femur-ACL Angle (°)[d]	Tibial Eminence Volume (cm^3)
M01149					
Left knee	Free	---	Did not fail	14.3	1.16
Right knee	Locked	127	Permanent elongation	17.3	1.24
M01431					
Left knee	Locked	80	Permanent elongation	26.4	2.03
Right knee	Free	---	Did not fail	23.9	1.98
F02341					
Left knee	Free	---	Did not fail	27.3	1.11
Right knee	Locked	38	Tibial avulsion	30.1	1.39
M02867					
Left knee	Free	---	Did not fail	19.4	1.27
Right knee	Locked	---	Did not fail	30.6	1.54

Specimen[a]	Internal Femoral Rotation	Cycles to Failure[b]	Failure Pattern[c]	Femur-ACL Angle (°)[d]	Tibial Eminence Volume (cm^3)
F10496					
Left knee	Locked	---	Did not fail	22.3	1.04
Right knee	Free	---	Did not fail	19.2	1.03
F20661					
Left knee	Locked	14	Complete tear at femoral enthesis	22.8	1.72
Right knee	Free	---	Did not fail	25.9	2.11
M21514					
Left knee	Locked	---	Did not fail	27.5	1.40
Right knee	Free	---	Did not fail	26.3	1.69
M22806					
Left knee	Free	---	Did not fail	30.7	1.41
Right knee	Locked	---	Did not fail	25.8	1.12
M30734					
Left knee	Free	---	Did not fail	22.7	2.07
Right knee	Locked	---	Did not fail	23.7	2.02
F34422					
Left knee	Free	---	Did not fail	19.6	1.22
Right knee	Locked	---	Did not fail	29.4	1.04
M34494					
Left knee	Locked	45	Partial tear of PL bundle at femoral enthesis	20.9	1.79
Right knee	Free	---	Did not fail	23.6	1.83
F34516					
Left knee	Free	---	Did not fail	30.4	1.06
Right knee	Locked	7	Partial tear of PL bundle at femoral enthesis and mid-substance	11.9	1.13
F34568					
Left knee	Locked	---	Did not fail	14.5	0.88
Right knee	Free	---	Did not fail	28.5	1.18
F40036					
Left knee	Locked	6	Tibial avulsion	33.9	1.05
Right knee	Free	10	Tibial avulsion	39.7	1.25
M40061					
Left knee	Locked	---	Did not fail	26.3	1.06
Right knee	Free	---	Did not fail	32.2	1.33
F71125					
Left knee	Free	---	Did not fail	21.1	1.12
Right knee	Locked	---	Did not fail	25.2	1.26

[a]M: male donor; F: female donor.

[b]Includes the five non-pivot trials at the beginning of each testing session.

[c]Permanent ACL elongation was defined as a 3-mm increase in cumulative anterior tibial translation relative to the first pivot trial. PL: posterolateral.

[d]Specimen knee flexion angle in the MR imaging system was standardized, with all specimens imaged in full extension.

The primary finding of this study is that the knee specimens with limited range of internal femoral rotation during repetitive *in vitro* pivot landings had a risk of ACL failure 8.3 times higher in comparison to the specimens with free rotation, when only this predictor variable was included in the statistical model (Wald X^2 = 3.90; p = 0.048) (Table 3.3, Model 1; Figure 3.3). The full statistical model, which included internal femoral rotation, sex of donor, femoral-ACL attachment angle, and tibial eminence volume, did not significantly predict ACL failure risk (Wald X^2 = 7.82; p = 0.098) (Table 3.3, Model 1). Although internal femoral rotation and sex of donor were found to be significant predictors in the full model, femoral-ACL attachment angle and tibial eminence volume did not significantly predict ACL failure risk. The best and final statistical model, therefore, only included internal femoral rotation and sex of donor as predictors of ACL fatigue failure risk (Wald X^2 = 7.50; p = 0.024) (Table 3.3, Model 3). When accounting for sex, risk of ACL failure was 17.1 times higher in the knee specimens loaded with a limited range of internal femoral rotation than those loaded with free rotation. When accounting for femoral rotation, the female knee specimens had a risk of ACL failure 26.9 times higher than the male specimens (Figure 3.3), though this did not reach statistical significance.

Table 3.3 Results of Cox regression models with shared frailty

Predictor Variable	Hazard Ratio	95% CI	P Value
Model 1			0.048[a]
Internal femoral rotation	8.30	1.02 - 67.85	0.048[a]
Model 2			0.098
Internal femoral rotation	13.13	1.32 - 130.96	0.028[a]
Sex	8.89	1.17 - 67.72	0.035[a]
Femoral-ACL attachment angle	1.12	0.93 - 1.36	0.237
Tibial eminence volume	9.23	0.74 - 114.98	0.084
Model 3			0.024[a]
Internal femoral rotation	17.09	1.70 - 171.85	0.016[a]
Sex	26.93	0.94 - 773.18	0.055

[a]Statistically significant.

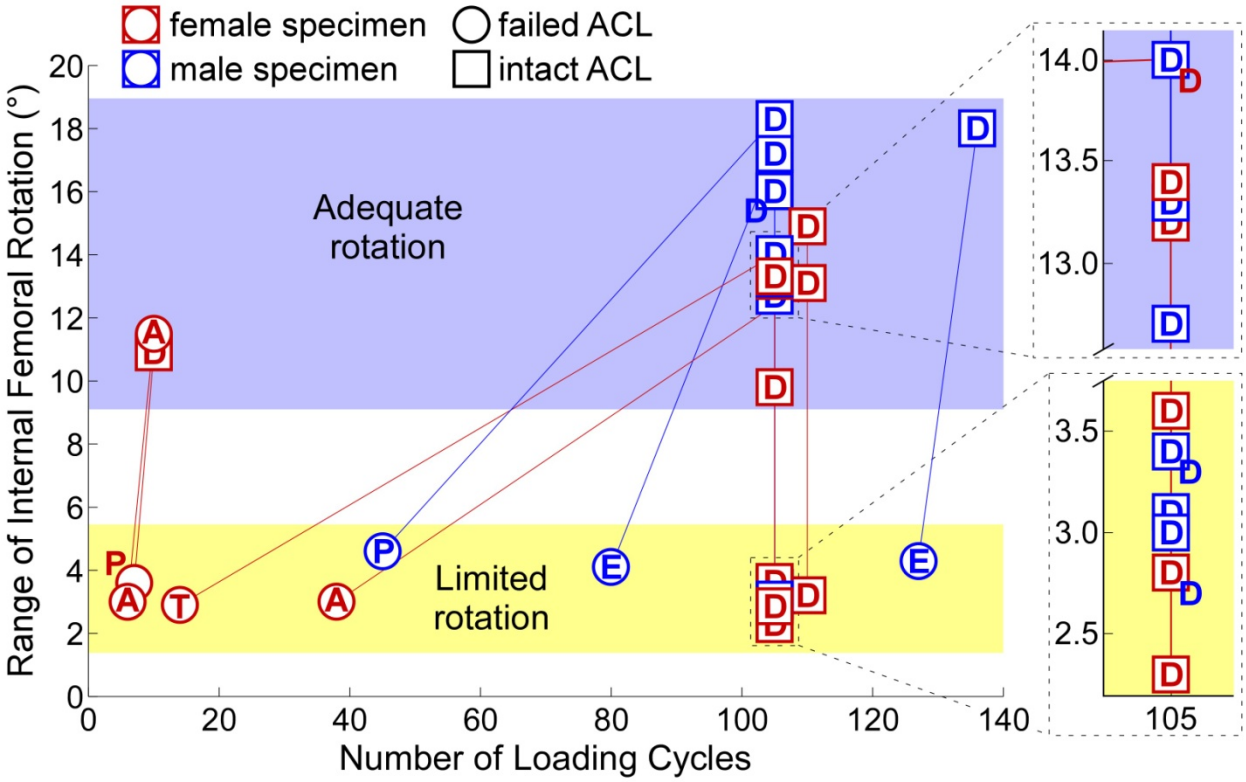

Figure 3.3 Scatterplot of the range of internal femoral rotation versus the maximum number of loading cycles of the knee specimens. A failed ACL is represented by a circle; whereas an intact ACL (at the end of the experiment) is represented by a square. The red and blue markers identify female and male knee specimens, respectively, with data from each donor connected with a solid line. A: tibial avulsion; D: did not fail; E permanent elongation; P: partial ACL tear; T: complete ACL tear.

3.5 Discussion

The current dogma that ACL injury results from a single loading cycle, such as a landing from a jump, has been challenged recently by evidence supporting repetitive loading, and thus fatigue failure of the ACL as the injury mechanism.[19] Greater impact load during cadaver-simulated pivot landings was found to increase risk of ACL injury.[19] Hence, we posed the question: what factors increase ACL loading magnitude, which would then reduce ACL fatigue life because of the inverse relationship between load magnitude and number of loading cycles?[19] Identifying such factors would be of significance in terms of injury prevention and rehabilitation.

Our results suggest that constraining the available range of hip internal rotation during single-leg pivot landings greatly increases the risk of sustaining an ACL rupture.

The primary hypothesis was supported that an *in vitro* repeated pivot landing model with a limited range of internal femoral rotation would have a significantly greater risk of ACL failure than that with free rotation. ACL failure risk was more than 8 times greater when internal femoral rotation was limited and more than 17 times greater when accounting for sex of donor. It is telling that only one knee specimen failed when internal femoral rotation was only resisted by springs, whereas 7 specimens failed when femoral rotation was locked. In addition, it is noteworthy that all ACLs that failed via a macroscopic tear ruptured at the femoral enthesis, especially of the PL bundle. Given the current literature,[4,19] this is not surprising. In a similar *in vitro* repeated pivot landing model, landing impact force was found to be related to ACL injury risk.[19] Specifically, a 1*BW increase in impact force increased injury risk by more than 32-fold, with impact force acting as the surrogate measure for ACL stress.[19] In fact, many materials are known to fail under a number of loading cycles that is inversely related to the tensile stress applied to them.[17] And most recently, we have shown that peak ACL strain increased in cadaver-simulated pivot landings as the available range of internal femoral rotation was decreased.[4] With ACL strain being positively related to ACL stress,[24] the results presented in the current study were expected. Since ACL strain, and thus ACL stress,[24] increased when the available range of internal femoral rotation was limited, the number of loading cycles to failure was expected to decrease with limited rotation. This may explain why athletes with decreased range of hip internal rotation have a greater risk of sustaining an ACL injury.[6,8]

Our results corroborate recently published evidence that the human ACL is susceptible to a repetitive loading injury[19] and that the femoral enthesis, especially that of the PL bundle, is at

risk of injury.[19,29] This may explain why athletes seem to rupture their ACL during maneuvers that they have performed over and over again.[16,23] So-called "fatigue" injuries have been reported in the leporine medial collateral ligament[37] and the human extensor digitorum longus tendon.[26] High ACL loading magnitudes and/or frequencies may induce tissue damage *in vivo* that is beyond the ACL's ability to adapt, thus leading to an accumulation of microdamage and then failure. Such a mechanism has also been described in rat patellar tendon[1] and may also occur in the ACL for several reasons: the ACL's lack of ability to remodel,[20] ligaments' similar collagen composition to tendon[2], and collagen's slow turnover rate.[32] If the ACL is indeed susceptible to fatigue-type failures *in vivo*, injury prevention efforts should focus on limiting the frequency of high ACL loading maneuvers thereby improving the fatigue life of the ACL. This may mean improving the functional range of motion available in a hip that has restricted internal rotation to reduce ACL loading,[4] or reducing the frequency of certain athletic maneuvers known to greatly increase load on the ACL, similar to the limit imposed on Little League pitchers in regard to the number of pitches allowed per day. Furthermore, the PL bundle may be at greater risk because of its significant role in resisting loads, especially internal tibial torque, when the knee is near full extension during pivot landings.[11,15] Further research is needed to elucidate the reasons for the vulnerability of the ACL's femoral enthesis to failure in comparison to the tibial enthesis.

One part of our secondary hypothesis, that the female specimens would have a significantly greater risk of ACL failure in comparison to the male specimens, was not supported. Although including sex of donor in our statistical model improved it and the female ACLs had a risk of failure nearly 27 times greater than the male ACLs, sex of donor failed to reach statistical significance by a small margin ($p = 0.055$). We believe that the small number of ACL failures—only 5 female and 3 male ACLs failed out of a total of 32 ACLs—contributed to

a lack of statistical power to reveal significant sex differences. However, a shorter fatigue life may explain why the ACL injury rate of women is two to five times greater than that of men.[31] The female ACLs were expected to fail in fewer cycles than the male ACLs because of sexual dimorphism in ACL size[18] and ultrastructure[14] and/or knee joint morphology.[18] For example, Lipps et al.[18,19] found not only that female knee specimens have a smaller ACL cross-sectional area than male specimens, but also that a smaller ACL cross-sectional area increases risk of a fatigue-type failure in a similar *in vitro* model. ACL cross-sectional area was not included in our regression model because we did not want to decrease its statistical power, especially given that this variable has already been shown to affect ACL injury risk during *in vitro* repeated pivot landings.[19]

The other part of our secondary hypothesis, stating that femoral-ACL attachment angle and tibial eminence volume would have a significant effect on ACL failure risk, was also not supported. Although an acute femoral-ACL attachment angle and a smaller tibial eminence volume may increase one's risk of sustaining an ACL injury,[21,30] these variables were not found to significantly influence risk of ACL failure (Table 3.3, Model 2). With regard to femoral-ACL attachment angle, its effect on injury risk may be specific to the type of failure pattern, with a smaller angle being a risk factor for partial or complete tears but not for tibial avulsions, for example. Thus, pooling the data of all failed knee specimens may have masked any present effect. For instance, the knee specimens that failed via a tibial avulsion appeared to have greater attachment angles than all other failed specimens (34.6 ± 4.9° vs. 19.9 ± 5.5°, Table 3.2). Isolating the specimens that failed via a complete or partial rupture at the femoral enthesis revealed smaller angles in these specimens in comparison to those in the specimens that did not fail (18.6 ± 5.8° vs. 25.4 ± 9.1°, Table 3.2). Unfortunately, the small number of ACL failures did

not allow us to analyze the data based on failure type. Similar data patterns were noticed with the tibial eminence volume data, with knee specimens that failed via a tibial avulsion having a relatively small volume in comparison to all other failed specimens (1.23 ± 0.17 cm^3 vs. 1.58 ± 0.38 cm^3, Table 3.2). We note that an ACL failure via a tibial avulsion is not the most common type of ACL injury among the population at greatest risk. This probably stems from the specimens having been harvested from older donors (45.0 ± 13.9 years). Hence, pooling the data of all failed knee specimens may have masked any present effect of tibial eminence volume. Another reason for the lack significant effect may be due to methodological reasons. Recently published data revealed that only the volume of the medial tibial eminence was inversely related to ACL injury risk, and in males only.[30] In the present study, volume was measured for the entire tibial eminence. Again, the small number of ACL failures did not allow us to analyze the data based on sex of donor.

We acknowledge several limitations of the present study. First, we investigated an ACL failure mechanism – ligament fatigue – with an *in vitro* model, which precludes the possibility of studying any adaptive biological response. Although the remodeling rate of the human ACL, whether intact or partially injured, is unknown, we do know that no remodeling occurs in the completely ruptured human ACL[20] and that Type 1 collagen has a slow turnover rate.[32] For these reasons, we believe that the role played by biological healing and remodeling is minimal over periods of days or even weeks; and hence, the results obtained from our *in vitro* model reflect behavior before any such remodeling can occur. Second, knee specimens were harvested from older donors in comparison to the younger population that sustains ACL injuries most frequently[27]. Hence, results cannot necessarily be generalized to this latter population. We believe, however, that the general qualitative trends remain valid, even though the number of

cycles to failure may have been underestimated because of the lower quality structural and mechanical properties of the older ACL.[36] Third, only two internal femoral rotation conditions ('locked' and 'free') were included in our experimental design. But we consider our paired knee specimen design one of the strengths of this study because it reduced the effect of inter-specimen variability. Although we cannot make definite conclusions about the relation between ACL failure risk and other available ranges of internal femoral rotation not tested herein, we have no reason to believe that a negative relation would not continue to exist if other available ranges of motion that fall within the condition tested (e.g., ~3° to 14°) had been included. This is especially true considering a similar relation has been reported between available range of internal femoral rotation and peak ACL strain during *in vitro* simulated pivot landings,[4] and that strain affects a ligament's potential for injury.[36] Lastly, only the monoarticular actions of the muscles were simulated in our *in vitro* model.

Our results confirm previous findings that the human ACL is susceptible to a fatigue failure when loaded repeatedly under large loads[19]. This suggests that limiting the frequency of high impact loading cycles and/or improving the fatigue life of the ACL as part of an ACL injury prevention program warrants further investigation. Our results also suggest that landing with a limited available range of hip internal rotation decreases the ACL's fatigue life. Hence, improving the functional range of motion available at the hip should decrease injury risk. This supports the justification for screening for restricted internal rotation at the hip as part of ACL injury prevention programs and evaluation protocols for individuals with ACL injuries and/or reconstructions. This is particular true for women, because the female knee specimens tended to have a greater risk of ACL failure than the male specimens. More research is needed to

determine the threshold of restricted range of hip internal rotation below which clinical intervention should occur.

3.6 Conclusion

Knee specimens with limited range of internal femoral rotation during repetitive *in vitro* simulated pivot landings had a risk of ACL failure more than 17 times higher than those with free rotation.

3.7 References

1. Andarawis-Puri N, Sereysky JB, Sun HB, Jepsen KJ, Flatow EL. (2012) Molecular response of the patellar tendon to fatigue loading explained in the context of the initial induced damage and number of fatigue loading cycles. *J Orthop Res*, 30(8): 1327-34.

2. Arnoczky SP. (1983) Anatomy of the anterior cruciate ligament. *Clin Orthop Relat Res*,(172): 19-25.

3. Bales J, Bales K. (2012) Swimming overuse injuries associated with triathlon training. *Sports Med Arthrosc*, 20(4): 196-9.

4. Beaulieu ML, Oh YK, Bedi A, Ashton-Miller JA, Wojtys EM. (2014) Does limited internal femoral rotation increase peak anterior cruciate ligament strain during a simulated pivot landing? *Am J Sports Med*, 42(12): 2955-63.

5. Bedi A, Dolan M, Leunig M, Kelly BT. (2011) Static and dynamic mechanical causes of hip pain. *Arthroscopy*, 27(2): 235-51.

6. Bedi A, Warren RF, Wojtys EM, Oh YK, Ashton-Miller JA, Oltean H, Kelly BT. (2014) Restriction in hip internal rotation is associated with an increased risk of ACL injury. *Knee Surg Sports Traumatol Arthrosc*, Sept 12. [Epub ahead of print].

7. DeFranco MJ, Bach BR, Jr. (2009) A comprehensive review of partial anterior cruciate ligament tears. *J Bone Joint Surg Am*, 91(1): 198-208.

8. Ellera Gomes JL, de Castro JV, Becker R. (2008) Decreased hip range of motion and noncontact injuries of the anterior cruciate ligament. *Arthroscopy*, 24(9): 1034-7.

9. Fleisig GS, Andrews JR. (2012) Prevention of elbow injuries in youth baseball pitchers. *Sports Health*, 4(5): 419-24.

10. Fufa DT, Goldfarb CA. (2013) Sports injuries of the wrist. *Curr Rev Musculoskelet Med*, 6(1): 35-40.

11. Gabriel MT, Wong EK, Woo SL, Yagi M, Debski RE. (2004) Distribution of in situ forces in the anterior cruciate ligament in response to rotatory loads. *J Orthop Res*, 22(1): 85-9.

12. Grood ES, Suntay WJ. (1983) A joint coordinate system for the clinical description of three-dimensional motions: application to the knee. *J Biomech Eng*, 105(2): 136-44.

13. Hashemi J, Bhuyian A, Mansouri H, Slauterbeck J, Beynnon B. (2013) ACL-injured subjects have a smaller tibial spine than uninjured controls and females have a smaller tibial spine than males. Presented at the *Annual Meeting of the Orthopaedic Research Society*. January 26-29. San Antonio, TX, USA.

14. Hashemi J, Chandrashekar N, Mansouri H, Slauterbeck JR, Hardy DM. (2008) The human anterior cruciate ligament: sex differences in ultrastructure and correlation with biomechanical properties. *J Orthop Res*, 26(7): 945-50.

15. Hosseini A, Gill TJ, Li G. (2009) In vivo anterior cruciate ligament elongation in response to axial tibial loads. *J Orthop Sci*, 14(3): 298-306.

16. Koga H, Nakamae A, Shima Y, Iwasa J, Myklebust G, Engebretsen L, Bahr R, Krosshaug T. (2010) Mechanisms for noncontact anterior cruciate ligament injuries: knee joint kinematics in 10 injury situations from female team handball and basketball. *Am J Sports Med*, 38(11): 2218-25.

17. Lipinski P, Barbas A, Bonnet AS. (2013) Fatigue behavior of thin-walled grade 2 titanium samples processed by selective laser melting. Application to life prediction of porous titanium implants. *J Mech Behav Biomed Mater*, 28: 274-90.

18. Lipps DB, Oh YK, Ashton-Miller JA, Wojtys EM. (2012) Morphologic characteristics help explain the gender difference in peak anterior cruciate ligament strain during a simulated pivot landing. *Am J Sports Med*, 40(1): 32-40.

19. Lipps DB, Wojtys EM, Ashton-Miller JA. (2013) Anterior cruciate ligament fatigue failures in knees subjected to repeated simulated pivot landings. *Am J Sports Med*, 41(5): 1058-66.

20. Murray MM, Martin SD, Martin TL, Spector M. (2000) Histological changes in the human anterior cruciate ligament after rupture. *J Bone Joint Surg Am*, 82-A(10): 1387-97.

21. Oh YK, Beaulieu ML, Lipps DB, Wojtys EM, Ashton-Miller JA. (2013) Is the strain concentration at the femoral enthesis a risk factor for anterior cruciate ligament injury? Presented at the *Annual Meeting of the American Society of Biomechanics*. September 4-7. Omaha, NE, USA.

22. Oh YK, Kreinbrink JL, Wojtys EM, Ashton-Miller JA. (2012) Effect of axial tibial torque direction on ACL relative strain and strain rate in an in vitro simulated pivot landing. *J Orthop Res*, 30(4): 528-34.

23. Olsen OE, Myklebust G, Engebretsen L, Bahr R. (2004) Injury mechanisms for anterior cruciate ligament injuries in team handball: a systematic video analysis. *Am J Sports Med*, 32(4): 1002-12.

24. Pioletti DP, Rakotomanana LR, Leyvraz PF. (1999) Strain rate effect on the mechanical behavior of the anterior cruciate ligament-bone complex. *Med Eng Phys*, 21(2): 95-100.

25. Riordan EA, Frobell RB, Roemer FW, Hunter DJ. (2013) The health and structural consequences of acute knee injuries involving rupture of the anterior cruciate ligament. *Rheum Dis Clin North Am*, 39(1): 107-22.

26. Schechtman H, Bader DL. (1997) In vitro fatigue of human tendons. *J Biomech*, 30(8): 829-35.

27. Shea KG, Pfeiffer R, Wang JH, Curtin M, Apel PJ. (2004) Anterior cruciate ligament injury in pediatric and adolescent soccer players: an analysis of insurance data. *J Pediatr Orthop*, 24(6): 623-8.

28. Shultz SJ, Schmitz RJ, Benjaminse A, Chaudhari AM, Collins M, Padua DA. (2012) ACL Research Retreat VI: an update on ACL injury risk and prevention. *J Athl Train*, 47(5): 591-603.

29. Sonnery-Cottet B, Barth J, Graveleau N, Fournier Y, Hager JP, Chambat P. (2009) Arthroscopic identification of isolated tear of the posterolateral bundle of the anterior cruciate ligament. *Arthroscopy*, 25(7): 728-32.

30. Sturnick DR, Argentieri EC, Vacek PM, DeSarno MJ, Gardner-Morse MG, Tourville TW, Slauterbeck JR, Johnson RJ, Shultz SJ, Beynnon BD. (2014) A decreased volume of the medial tibial spine is associated with an increased risk of suffering an anterior cruciate ligament injury for males but not females. *J Orthop Res*, 32(11): 1451-7.

31. Swenson DM, Collins CL, Best TM, Flanigan DC, Fields SK, Comstock RD. (2013) Epidemiology of knee injuries among US high school athletes, 2005/06-2010/11. *Med Sci Sports Exerc*, 45(3): 462-9.

32. Thorpe CT, Streeter I, Pinchbeck GL, Goodship AE, Clegg PD, Birch HL. (2010) Aspartic acid racemization and collagen degradation markers reveal an accumulation of damage in tendon collagen that is enhanced with aging. *J Biol Chem*, 285(21): 15674-81.

33. Triantafillou KM, Lauerman W, Kalantar SB. (2012) Degenerative disease of the cervical spine and its relationship to athletes. *Clin Sports Med*, 31(3): 509-20.

34. Walden M, Hagglund M, Werner J, Ekstrand J. (2011) The epidemiology of anterior cruciate ligament injury in football (soccer): a review of the literature from a gender-related perspective. *Knee Surg Sports Traumatol Arthrosc*, 19(1): 3-10.

35. Weisman G, Pope MH, Johnson RJ. (1980) Cyclic loading in knee ligament injuries. *Am J Sports Med*, 8(1): 24-30.

36. Woo SL, Hollis JM, Adams DJ, Lyon RM, Takai S. (1991) Tensile properties of the human femur-anterior cruciate ligament-tibia complex. The effects of specimen age and orientation. *Am J Sports Med*, 19(3): 217-25.

37. Zec ML, Thistlethwaite P, Frank CB, Shrive NG. (2010) Characterization of the fatigue behavior of the medial collateral ligament utilizing traditional and novel mechanical variables for the assessment of damage accumulation. *J Biomech Eng*, 132(1): 011001.

CHAPTER 4

A QUANTITATIVE COMPARISON OF THE MICROSCOPIC ANATOMY OF THE HUMAN ACL FEMORAL AND TIBIAL ENTHESES

This chapter has been submitted for consideration of publication:

Beaulieu ML, Carey GE, Schlecht SH, Wojtys EM, Ashton-Miller JA. *J Orthop Res*. [In review]

4.1 Abstract

The femoral enthesis of the human anterior cruciate ligament (ACL) is known to be more susceptible to injury than the tibial enthesis. To determine whether anatomic differences might help explain this difference, we quantified the microscopic appearance of both entheses in 15 unembalmed knee specimens using light microscopy, toluidine blue stain and image analysis. The amount of calcified fibrocartilage and uncalcified fibrocartilage, and the ligament entheseal attachment angle were then compared between the femoral and tibial entheses via linear mixed-effects models. The results showed marked differences in anatomy between the two entheses. The femoral enthesis exhibited a 3.9-fold more acute ligament attachment angle than the tibial enthesis ($p < 0.001$), a 43% greater calcified fibrocartilage tissue area ($p < 0.001$), and a 226% greater uncalcified fibrocartilage depth ($p < 0.001$), with the latter differences being particularly pronounced in the central region. We conclude that the ACL femoral enthesis has more fibrocartilage and a more acute ligament attachment angle than the tibial enthesis, which provides insight into why it is more vulnerable to failure.

4.2 Introduction

Injuries to the anterior cruciate ligament (ACL) pose extensive health and financial difficulties, both short- and long-term.[17,22] The majority of ACL ruptures occur near its femoral origin or "enthesis",[16,29] rather than elsewhere, but the underlying reason for this remains unknown. We speculate that the anatomy of the ACL femoral enthesis may be significantly different than the tibial enthesis. If confirmed, it might help explain the higher failure rate at, or near, the femoral enthesis.

The microscopic anatomy of ligament and tendon entheses minimizes stress concentrations and distributes forces across the entire attachment area.[5,24] Entheses are classified as either fibrous or fibrocartilaginous according to the type of tissue comprising the attachment site.[5] Fibrocartilaginous entheses are characterized by four zones of tissue: dense fibrous connective tissue, uncalcified fibrocartilage (UF), calcified fibrocartilage (CF), and bone.[5] The quantity of each tissue type is characteristic of the mechanical loading at the enthesis.[4,8,9] For example, the quantity of UF has been positively related to the change in angle that occurs between the ligament/tendon and the bone to which it attaches during joint motion;[4,8] while the quantity of cortical calcified tissue has been positively related to the size of the ligament/tendon, and thus the tensile force applied to the bone.[4,9] Most fibrocartilaginous entheses, however, do not contain fibrocartilage across the entire attachment site, with the superficial portions frequently being more fibrous.[5]

Descriptions of the ACL entheses have mostly focused on their macroscopic characteristics and dimensions.[10,20] Few studies have explored these entheses at a microscopic level, and those that have, focused on the femoral enthesis.[1,12,18,23,26] Arnoczky characterized the ACL entheses as fibrocartilaginous, with a description of the transitional zones of UF and CF.[1]

Tissue quantification has not been reported for UF, either at the femoral or the tibial entheses. Greater UF may be expected at the femoral enthesis than the tibial enthesis given the greater change in ACL-bone angle reported at the femur during passive knee flexion.[28]

Lastly, the oblique angle at which a tendon/ligament attaches to the bone has been shown, by computer simulations, to induce a strain concentration where the shortest longitudinal fibers of the tendon/ligament originate from, or insert into, bone at the enthesis.[13,19] And that strain concentration increased with more acute attachment angles.[13] It is unknown, however, whether the femoral ACL entheseal attachment angle is more acute than the tibial attachment angle, thereby inducing greater strain concentration at the femur.

The purpose of this study was to quantify and compare the microscopic anatomy of the human ACL femoral and tibial entheses by means of histological analyses. We tested the primary null hypothesis that there would be no difference in relative area of CF, or the average depth of UF, between the femoral and tibial entheses. We also tested the secondary null hypothesis that there would be no difference between the femoral and tibial ACL entheseal attachment angles.

4.3 Materials and Methods

Specimen Procurement and Preparation. Fifteen unembalmed human knee specimens, including seven pairs, were harvested from four male and four female donors (age = 52.1 ± 8.4 years; height = 1.70 ± 0.10 m; mass = 70.5 ± 15.9 kg; BMI = 24.1 ± 4.3 kg/m^2) through the University of Michigan Anatomical Donations Program. All specimens were dissected so as to leave only the ACL, distal femur, and proximal tibia. No macroscopic evidence of previous ACL injury was observed in the dissected specimens. The femur-ACL-tibia complexes were fixed in 10% neutral buffered formalin for 48 hours, with the knee in 15° of flexion, 0° of

abduction/adduction, and 0° of axial rotation, by means of a custom-built fixation device, to maintain the ligament's natural twist and angle of attachment to each bone. Then, two smaller samples were cut from each femur-ACL-tibia complex for histochemical processing (Table 4.1): the ACL-femur and ACL-tibia attachment sites. Once processed and embedded in methyl methacrylate, tissue samples were sectioned using a commercially available precision sectioning saw (IsoMet™ Low Speed Saw, Buehler, Lake Bluff, IL, USA). For each tissue sample, four thick sections were extracted, mounted on a slide, ground, and polished (EcoMet™ 300 Pro-Grinder/Polisher, Buehler, Lake Bluff, IL, USA) to obtain tissue sample of approximately 100 μm in thickness. Tibial tissue samples were sectioned in a parasagittal plane. Femoral samples were sectioned along the longitudinal axis of the ACL, with both tissue samples sectioned at 20%, 40%, 60%, and 80% of the width of the enthesis (Figure 4.1). The mounted sections were surface stained with toluidine blue for light microscopy viewing. High resolution digital images (4,000 dpi) of all sections were obtained with a film scanner (Nikon Super CoolScan 5000ED) for further analyses.

Table 4.1 Tissue processing protocol for histological analysis

Solution	Time (hrs)
Defat	
ethanol:ether (1:1)	8
chloroform:methanol (2:1)	16
Rinse	
Chloroform	1
Chloroform	1
ethylene glycol monoethyl ether	12
Dehydration	
ethylene glycol monoethyl ether	8
ethylene glycol monoethyl ether	8
ethylene glycol monoethyl ether	8
ethylene glycol monoethyl ether	8
Rinse	
2-propanol	8
2-propanol	8
2-propanol	8
Clear	
methyl salicylate	8
methyl salicylate	8
Process	
methyl methacrylate I[a]	24
Clear	
methyl methacrylate I[a]	96
methyl methacrylate II[a]	96
methyl methacrylate III[a]	96
Embed	
methyl methacrylate IV[b]	~ 432

[a]methyl methacrylate (MMA) and n-butyl phthalate.
[b]MMA, n-butyl phthalate, and dry benzoyl peroxide (varying amounts of benzoyl peroxide in MMA II-IV).

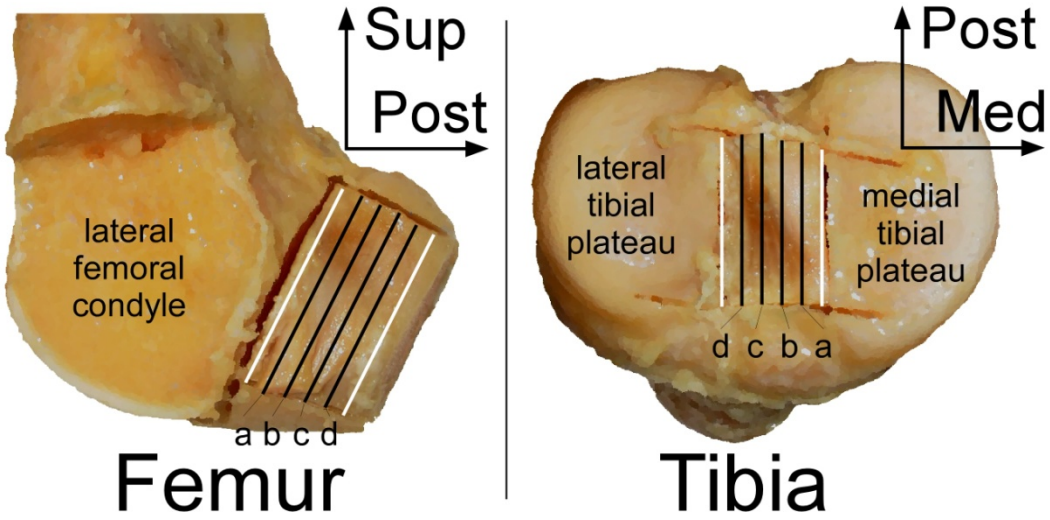

Figure 4.1 Location of tissue sections (black lines) prepared for histological analysis on the femoral and tibial tissue blocks of a right knee specimen. White lines indicate the edges of the entheses. a: 20%; b: 40%; c: 60%; d: 80% of the width of the enthesis.

Quantitative Analysis. From the digital images of tissue sections, the diameters of the femoral and tibial entheses were measured and averaged over all four sections. The diameter was measured along the longitudinal axis of the ligament and along an antero-posterior axis for the femoral and tibial entheses, respectively. The relative area of CF was also quantified by outlining this tissue using a pen display (Cintiq 24HD w/ grip pen, Wacomb, Kazo, Saitama, Japan) and dividing this area by the length of the enthesis (Figure 4.2A). We measured CF relative area because the area measurement includes all CF in the enthesis rather than a sampling of its depth at discrete intervals. In addition, the depth of UF was measured at 500-μm intervals along the entire enthesis (Figure 4.2B). A sample of depth was selected here as the quantification method because the interface between the UF and the dense fibrous connective tissue was less apparent than for the CF, making a relative area measurement impractical (Figure 4.2A-4.2B). Also, sampling UF depth at a constant interval has been used previously to quantify UF in human quadriceps tendons and patellar ligaments.[8] This variable was defined as the perpendicular distance from the tidemark to the end of the UF tissue, delineated by the furthest chondrocyte[8]

viewed with a light microscope (BX-51, Olympus, Center Valley, PA, USA) at x100 and x400 magnifications (Figure 4.2B). Finally, the ligament entheseal attachment angle, defined as the angle between a line parallel to the fibers of the dense fibrous connective tissue and a line of best fit to the digitized entheseal surface (i.e., tidemark), was measured in each tissue section (Figure 4.2C). All measurements were made in ImageJ.[25] CF relative area was quantified over the diameter of the enthesis, as well as for the middle 50% and outer 50% of the enthesis diameter (Figure 4.2D), and averaged over all four tissue sections. UF depth was averaged over the diameter of the enthesis, as well as over the middle 50% and outer 50% of the diameter of the enthesis, and then averaged over all sections. The entheseal attachment angle was averaged over all sections. The intraclass correlation coefficients for the measurements were excellent, with 0.98 for CF relative area, 0.83 for the UF depth, and 0.99 for the ligament entheseal angle.

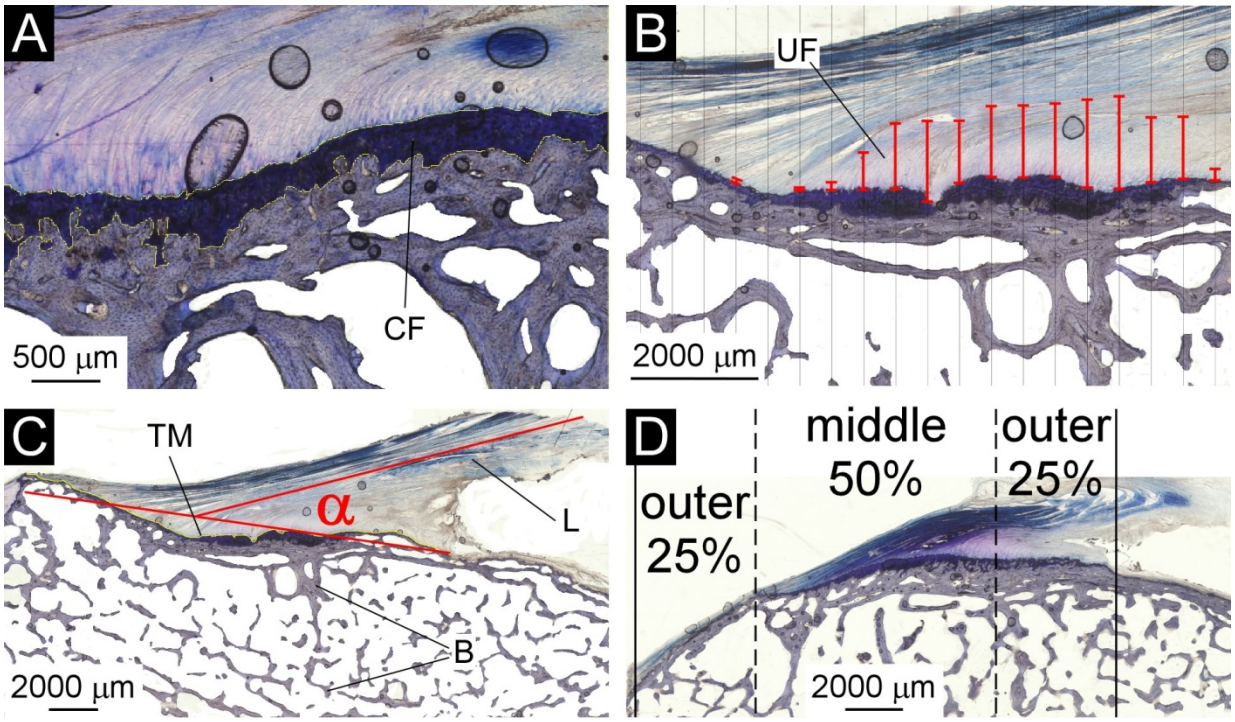

Figure 4.2 Example of the (**A**) outline of CF area, (**B**) UF depth measured at 500-μm intervals, and (**C**) ligament entheseal attachment angle measurement. (**D**) Definition of the enthesis regions for which the dependent variables were quantified. cf: calcified fibrocartilage; uf: uncalcified fibrocartilage; tm: tidemark; b: bone; l: ligament. Toluidine blue strain.

Statistical Analysis. The hypotheses were statistically tested by means of a series of linear mixed-effects models with CF relative area, UF depth, and entheseal attachment angle as the outcome variables and enthesis (coded as '1' = femur and '2' = tibia), knee specimen, and knee donor as the predictor variables. A second series of linear mixed-effects models were run to gain further insight on quantitative differences between femoral and tibial entheses. For these models, CF relative area and UF depth were the outcome variables and enthesis region (coded as '1' = middle 50% of femoral enthesis, '2' = outer 50% of femoral enthesis, '3' = middle 50% of tibia enthesis, and '4' = outer 50% of tibia enthesis), knee specimen, and knee donor were the predictor variables. Knee donor was included in the models to account for the correlation between specimens harvested from the same donor. An alpha level below 0.05 indicated statistical significance.

4.4 Results

Qualitative Analysis. The femoral entheses were fibrocartilaginous in that they comprised four distinct zones of tissue: dense fibrous connective tissue, UF, CF, and bone (Figure 4.3A-4.3D and 4.3I). The periphery, especially the most superior and posterior regions, however, contained little or no fibrocartilage. The superior fibers were found to extend to, and blend into, the posterior articular cartilage (Figure 4.3J); the inferior fibers originated adjacent to the lateral intercondylar ridge. The shape of the femoral enthesis was generally convex in the most anterior section (section 'a' in Figure 4.1 and Figure 4.3A), but generally concave in the most posterior section (section 'd' in Figure 4.1 and Figure 4.3D), and more complex in the middle sections (Figure 4.3B-4.3C). Finally, in the regions with a large quantity of UF, typically the middle to inferior one-third of the enthesis, the fibrocartilage transitioned from calcified to uncalcified, and

thus arose from the tidemark, at a less acute angle and curved to align with the primary collagen fiber direction of the ligament (Figure 4.3I).

The tibial entheses were also fibrocartilaginous, but with smaller and relatively uniform quantities of fibrocartilage across the enthesis in comparison with the femoral entheses (Figure 4.3E-4.3H and 4.3K). They inserted into a bony depression delineated anteriorly by the anterior ridge and posteriorly by the anterior intertubercular fossa. In comparison with the femoral enthesis, the trabecular bone appeared to be more anisotropic (Figure 4.3A-4.3H).

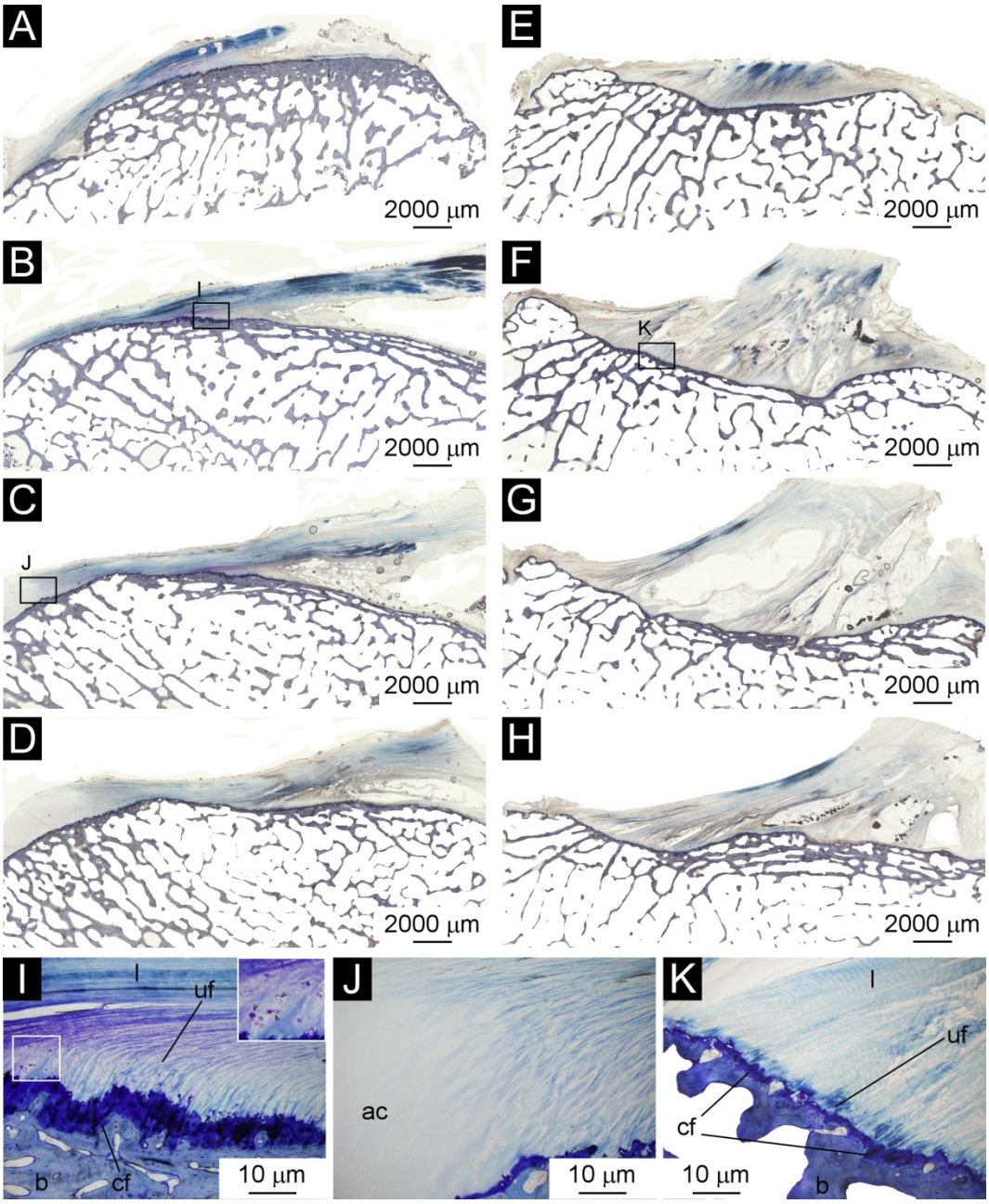

Figure 4.3 Histology of the four tissue sections of the ACL femoral (**A**: 20%; **B**: 40%; **C**: 60%; **D**: 80% of the width of the enthesis) and tibial (**E**: 20%; **F**: 40%; **G**: 60%; **H**: 80% of the width of the enthesis) entheses in a representative specimen in terms of fibrocartilage quantity, entheseal tidemark profile, and ligament entheseal attachment angle. The large voids in the tibia may be fat deposits. (**I**) Femoral entheses had four zones of tissue: ligamentous tissue (l), uncalcified fibrocartilage (uf), calcified fibrocartilage (cf), and bone (b). Note how the ligamentous tissue transitions into uncalcified fibrocartilage and curves to insert into the calcified tissue at a less acute angle. *Inset*: High power view of tissue outlined in white showing uncalcified fibrocartilage with its fibrocartilage cells (arrow heads). (**J**) The femoral enthesis often extended to, and blended into, the posterior articular cartilage (ac). (**K**) Tibial entheses also had four zones of tissue, but with less fibrocartilage. Toluidine blue stain.

Quantitative Analysis. The mean entheseal diameters, averaged over all sections of the femoral and tibial entheses, were 14.8 ± 3.2 mm and 15.8 ± 2.0 mm, respectively. Overall, the relative area of CF and average depth of UF were 43% and 226% greater at the femoral enthesis than the tibial enthesis, respectively (p's < 0.001) (Figure 4.4A-4.4B). Additional region-specific comparisons revealed that this difference in CF relative area between entheses was significant only in the middle 50% of the enthesis (p < 0.001) (Figure 4.4A). Furthermore, the difference in average UF depth between the femoral and tibial entheses was significant in the middle 50% (p < 0.001) as well as the outer 50% of the enthesis (p = 0.009) (Figure 4.4B). As for the entheseal attachment angle, it was 3.9 times smaller at the femoral enthesis compared with the tibial enthesis (p < 0.001) (Figure 4.4C).

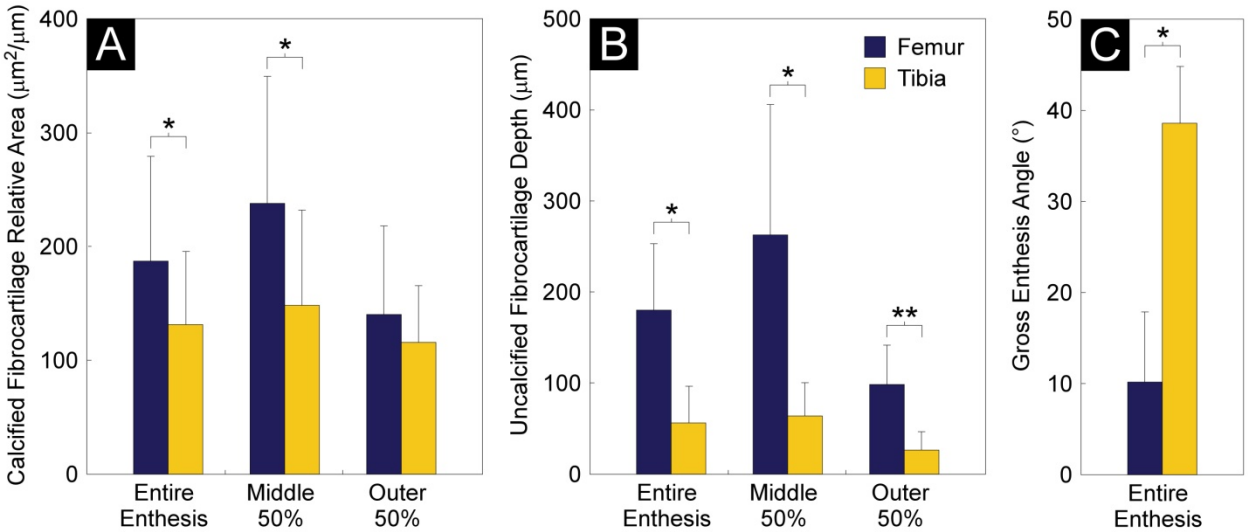

Figure 4.4 Mean and standard deviation of (**A**) relative area of calcified fibrocartilage and (**B**) depth of uncalcified fibrocartilage of all tissue sections for the entire enthesis and by region, as well as (**C**) ligament entheseal attachment angle of all tissue sections for the entire enthesis presented for the femoral and tibial entheses. *significantly different, p < 0.001; **significantly different, p < 0.010.

4.5 Discussion

The goal of this study was to compare the microscopic anatomy of the ACL tibial and femoral entheses. Our histological analyses revealed significant differences in the quantity of

fibrocartilage, and especially the angle at which the ACL attaches to the bone (i.e., the "entheseal attachment angle") at the femoral and tibial entheses. When these anatomic differences are interpreted in a biomechanical context, they help provide new insight into why the femoral enthesis is more vulnerable to failure.

The primary null hypothesis was rejected because more CF and UF were found at the femoral enthesis, especially in its middle region. Although the ACL entheses have been the subject of several histological analyses,[1,12,18,23,26] we were unable to find quantitative comparisons of femoral and tibial entheseal anatomy. The only other study to quantify fibrocartilage did so at the femoral enthesis and measured the combined depth of the calcified fibrocartilage and subchondral bone (CFB).[23] We also made this measurement, but did not present those data to avoid redundancy, given similar trends in CF relative area and CFB depth. Therefore, our results corroborate those of Sasaki;[23] qualitatively more calcified tissue appears to be present in the central region of the femoral enthesis in both studies.

The magnitude of UF and CF at an enthesis has been proposed to be positively related to the change in angle between the ligament and the bone to which it attaches and to the tensile force applied to the bone, respectively.[4,8,9] It is not surprising, therefore, that more UF was present at the femoral enthesis than at the tibial enthesis given the greater change in ACL-bone angle at the femoral enthesis measured *in vitro* during passive knee flexion.[28] Specifically, the ACL-femur angle increases 54° during knee flexion (0 - 140°), on average, in comparison with the ACL-tibia angle, which only decreases an average of 23°.[28] The greater quantity of UF at the femoral enthesis, therefore, may help reduce bending moments at the enthesis calcified-uncalcified junction.[6] As for the CF, its greater quantity at the femoral enthesis may indicate greater stress there than at the tibia, as suggested by Evans et al.[9] Given that the load magnitude

applied to the enthesis should be the same at the femoral and tibial attachments of a given ACL, we speculate that the larger footprint of the tibial enthesis[11] and the concavity into which it inserts, which lengthens the entheseal 'bond' between soft and hard tissue, reduces the average tensile stress (i.e., force per unit area) at the tibial enthesis. Hence, less CF may be required at the tibial enthesis in comparison with the femoral enthesis. Benjamin and colleagues,[5] on the other hand, suggested that less calcified tissue (CF and subchondral bone) allows for greater deformation of the enthesis, and thus greater dissipation of energy. They have also proposed that the lateral tibial spine reduces stress at the tibial enthesis by allowing the ACL to bend over it, as the spine acts like a pulley.[7] However, we did not observe such bending in our specimens. Perhaps this is only a factor at greater angles of knee flexion, given that the angle at which the ACL inserts into the tibia decreases with knee flexion[28]. All our knee specimens were fixed at 15° of flexion—the mean knee flexion angle at initial contact during ACL injury scenarios,[15] and that used for *in vitro* studies.[2] The angle at which the ACL-bone specimens were fixed by Benjamin et al., however, was not reported.[7] Even though it appears to be dimensioned appropriately (i.e., more CF), the smaller femoral enthesis is systematically loaded by a greater average tensile stress than the tibial enthesis. It is logical, therefore, that it could accumulate microdamage over time, especially given recent evidence that the ACL is indeed susceptible to fatigue failure.[3,16]

We rejected the secondary null hypothesis in that the ACL was found to arise from the femur at a nearly four-fold more acute angle than it inserts into the tibia. Zaffagnini and colleagues[28] also examined ACL-bone angles, but they did not use a plane representative of the entheseal surface (or "tidemark"). Rather, they used a plane that was representative of the articular surface of the bones to calculate these angles. From a biomechanical viewpoint, the

more acute femoral entheseal angle will induce a greater strain concentration at the inferior margin of the femoral enthesis than at the tibial enthesis, based on *in silico* evidence.[13] In a computer model of the pubovisceral muscle and its enthesis, an inverse relation was found between enthesis angle and strain energy concentration: the smaller the attachment angle, the greater the strain concentration.[13] Hence, the more acute entheseal attachment angle at the femur and the putative greater strain concentration might help explain why the ACL often fails there.

We note several limitations of this study. First, we used older specimens (age = 52.1 ± 8.4 years) to gain insight on an injury that mainly occurs in adolescents and young adults.[14] Fibrocartilaginous entheses are known to be affected by age-related degenerative changes, such as microdamage and an increase in thickness of the CF.[27] There is no evidence that these changes would affect the femoral and tibial entheses differently, so the general qualitative trends should remain valid. Second, the donors' history of physical activity was unknown; certain activities could have induced entheseal trauma and micro-trauma, thereby producing architectural changes at the enthesis.[21] Without a detailed history, however, we cannot interpret with confidence any variations/abnormalities.

4.6 Conclusion

More fibrocartilage tissue was found at the femoral enthesis than at the tibial enthesis. Furthermore, the ACL was found to arise from the femur at a significantly more acute angle than that at which it inserts into the tibia.

4.7 References

1. Arnoczky SP. (1983) Anatomy of the anterior cruciate ligament. *Clin Orthop Relat Res*,(172): 19-25.

2. Beaulieu ML, Oh YK, Bedi A, Ashton-Miller JA, Wojtys EM. (2014) Does limited internal femoral rotation increase peak anterior cruciate ligament strain during a simulated pivot landing? *Am J Sports Med*, 42(12): 2955-63.

3. Beaulieu ML, Wojtys EM, Ashton-Miller JA. (In review) Risk of ACL fatigue failure is increased by limited internal femoral rotation during in vitro repeated pivot landings. *Am J Sports Med*. [In review].

4. Benjamin M, Evans EJ, Rao RD, Findlay JA, Pemberton DJ. (1991) Quantitative differences in the histology of the attachment zones of the meniscal horns in the knee joint of man. *J Anat*, 177: 127-34.

5. Benjamin M, Kumai T, Milz S, Boszczyk BM, Boszczyk AA, Ralphs JR. (2002) The skeletal attachment of tendons--tendon "entheses". *Comp Biochem Physiol A Mol Integr Physiol*, 133(4): 931-45.

6. Benjamin M, McGonagle D. (2001) The anatomical basis for disease localisation in seronegative spondyloarthropathy at entheses and related sites. *J Anat*, 199(Pt 5): 503-26.

7. Benjamin M, Moriggl B, Brenner E, Emery P, McGonagle D, Redman S. (2004) The "enthesis organ" concept: why enthesopathies may not present as focal insertional disorders. *Arthritis Rheum*, 50(10): 3306-13.

8. Evans EJ, Benjamin M, Pemberton DJ. (1990) Fibrocartilage in the attachment zones of the quadriceps tendon and patellar ligament of man. *J Anat*, 171: 155-62.

9. Evans EJ, Benjamin M, Pemberton DJ. (1991) Variations in the amount of calcified tissue at the attachments of the quadriceps tendon and patellar ligament in man. *J Anat*, 174: 145-51.

10. Ferretti M, Doca D, Ingham SM, Cohen M, Fu FH. (2012) Bony and soft tissue landmarks of the ACL tibial insertion site: an anatomical study. *Knee Surg Sports Traumatol Arthrosc*, 20(1): 62-8.

11. Iriuchishima T, Shirakura K, Yorifuji H, Aizawa S, Murakami T, Fu FH. (2013) ACL footprint size is correlated with the height and area of the lateral wall of femoral intercondylar notch. *Knee Surg Sports Traumatol Arthrosc*, 21(4): 789-96.

12. Iwahashi T, Shino K, Nakata K, Otsubo H, Suzuki T, Amano H, Nakamura N. (2010) Direct anterior cruciate ligament insertion to the femur assessed by histology and 3-dimensional volume-rendered computed tomography. *Arthroscopy*, 26(9 Suppl): S13-20.

13. Kim J, DeLancey JO, Ashton-Miller JA. (2011) Why does the pubovisceral muscle fail at its enthesis, and not elsewhere, during the second stage of labor? A computational study. Presented at the *Annual Meeting of the American Society of Biomechanics*. Aug 10-13. Long Beach, CA, USA.

14. Kobayashi H, Kanamura T, Koshida S, Miyashita K, Okado T, Shimizu T, Yokoe K. (2010) Mechanisms of the anterior cruciate ligament injury in sports activities: A twenty-year clinical research of 1,700 athletes. *J Sports Sci Med*, 9(4): 669-75.

15. Krosshaug T, Nakamae A, Boden BP, Engebretsen L, Smith G, Slauterbeck JR, Hewett TE, Bahr R. (2007) Mechanisms of anterior cruciate ligament injury in basketball: video analysis of 39 cases. *Am J Sports Med*, 35(3): 359-67.

16. Lipps DB, Wojtys EM, Ashton-Miller JA. (2013) Anterior cruciate ligament fatigue failures in knees subjected to repeated simulated pivot landings. *Am J Sports Med*, 41(5): 1058-66.

17. Lohmander LS, Englund PM, Dahl LL, Roos EM. (2007) The long-term consequence of anterior cruciate ligament and meniscus injuries: osteoarthritis. *Am J Sports Med*, 35(10): 1756-69.

18. Mochizuki T, Fujishiro H, Nimura A, Mahakkanukrauh P, Yasuda K, Muneta T, Akita K. (2014) Anatomic and histologic analysis of the mid-substance and fan-like extension fibres of the anterior cruciate ligament during knee motion, with special reference to the femoral attachment. *Knee Surg Sports Traumatol Arthrosc*, 22(2): 336-44.

19. Oh YK, Beaulieu ML, Lipps DB, Wojtys EM, Ashton-Miller JA. (2013) Is the strain concentration at the femoral enthesis a risk factor for anterior cruciate ligament injury? Presented at the *Annual Meeting of the American Society of Biomechanics*. Sept 4-7. Omaha, NE, USA.

20. Otsubo H, Shino K, Suzuki D, Kamiya T, Suzuki T, Watanabe K, Fujimiya M, Iwahashi T, Yamashita T. (2012) The arrangement and the attachment areas of three ACL bundles. *Knee Surg Sports Traumatol Arthrosc*, 20(1): 127-34.

21. Resnick D, Niwayama G. (1983) Entheses and enthesopathy. Anatomical, pathological, and radiological correlation. *Radiology*, 146(1): 1-9.

22. Riordan EA, Frobell RB, Roemer FW, Hunter DJ. (2013) The health and structural consequences of acute knee injuries involving rupture of the anterior cruciate ligament. *Rheum Dis Clin North Am*, 39(1): 107-22.

23. Sasaki N, Ishibashi Y, Tsuda E, Yamamoto Y, Maeda S, Mizukami H, Toh S, Yagihashi S, Tonosaki Y. (2012) The femoral insertion of the anterior cruciate ligament: discrepancy between macroscopic and histological observations. *Arthroscopy*, 28(8): 1135-46.

24. Schlecht SH. (2012) Understanding entheses: bridging the gap between clinical and anthropological perspectives. *Anat Rec (Hoboken)*, 295(8): 1239-51.

25. Schneider CA, Rasband WS, Eliceiri KW. (2012) NIH Image to ImageJ: 25 years of image analysis. *Nat Methods*, 9(7): 671-5.

26. Tensho K, Shimodaira H, Aoki T, Narita N, Kato H, Kakegawa A, Fukushima N, Moriizumi T, Fujii M, Fujinaga Y, Saito N. (2014) Bony landmarks of the anterior cruciate ligament tibial footprint: A detailed analysis comparing 3-dimensional computed tomography images to visual and histological evaluations. *Am J Sports Med*, 42(6): 1433-40.

27. Villotte S, Knüsel CJ. (2013) Understanding entheseal changes: definition and life course changes. *Int J Osteoarchaeol*, 23(2): 135-146.

28. Zaffagnini S, Martelli S, Acquaroli F. (2004) Computer investigation of ACL orientation during passive range of motion. *Comput Biol Med*, 34(2): 153-63.

29. Zantop T, Brucker PU, Vidal A, Zelle BA, Fu FH. (2007) Intraarticular rupture pattern of the ACL. *Clin Orthop Relat Res*, 454: 48-53.

CHAPTER 5

A QUANTITATIVE ANALYSIS OF THE REGIONAL AND BILATERAL VARIATIONS IN THE MICROSCOPIC ANATOMY OF THE HUMAN ACL FEMORAL ENTHESIS

This chapter has been submitted for consideration of publication:

Beaulieu ML, Carey GE, Schlecht SH, Wojtys EM, Ashton-Miller JA. *J Orthop Res*. [In review]

5.1 Abstract

The anterior cruciate ligament (ACL) often ruptures near its femoral enthesis, with the posterolateral fibers of the ligament being vulnerable during pivot landings. To determine whether regional variations in entheseal microscopic anatomy exist as a potential risk factor for injury, a secondary analysis was performed of data from 15 human ACL femoral entheses. We quantified the regional differences in calcified and uncalcified fibrocartilage, the angle at which the ligament originates from the bone, and the profile of the tidemark in four entheseal sections cut parallel to the ACL longitudinal axis. The results demonstrate at least 33% more calcified fibrocartilage and 143% more uncalcified fibrocartilage in the antero-inferior region, which corresponds to the inferior margin of the origin of the anteromedial ACL fibers (p's < 0.050). The anteromedial ACL fibers originated from the femur at an angle six times greater than its posterolateral fibers (p = 0.032). Finally, average entheseal tidemark profiles correlated bilaterally (Pearson's r = 0.79; p = 0.036), with the most common profile being convex with a single re-entrant. In conclusion, systematic regional differences in fibrocartilage quantity and

collagen fiber attachment angles were found. We argue that these differences may affect the biomechanics of entheseal injury.

5.2 Introduction

Anterior cruciate ligament (ACL) injuries occur at a rate of more than 250,000 incidences per year in the United States[9] and present with long-term debilitative sequelae.[13] Better prevention is needed to reduce the considerable financial and health costs associated with such injuries.[18] Most ruptures occur at, or near, the ACL's femoral origin (or "enthesis"),[25] with the posterolateral (PL) fibers being especially vulnerable during pivot landings,[2,12,15] A recent investigation of the microscopic anatomy of the ACL entheses revealed significant differences in fibrocartilage quantity and ligament attachment angle between the femoral and tibial entheses that may explain the difference in entheseal injury rates.[1] The reasons the femoral enthesis of the PL fibers is susceptible to injury during pivot landings, however, are unknown. Investigating regional differences in the microscopic anatomy of the ACL femoral enthesis may help us explain injury patterns, which in turn could guide injury prevention efforts.

The amount of calcified and uncalcified fibrocartilage within an enthesis is of particular interest because it relates to differences in mobility and in the forces experienced by the structure, and varies within an enthesis.[6,7] Specifically, the quantity of calcified fibrocartilage (CF) is positively related to the magnitude of the tensile forces applied to the enthesis;[7]while the quantity of uncalcified fibrocartilage (UF) is positively related to the magnitude of the change in angle between the bone and ligament/tendon during joint motion.[6] Although regional variations in fibrocartilage have been reported in the entheses of the quadriceps tendon, patellar ligament, and meniscal horns,[3,6,7] they have not been investigated in the ACL entheses. Sasaki et al.[19] reported the combined depth of calcified fibrocartilage and subchondral bone for various regions

of the ACL's femoral enthesis, but without statistical comparisons. Even so, their tabular data showed greater depths in the central region, as well as in the sections corresponding to the origin of the ACL's anteromedial (AM) fibers in comparison with those of the PL fibers.[19] It appears, therefore, that heterogeneity in fibrocartilage quantity within the ACL's femoral enthesis may exist, which may reflect the presence of stress concentrations in regions with more fibrocartilage.

In terms of injury mechanisms, the ligament entheseal attachment angle—the oblique angle at which a tendon/ligament attaches to the bone—can induce a strain concentration in the shortest collagen fibers of the tendon/ligament.[10,17] In fact, a computer simulation has demonstrated that this strain concentration increases when the entheseal attachment angle becomes more acute.[10] Although the entheseal attachment angle is more acute at the femoral enthesis than at the tibial enthesis,[1] it is not known if it varies regionally within the femoral enthesis. The presence of regional differences in attachment angle would indicate differences in injury risk, with regions of the femoral enthesis having a more acute attachment angle being at greater risk for injury.

In a secondary analysis of data from a study of the human ACL entheses,[1] we tested the primary null hypotheses that there would be no regional difference in the relative area of CF, the average depth of UF, or the ligament entheseal attachment angle. We also quantified the profile of the femoral entheseal tidemark and tested the secondary null hypotheses that all entheses, including paired entheses, have the same general tidemark surface shape.

5.3 Materials and Methods

Specimen Procurement and Preparation. To test our hypotheses, we harvested 15 unembalmed human knee specimens, including 14 paired and 1 unpaired specimens, from four male and four female donors (age = 52.1 ± 8.4 years; height = 1.70 ± 0.10 m; mass = 70.5 ± 15.9

kg; BMI = 24.1 ± 4.3 kg/m^2) through the University of Michigan Anatomical Donations Program. A detailed description of the methods used to process the specimens and prepare the slides for histological analysis have been published.[1] Briefly, the knee specimens were dissected down to the distal femur, proximal tibia, and ACL, and then fixed in 10% neutral buffered formalin in 15° of flexion. With the ACL cut cross-sectionally at mid-substance, the femoral attachment site was extracted with an oscillating saw with plunge blade (Bosch, Stuttgart, Germany) and trimmed with a diamond band pathology saw (EXAKT, Norderstedt, Germany). All tissue blocks were processed and embedded in methyl methacrylate according to a published processing schedule.[1] For each enthesis, four thick sections (approximately 100 μm in thickness) were prepared, stained with toluidine blue, and digitized (resolution: 4,000 dpi). Sections were obtained parallel to the longitudinal axis of the ACL at 20%, 40%, 60%, and 80% of the width of the femoral entheses (Figure 1).

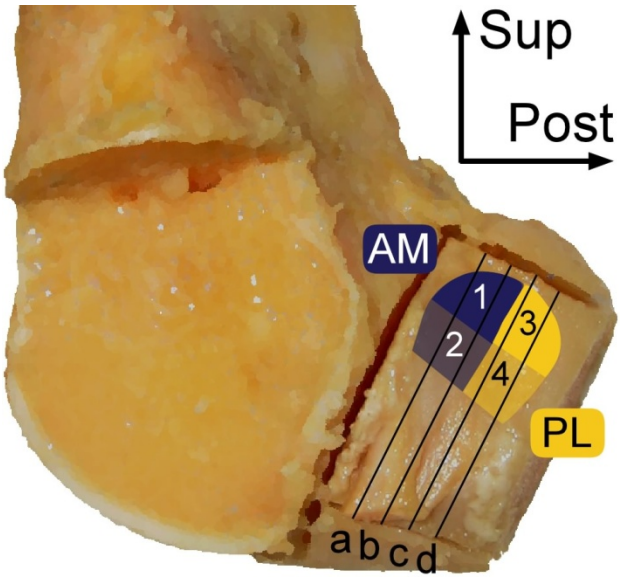

Figure 5.1 Excised femoral attachment site from a right distal femur showing the location of the tissue sections (black lines) processed and prepared, as well as the location of the regions of interest defined for histological analysis. a: 20%; b: 40%; c: 60%; d: 80% of the width of the enthesis. 1: antero-superior; 2: antero-inferior; 3: postero-superior; 4: postero-inferior regions. Regions 1-2 corresponded to the origin of the anteromedial (AM) fibers; meanwhile regions 3-4 corresponded to the origin of the posterolateral (PL) fibers.

Quantitative Analysis. For each tissue section, the relative area of CF was quantified by outlining the CF tissue and dividing its area by the length of the enthesis; whereas the depth of UF was measured at 500-μm intervals across the entire enthesis.[1] The ligament entheseal attachment angle was also quantified by measuring the angle between a line parallel to the fibers of the ligament and a line of best fit to the profile of the digitized interface between the entheseal calcified and uncalcified tissue, also known as the "tidemark".[1] The average CF relative area and UF depth was calculated for four regions of interest of the femoral enthesis (Figure 1): (1) antero-superior; (2) antero-inferior; (3) postero-superior; and (4) postero-inferior. Anatomically, regions 1-2 correspond to the origin of the AM fibers, while regions 3-4 correspond to the origin of the PL fibers. These four regions were selected to allow for comparisons between the AM and PL fibers of the ACL, as well as between the superior and inferior margins. Lastly, the entheseal attachment angle was averaged over the two most anterior sections (Figure 1, a-b), as well as over the two most posterior sections (Figure 1, c-d), of each enthesis.

To measure the overall surface shape of the entheseal tidemark, the profile of the tidemark was quantified in each of the four tissue sections using custom Matlab code. Specifically, digital images of all sections were imported into Matlab, cropped to the width and height of the tidemark and resized so that all images were normalized to have the same width and height. Then, the tidemark profile was digitized and a 5th order polynomial was fit to it. This order was selected because it was the lowest order polynomial that adequately represented the tidemark profile. For bilateral comparisons, the polynomial coefficients were averaged over all sections, resulting in an average polynomial, or "surface shape", for each entheseal tidemark.

Statistical Analysis. A series of linear mixed-effects models were used to test whether regional differences existed in the amount of fibrocartilage and the magnitude of the ligament

entheseal attachment angle within the femoral enthesis. The outcome variables for each model were CF relative area, UF depth, and entheseal attachment angle. The predictor variables for all models were enthesis region (coded as 1 = antero-superior, 2 = antero-inferior, 3 = postero-superior, and 4 = postero-inferior for CF and UF; and 1 = anterior sections and 2 = posterior sections for the entheseal attachment angle). Knee donor was included in the models to account for the correlation between specimens harvested from the same donor. To test whether the average polynomial describing the tidemark surface shape correlated bilaterally, the association between each polynomial coefficient was estimated with Pearson's product moment correlation coefficient. One enthesis was excluded for this correlation analysis because its contralateral enthesis was not among the specimens included in this study. An alpha level below 0.05 indicated statistical significance.

5.4 Results

The relative area of CF was significantly greater at the antero-inferior region of the ACL femoral enthesis than any other region (Figure 2A, 2D, and 2E). In comparison with the antero-superior region, it exhibited 33% more CF ($p = 0.041$). Within the posterior sections, however, no significant difference in CF relative area was found ($p > 0.050$). Comparing the entheseal (anterior) sections that approximate the origin of the AM fibers of the ACL to those (posterior) sections that approximate the origin of the PL fibers, significant differences in CF relative area were found within the inferior margin: specifically, the antero-inferior region exhibited 39% more CF than the postero-inferior region ($p = 0.020$).

The average depth of UF was also found to be heterogeneous, with significantly more UF in the antero-inferior region of the enthesis than in the other regions (Figure 2B, 2D, and 2E). In fact, average UF depth in this region (which approximates the inferior margin of the origin of the

ACL's AM fibers) was 2.5 times greater than in the postero-inferior region (which approximates the inferior margin of the origin of the ACL's PL fibers) ($p < 0.001$). Within the anterior sections, the inferior region exhibited 2.8 times more UF than the superior region ($p < 0.001$). Within the posterior sections, the inferior region exhibited 2.2 times more UF than the superior region ($p = 0.032$).

The ligament entheseal attachment angle was six-fold larger in the posterior sections than in the anterior sections ($p < 0.001$) (Figure 2C), which correspond to the origin of the ACL's PL and AM fibers, respectively.

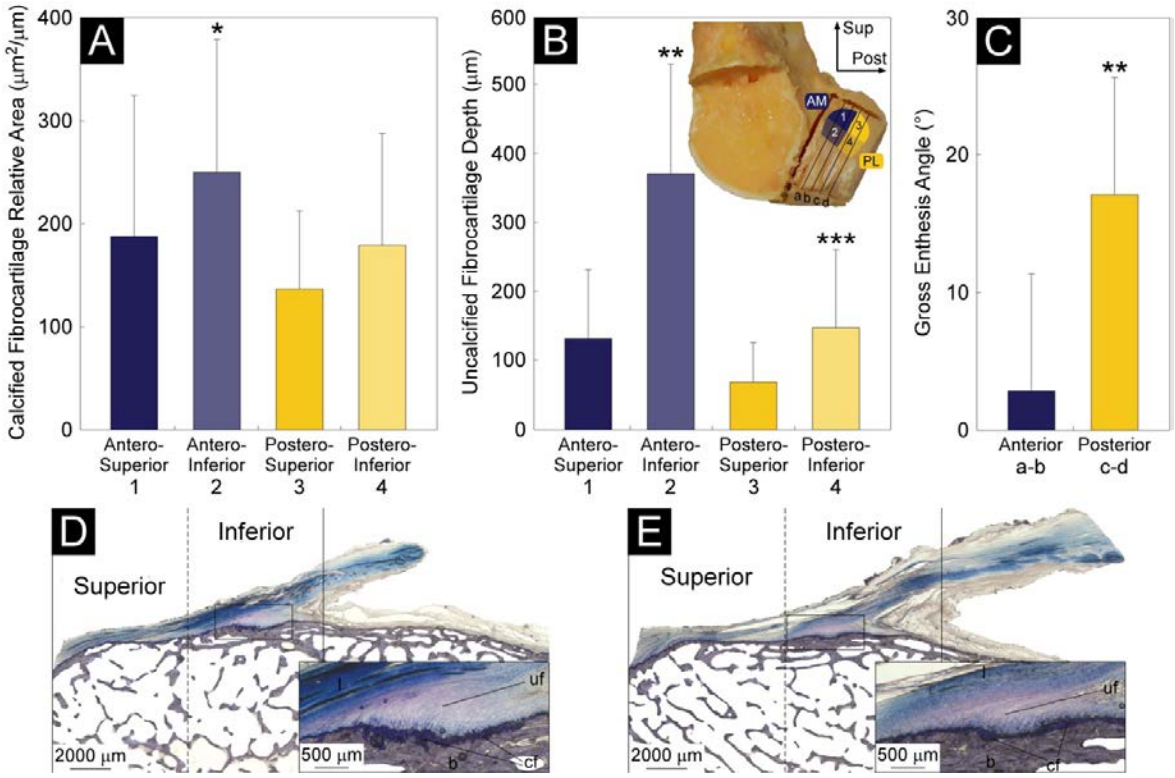

Figure 5.2 Mean and standard deviation of (A) relative area of calcified fibrocartilage and (B) depth of uncalcified fibrocartilage for each entheseal region of interest (1-4), as well as (C) ligament entheseal attachment angle of the anterior (a-b) and posterior (c-d) tissue sections presented for the femoral entheses. Example of (D) anterior (section b in Fig. 1) and (E) posterior (section c in Fig. 1) tissue sections of the ACL femoral enthesis of a representative specimen. *Insets*: High power views of tissue outlined in black showing four zones of tissue: ligamentous tissue (l), uncalcified fibrocartilage (uf), calcified fibrocartilage (cf), and bone (b). *significantly greater than region 1 ($p = 0.041$), region 3 ($p < 0.001$), and region 4 ($p = 0.020$); **significantly greater than all other regions ($p < 0.001$); ***significantly greater than region 3 ($p = 0.032$).

As for the profiles of the entheseal tidemarks, six profiles predominated (Figure 3). The most common profile (21 out of 60 sections) was a convex profile with a single re-entrant (Figure 3C). Most (8 out 9 sections) of the sections with a convex profile (Figure 3A) were anterior sections of the entheses (Figure 1, sections a-b). All the sections with a concave profile (Figure 3B) were the most posterior section of the entheses (Figure 1, section d). The occurrence of the other four types of entheseal profiles was more evenly distributed between the anterior and posterior entheseal sections (number of anterior/posterior sections per entheseal profile: 10/11 (C); 3/4 (D); 5/7 (E); 4/2 (F)). Lastly, the average entheseal tidemark profiles correlated bilaterally (fifth order coefficient, $p = 0.036$) (Figure 4 and Table 1). No other coefficients were significantly correlated bilaterally (p's > 0.050).

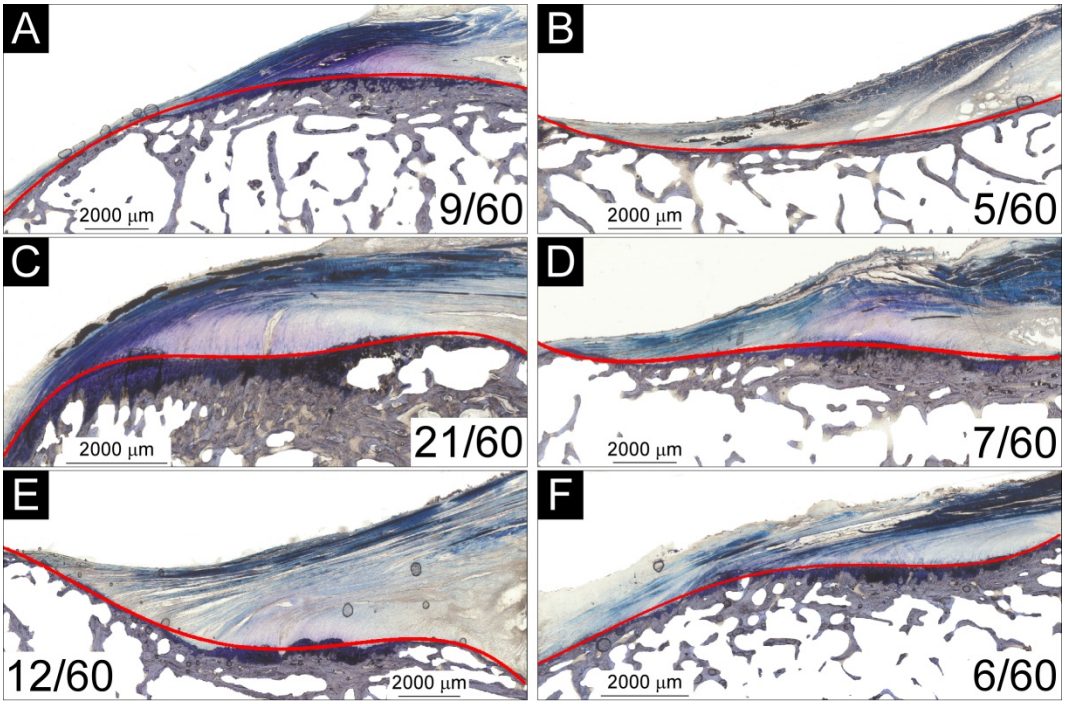

Figure 5.3 Examples of the six types of entheseal tidemark profiles: A: convex; B: concave; C: convex with a single re-entrant; D: concave with a single re-entrant; E: half concave, half convex; F: half convex, half concave. The portion of sections classified as being of a given tidemark profile is shown in the lower corner of each image.

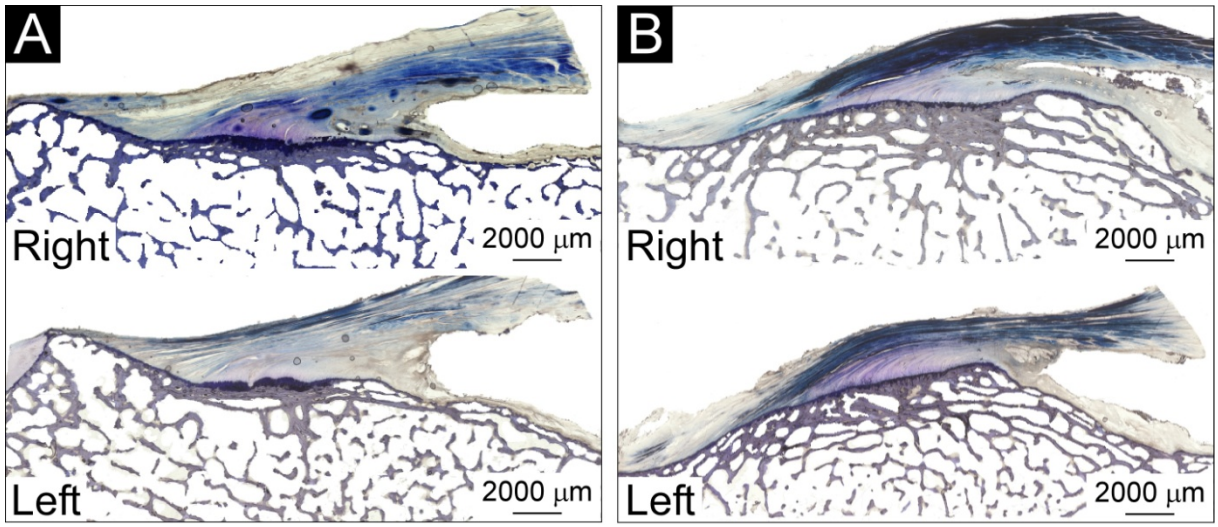

Figure 5.4 Examples of bilateral correlation in entheseal tidemark profiles. Sections from the right and left ACL femoral entheses from (A) specimen #34578 and (B) specimen #34593.

Table 5.1 Mean (standard deviation) coefficients of fifth-order polynomial fit to tidemark profiles of the left and right ACLs, including correlation coefficient and p values.

Polynomial Coefficients			Pearson Correlation Coefficient	P Value
Order	**Left**	**Right**		
0	226×10^{-17} (550×10^{-17})	9.7×10^{-17} (440×10^{-17})	0.451	0.310
1	-238×10^{-13} (669×10^{-13})	-6.3×10^{-13} (499×10^{-13})	0.374	0.409
2	78×10^{-9} (287×10^{-9})	4.7×10^{-9} (207×10^{-9})	0.253	0.585
3	-4.5×10^{-5} (52×10^{-5})	-1.7×10^{-5} (45×10^{-5})	0.131	0.779
4	-22.0×10^{-2} (50×10^{-2})	-5.4×10^{-2} (65×10^{-2})	0.425	0.342
5	718.0 (290.6)	590.1 (303.2)	0.786	0.036

5.5 Discussion

The present work aimed at understanding why the femoral enthesis of the ACL's PL fibers is vulnerable to injury during pivot landings. Our results indicate that the amount of fibrocartilage and the magnitude of the ligament entheseal attachment angle do indeed exhibit systematic regional heterogeneity in the femoral enthesis; hence we rejected the primary null hypotheses. The most fibrocartilage, whether CF or UF, was found at the antero-inferior region

of the femoral enthesis, corresponding to the inferior margin of the origin of the ACL's AM fibers. The heterogeneity in the amount of fibrocartilage at the femoral enthesis may reflect regional differences in the loading history applied to the enthesis. This is because the amounts of CF and UF are thought to positively relate to the tensile force applied to the bone and to the change in angle between the ligament and the bone to which it attaches, respectively.[3,6,7] Hence, the inferior margin of the origin of the AM fibers may have been subjected to greater loading on a regular basis than other regions. This explanation is consistent with evidence that the ACL load is carried by only a few fiber groups at each knee flexion angle, with location of the fibers carrying the load varying with knee flexion angle.[16] It is also consistent with results from a simplified finite element model of the pubovisceral muscle enthesis which, like the ACL femoral enthesis[16], is a tensile structure that also arises from bone at an acute angle. The model revealed a strain concentration in the entheseal region where the shortest fibers of the tensile structure attach,[10] corresponding to the inferior margin of the ACL femoral origin. So, why might the tensile loading history be greater at the inferior margin of the AM fibers than the PL fibers?

The answer may lie in their complementary roles in resisting anterior tibial translation and internal tibial rotation. Although all ACL fibers resist these loads to some degree, the AM fibers primarily resist anterior tibial translation;[5,14] while the PL fibers primarily resist internal tibial rotation.[26] In activities of daily living, such as walking and ascending/descending stairs, the knee mainly moves in the sagittal plane including anterior tibial translation,[20,21,24] thereby primarily loading the AM fibers more than the PL fibers. Hence, the inferior margin of the AM fibers and their enthesis may be subjected to greater loads on a daily basis during activities of daily living than the PL fibers and their enthesis. This would explain the greater amount of CF we found at the former location. However, the PL fibers' femoral enthesis may be at greater risk

of injury during pivot landings because they will be subjected to greater loads as the knee resists the internal tibial rotation that occurs during these landings.[26] In fact, a recent finite element model of the ACL, to which impulsive loads consistent with a pivot landing were applied, revealed a strain concentration at the inferior margin of the PL fiber enthesis.[17] Hence, we speculate that there may be a shift in the location of the strain concentration at the femoral enthesis from the inferior margin of the AM fibers during activities of daily living to that of the PL fibers during athletic activities with high internal tibial torque. Less fibrocartilage at the PL enthesis could make it vulnerable to injury during such pivoting activities. It remains to be seen whether athletes who regularly perform these activities have a different regional distribution of fibrocartilage quantities than we found.

Our results corroborate the qualitative observation of Sasaki et al.[19] that less fibrocartilage tissue exists in the superior regions (previously identified as "posterior"[19]) of the femoral enthesis. They measured the combined depth of the CF and subchondral bone at the femoral enthesis,[19] but no regional statistical comparisons were made and the calcified and uncalcified fibrocartilage were not assessed independently. They also categorized the enthesis as both a direct and indirect enthesis,[19] termed fibrocartilaginous and fibrous, respectively, herein. The fibrocartilaginous portion of the femoral enthesis, which consists of four zones of tissue—ligamentous tissue, UF, CF, and bone,[4] has been described as the central and inferior regions of the enthesis; while the fibrous portion, where the ligament originates directly from the bone without fibrocartilage,[4] has been said to comprise the most superior region of the enthesis.[19] Because we did find some CF and, to a lesser extent, UF in this region, we believe the ACL femoral enthesis is more properly categorized as a fibrocartilaginous enthesis.[4]

The ligament entheseal attachment angle was significantly larger in the posterior rather

than the anterior sections. This angle difference may be attributed to differences in entheseal profile between anterior and posterior sections since the most convex and concave profiles were found in the anterior and posterior sections, respectively. To our knowledge, the entheseal attachment angle and its regional differences have not been reported before. According to the simplified finite element model of the pubovisceral muscle enthesis, the entheseal attachment angle is inversely related to the strain concentration magnitude in the inferior margin. This suggests that, within the inferior margin of the femoral enthesis, the anterior region may experience a greater strain concentration than the posterior region, at least in the knee position examined herein (15° of knee flexion). This may partly explain the greater amount of fibrocartilage in the antero-inferior region than the postero-inferior region. Conversely, the greater attachment angle in the posterior enthesis section, in part caused by the concave surface profile there, may be an architectural mechanism to reduce the entheseal strain concentration in that region.

The secondary null hypothesis that the tidemark of all entheses, including paired entheses, would have the same general surface shape was rejected. Several tidemark profiles were observed, which varied from generally convex to concave as one moved from anterior to posterior sections. In addition, the average tidemark profiles, or "tidemark surface shapes", were more strongly correlated bilaterally than between individuals. Our findings are not surprising given that entheseal surface shape is determined by the history of the tensile forces applied to the enthesis by the ligament during puberty.[8] Assuming that the donors of our knee specimens subjected their ACL femoral entheses to different loading histories, one might expect the variations in entheseal surface shape to be greater between individuals than bilaterally within an individual, which is indeed what we found. Interestingly, some images exhibited local

concentrations in calcification (Figure 5) reminiscent of nascent Pellegrini Stieda known to form in other knee ligaments.[23] It remains to be seen whether these regions are evidence of local remodeling of injured fibrous regions.

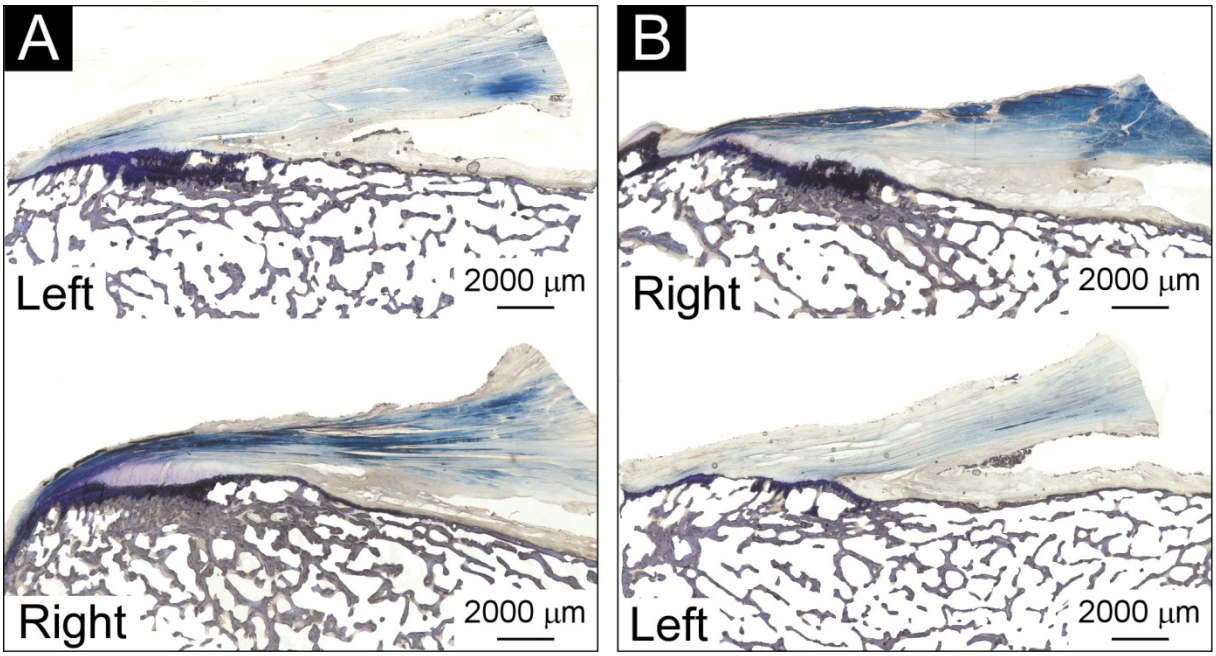

Figure 5.5 Histological images of (A) anterior sections (Fig. 1, b) and (B) posterior sections (Fig. 1, c) showing local concentrations in calcification (top) and the corresponding sections in the paired enthesis (bottom) from specimen #34602.

Our study was not without limitations. First, ACL entheseal tissues were harvested from older donors. Although fibrocartilaginous entheses, such as the ACL femoral enthesis, can be affected by age-related degenerative changes,[22] no evidence exists to suggest that these changes would affect one region of the enthesis differently than another. Second, the physical activity history of our specimens' donors was unknown. We cannot assume, therefore, that our results can be generalized to the young, active population that suffers the most ACL injuries.[11]

5.6 Conclusion

Most calcified and uncalcified fibrocartilage was found at the antero-inferior region of the femoral enthesis. The ligament entheseal attachment angle was more acute in the anterior

rather than the posterior sections. Finally, the profile of the femoral entheseal tidemark varied within an enthesis and between individuals, but some bilateral similarity was evident.

5.7 References

1. Beaulieu ML, Carey GE, Schlecht SH, Jepsen KJ, Wojtys EM, Ashton-Miller JA. A quantitative comparison of the microscopic anatomy of the human ACL femoral and tibial entheses. *J Orthop Res*. [In review].

2. Beaulieu ML, Wojtys EM, Ashton-Miller JA. Risk of ACL fatigue failure is increased by limited internal femoral rotation during in vitro repeated pivot landings. *Am J Sports Med*. [In review].

3. Benjamin M, Evans EJ, Rao RD, Findlay JA, Pemberton DJ. (1991) Quantitative differences in the histology of the attachment zones of the meniscal horns in the knee joint of man. *J Anat*, 177: 127-34.

4. Benjamin M, Kumai T, Milz S, Boszczyk BM, Boszczyk AA, Ralphs JR. (2002) The skeletal attachment of tendons--tendon "entheses". *Comp Biochem Physiol A Mol Integr Physiol*, 133(4): 931-45.

5. Christel PS, Akgun U, Yasar T, Karahan M, Demirel B. (2012) The contribution of each anterior cruciate ligament bundle to the Lachman test: a cadaver investigation. *J Bone Joint Surg Br*, 94(1): 68-74.

6. Evans EJ, Benjamin M, Pemberton DJ. (1990) Fibrocartilage in the attachment zones of the quadriceps tendon and patellar ligament of man. *J Anat*, 171: 155-62.

7. Evans EJ, Benjamin M, Pemberton DJ. (1991) Variations in the amount of calcified tissue at the attachments of the quadriceps tendon and patellar ligament in man. *J Anat*, 174: 145-51.

8. Gao J, Messner K. (1996) Quantitative comparison of soft tissue-bone interface at chondral ligament insertions in the rabbit knee joint. *J Anat*, 188 (Pt 2): 367-73.

9. Griffin LY, Albohm MJ, Arendt EA, Bahr R, Beynnon BD, Demaio M, Dick RW, Engebretsen L, Garrett WE, Jr., Hannafin JA, Hewett TE, Huston LJ, Ireland ML, Johnson RJ, Lephart S, Mandelbaum BR, Mann BJ, Marks PH, Marshall SW, Myklebust G, Noyes FR, Powers C, Shields C, Jr., Shultz SJ, Silvers H, Slauterbeck J, Taylor DC, Teitz CC, Wojtys EM, Yu B. (2006) Understanding and preventing noncontact anterior cruciate ligament injuries: a review of the Hunt Valley II meeting, January 2005. *Am J Sports Med*, 34(9): 1512-32.

10. Kim J, DeLancey JO, Ashton-Miller JA. (2011) Why does the pubovisceral muscle fail at its enthesis, and not elsewhere, during the second stage of labor? A computational study.

Presented at the *Annual Meeting of the American Society of Biomechanics*. Aug 10-13. Long Beach, CA, USA.

11. Kobayashi H, Kanamura T, Koshida S, Miyashita K, Okado T, Shimizu T, Yokoe K. (2010) Mechanisms of the anterior cruciate ligament injury in sports activities: A twenty-year clinical research of 1,700 athletes. *J Sports Sci Med*, 9(4): 669-75.

12. Lipps DB, Wojtys EM, Ashton-Miller JA. (2013) Anterior cruciate ligament fatigue failures in knees subjected to repeated simulated pivot landings. *Am J Sports Med*, 41(5): 1058-66.

13. Lohmander LS, Englund PM, Dahl LL, Roos EM. (2007) The long-term consequence of anterior cruciate ligament and meniscus injuries: osteoarthritis. *Am J Sports Med*, 35(10): 1756-69.

14. Markolf KL, Park S, Jackson SR, McAllister DR. (2008) Contributions of the posterolateral bundle of the anterior cruciate ligament to anterior-posterior knee laxity and ligament forces. *Arthroscopy*, 24(7): 805-9.

15. Meyer EG, Baumer TG, Slade JM, Smith WE, Haut RC. (2008) Tibiofemoral contact pressures and osteochondral microtrauma during anterior cruciate ligament rupture due to excessive compressive loading and internal torque of the human knee. *Am J Sports Med*, 36(10): 1966-77.

16. Mommersteeg TJ, Huiskes R, Blankevoort L, Kooloos JG, Kauer JM. (1997) An inverse dynamics modeling approach to determine the restraining function of human knee ligament bundles. *J Biomech*, 30(2): 139-46.

17. Oh YK, Beaulieu ML, Lipps DB, Wojtys EM, Ashton-Miller JA. (2013) Is the strain concentration at the femoral enthesis a risk factor for anterior cruciate ligament injury? Presented at the *Annual Meeting of the American Society of Biomechanics*. Sept 4-7. Omaha, NE, USA.

18. Riordan EA, Frobell RB, Roemer FW, Hunter DJ. (2013) The health and structural consequences of acute knee injuries involving rupture of the anterior cruciate ligament. *Rheum Dis Clin North Am*, 39(1): 107-22.

19. Sasaki N, Ishibashi Y, Tsuda E, Yamamoto Y, Maeda S, Mizukami H, Toh S, Yagihashi S, Tonosaki Y. (2012) The femoral insertion of the anterior cruciate ligament: discrepancy between macroscopic and histological observations. *Arthroscopy*, 28(8): 1135-46.

20. Shelburne KB, Pandy MG, Anderson FC, Torry MR. (2004) Pattern of anterior cruciate ligament force in normal walking. *J Biomech*, 37(6): 797-805.

21. Taylor WR, Heller MO, Bergmann G, Duda GN. (2004) Tibio-femoral loading during human gait and stair climbing. *J Orthop Res*, 22(3): 625-32.

22. Villotte S, Knüsel CJ. (2013) Understanding entheseal changes: definition and life course changes. *Int J Osteoarchaeol*, 23(2): 135-146.

23. Wang JC, Shapiro MS. (1995) Pellegrini-Stieda syndrome. *Am J Orthop (Belle Mead NJ)*, 24(6): 493-7.

24. Zabala ME, Favre J, Scanlan SF, Donahue J, Andriacchi TP. (2013) Three-dimensional knee moments of ACL reconstructed and control subjects during gait, stair ascent, and stair descent. *J Biomech*, 46(3): 515-20.

25. Zantop T, Brucker PU, Vidal A, Zelle BA, Fu FH. (2007) Intraarticular rupture pattern of the ACL. *Clin Orthop Relat Res*, 454: 48-53.

26. Zantop T, Herbort M, Raschke MJ, Fu FH, Petersen W. (2007) The role of the anteromedial and posterolateral bundles of the anterior cruciate ligament in anterior tibial translation and internal rotation. *Am J Sports Med*, 35(2): 223-7.

CHAPTER 6

GENERAL DISCUSSION

The overall objective of this dissertation was to address several knowledge gaps in the area of ACL injury mechanisms and prevention. First, we did not understand why athletes with a restricted range of hip internal rotation were more prone to anterior cruciate ligament (ACL) injuries. Second, it was unknown whether such a limitation in hip internal rotation could increase the ACL's susceptibility to a fatigue failure via repetitive loading. Third, we did not know why the ACL ruptures more frequently near its femoral enthesis, neither *in vivo* nor *in vitro*. Last, it was unknown why the ACL's posterolateral (PL) fibers appear to be more susceptible to injury than the anteromedial (AM) fibers during pivot landings.

6.1 Restriction in Hip Internal Rotation

Most ACL injuries occur upon landing on one leg after a jump and/or during a change of direction with knee flexion, abduction, and internal rotation, without any direct contact to the knee.[6,28,30,46] *In vitro* and *in silico* work has confirmed that, indeed, a combination of knee axial compression force, knee flexion moment, internal tibial torque, and knee abduction moment is the 'worst-case' dynamic loading scenario in terms of peak ACL strain.[10,41,45,49,55] The strains experienced by a ligament directly impacts its potential for injury.[65] As the peak ACL strain in a single loading cycle increases, it approaches the ultimate tensile strain of the structure. By definition, rupture will ensue when ACL strain exceeds that ultimate tensile strain. Several factors can increase ACL strain during a single-leg landing, from morphological factors, such as

a larger posterior-directed slope of the tibial plateau,[7,53,57,59,61,63,70] to material properties, such as lower quadriceps tensile stiffness.[33] Knowledge of the factors that increase ACL injury risk, as well as an understanding of how they influence that risk, is critical if our goal is to target such factors within an injury prevention and screening framework (Figure 6.1).

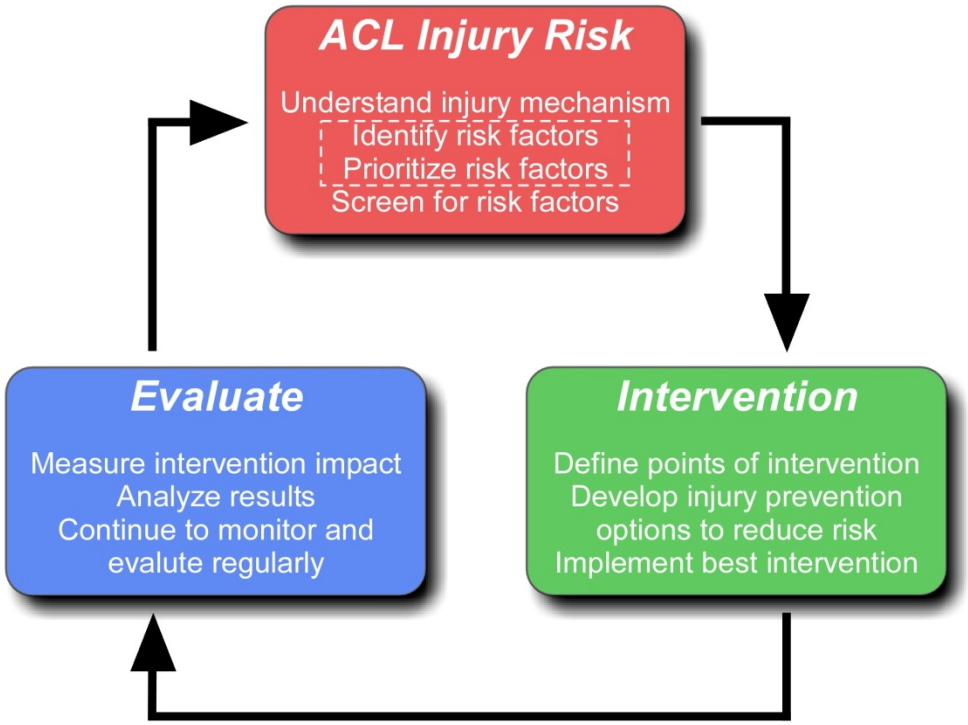

Figure 6.1 An ACL injury and prevention conceptual model. This dissertation was aimed at identifying contributing factors to ACL injury risk, as well as the magnitude of the associated risk (items highlighted by dashed box). Adapted from the Physical Activity Injury Reduction tool.[9]

Recently, epidemiological evidence has emerged that a restriction in hip internal rotation is a contributing factor to ACL injury risk.[4,12,13] For example, soccer and football athletes presenting with a restricted passive range of internal rotation at the hip were found to be more susceptible to an ACL rupture or rerupture in comparison with athletes with unrestricted rotation.[4,12,13] The present dissertation has revealed how and why such athletes with limited hip internal rotation may be at greater risk of sustaining an ACL injury (Chapters 2-3). Using an *in vitro* landing model, an inverse relationship was established between the range of internal

femoral rotation and peak strain in the AM fibers of the ACL (Chapter 2) and also ACL injury risk (Chapter 3). Limiting internal femoral rotation increased ACL strain by increasing internal tibial rotation and anterior tibial translation, both of which are known to load the ACL.[45] Hence, restriction in rotation in one joint led to compensatory rotation in an adjacent joint. For every 10° decrease in internal femoral rotation, there was a 1.3% increase in peak ACL strain. To put this into perspective, that represents a 20% relative increase in peak strain from a landing with average hip internal rotation upon landing (15°)[22] to one with limited rotation (5°). This suggests that athletes with limited hip internal rotation are systematically exposed to greater ACL strain than those individuals with unrestricted hips.

This dissertation research also showed that limited internal femoral rotation increases risk of ACL injury by decreasing ACL fatigue life (i.e., the number of loading cycles to ACL failure) (Chapter 3), thereby extending the findings of Chapter 2. For example, decreasing the range of internal femoral rotation by 11°, on average, increased injury risk more than 17-fold. Current dogma is that ACL injury results from a single awkward landing. Only recently has fatigue failure of the ligament been suggested as an ACL injury mechanism.[34] Lipps et al.[34] showed that the number of cycles needed to fail the ACL is inversely related to knee loading magnitude, the latter being used as a surrogate for ACL loading, and positively related to ACL cross-sectional area. In other words, as the repetitive load applied to the knee was increased, the risk of ACL injury also increased, with smaller diameter ACLs failing in fewer cycles.[34] Chapter 3 of this dissertation extends that work to show that limited hip internal rotation is an additional contributing factor to the risk of ACL fatigue failure.

If the ACL can indeed fail due to material fatigue *in vivo*, it means that loads below those which would cause a ligament to rupture in a single loading cycle can rupture the ACL if that

load is applied enough times. This insight can help explain why athletes appear to rupture their ACL during landing maneuvers that they have performed successfully, without injury, thousands if not millions of times before.[29,46] One can speculate that if loading is of a sufficient magnitude and occurs enough times within a given period, the ACL is unable to maintain homeostasis, and thus catabolism occurs. Microdamage may occur in one or more regions of the ACL. If the microdamage accumulates spatially over repeated loading cycles then the multitude of localized failures will eventually coalesce to cause a tear in a major portion of the structure, or even the whole structure, causing what is termed a fatigue failure. This means that ACL injuries may be prevented by simply monitoring the magnitude and frequency of ACL loading cycles and limiting the number of high loading cycles within a specified time period to maintain homeostatis. Such a concept is currently used in Little League Baseball whereby a limit, termed a 'pitch count', is imposed on pitchers of a certain age in regard to the number of fast pitches allowed per day and per week. In the case of the ACL, however, several knowledge gaps remain before such a monitoring program can be established. First, the relation between ACL loading and number of cycles to ACL failure is currently unknown *in vivo*. Second, no noninvasive method exists to estimate ACL loading in the field (i.e., during a soccer game). Addressing these gaps, for example, might lead to body-worn inertial measurement units being used to quantify knee joint loading, and therefore monitor loading frequency and magnitude during soccer matches to prevent ACL failures due to an excessive number of severe loading cycles.

In terms of implications for injury prevention and screening, we need to know the importance of each contributing factor to ACL fatigue injury risk, as well as any additional potential factors yet to be investigated. Results from Chapters 2 and 3 underline the importance of screening for restrictions in hip internal rotation to prevent ACL ruptures and reruptures.

Screening for restricted internal rotation at the hip is recommended not only for ACL injury prevention programs, but also for evaluation protocols in individuals with ACL injuries and/or reconstructions to prevent rerupture. With a simple examination of passive range of hip internal rotation before preseason training, for example, at-risk athletes could be identified and targeted for injury prevention interventions. However, this raises several questions. On which individuals would we choose to intervene? This is especially important when surgical intervention is needed to attempt to improve range of motion when limited by bony impingement, as seen in femoroacetabular impingement (FAI).[3] In other words, how critical is limited hip internal rotation to ACL injury risk, knowing that several other contributing factors exist, such as a small ACL cross-sectional area?[34] Will addressing a hip with limited internal rotation significantly lower one's risk of sustaining an ACL fatigue failure in the presence of a small ACL or other contributing factors to ACL fatigue injury risk? What are those other factors, if any? Future research aimed at answering these questions is needed.

6.2 Microscopic Anatomy of the ACL Entheses

The majority of ACL ruptures occur near its femoral rather than its tibial enthesis,[34,37,56,58,68] with the PL fibers being especially vulnerable during pivot landings, as seen in Chapter 3 and previous work.[34,37] To try to understand the reasons for this systematic bias in ACL injury location, an investigation of the microscopic anatomy of the ACL entheses was carried out (Chapters 4-5). I propose that the ACL femoral enthesis is at greater risk of injury, in part, because it is systematically subjected to higher average stresses than the tibial enthesis. Evidence for this is four-fold (Chapter 4). First, and most importantly, the literature provides evidence that the footprint of the femoral enthesis is 18% smaller than the tibial enthesis.[11,21] This means that the average stress on the femoral enthesis is 18% larger than on the tibial

enthesis because essentially the same resultant force has to be carried by the ligament at both attachment sites. Secondly, indirect evidence of greater loading comes from the amount of calcified fibrocartilage being greater in the femoral enthesis, which suggests that greater tensile forces are applied to the femoral enthesis.[5,15] Thirdly, the amount of uncalcified fibrocartilage was also greater in the femoral enthesis. This suggests that there are greater changes in the angle of pull of the ligament as the knee rotates and translates, and thus greater bending between the ACL and the femur than between the ACL and the tibia.[5,14] In fact, greater changes in the ACL-bone angle have been reported at the femur than the tibia during passive knee flexion.[67] Lastly, the ACL originated from the femur at a nearly four-fold more acute angle than it inserts onto the tibia. Based on *in silico* evidence, a greater strain concentration at the apex of the ligament entheseal angle will occur in entheses with more acute ligament attachment angles.[27] A greater strain concentration in the femoral enthesis would also explain the greater amount of calcified fibrocartilage in comparison with the tibial enthesis, based on evidence presented by Benjamin and colleagues.[5,15] Their work suggests that the quantity of calcified fibrocartilage is positively related to the tensile force applied to the bone by the ligament.[5,15] Differences previously reported in the material properties between the proximal and distal ACL,[8] however, should also be kept in mind. For example, the proximal region of the ACL has been found to be more compliant than its distal region in rats.[35] For a given tensile stress, therefore, the more compliant proximal region will experience greater tensile strain. This may explain why the average collagen fibril diameter is larger near the femoral enthesis than the tibial enthesis in the human ACL, with the number of fibrils being the same along the length of the ligament.[2] Larger fibrils suggest larger tensile stresses at the femoral enthesis since collagen fibril diameter are related to the applied stress.[47] In short, results from Chapter 4, when interpreted within the context of the

literature, suggest that the femoral enthesis is systematically subjected to higher loads and experiences greater bending than the tibial enthesis. Both of these factors would tend to increase the susceptibility of the ACL femoral enthesis to fatigue failure.

Within the ACL femoral enthesis, why are the PL fibers at greater risk of injury than the AM fibers during pivot landings?[34,37] Regional anatomic differences within the femoral enthesis, and shape differences within and between femoral entheses, also exist (Chapter 5). More fibrocartilage, both calcified and uncalcified, was found in the antero-inferior region of the femoral enthesis, which corresponds to the inferior margin of the AM fibers.[11] The AM fibers were also found to arise from the bone at an angle six times more acute than the PL fibers, at least when the knee is in 15° of flexion. Although these regional differences suggest that greater forces are applied to the AM fibers enthesis,[5,14,15] and thus suggest that the AM fibers may be at greater risk of injury, I propose that the ACL injury pattern may be specific to the type of knee loading. Pivot landings load the knee with additional internal tibial torque, as well as the ubiquitous inertial and muscular compressive forces and knee flexion moment during the landing. This internal torque loads the ACL,[45] especially its PL fibers.[69] In fact, a recent finite element model of the ACL loaded during a pivot landing revealed a strain concentration at the inferior margin of the PL fiber enthesis.[43] Less fibrocartilage in this region may make it vulnerable to injury during activities with high internal tibial torques. Although the greater ligament attachment angle of the PL fibers appears to protect these fibers in comparison with the AM fibers, these angles are unknown when the tibia is internal rotated. For the purposes of this dissertation, the knee specimens were fixed in 15° of flexion, 0° of abduction/adduction, and 0° of axial rotation. Further research is needed to study the effects of other knee angles.

Results from Chapter 5 also revealed interesting differences in the shape of the femoral entheseal surface, not only within an enthesis, but also between entheses from different donors. Similarities in shape, however, were found between the right and left femoral entheses of each donor. These findings raise several questions:

- Why does this variability in entheseal surface shape exist?
- Is there a characteristic shape that enhances stress dissipation at the enthesis?
- Does enthesis shape change over one's lifespan?

Gao and Messner[20] suggest that entheseal surface shape is determined by the history of the tensile forces applied to the enthesis by the ligament during puberty, but that after puberty, it is the amount of fibrocartilage that fluctuates as it adapts to the forces applied to the enthesis. Interestingly, Schlecht[51] suggests that morphological changes in entheses may only occur when entheseal stress magnitudes exceed those resulting from habitual loading, and thus exceed remodeling thresholds. He also suggests that a rough entheseal surface may be due to microdamage, perhaps from frequent low-magnitude loads applied to the enthesis during habitual activity or from infrequent high-magnitude loads applied during more strenuous activity.[51] Or perhaps both. This hypothesis would parallel the theory that the ACL can fail due to material fatigue and that the number of loading cycles is related to the magnitude of loading.[34] If load magnitude and/or frequency exceeds remodeling threshold of entheseal tissue, then microdamage may occur. Evidence of such rough entheseal surface, including calcification, was presented in Chapter 5, though its cause is unknown. Hence, this histological work has revealed entheseal and regional differences in the microscopic anatomy of the ACL entheses, but has also raised several questions regarding entheseal development, the effect of habitual loading before, during, and after puberty on entheseal tissue and shape, and entheseal remodeling responses to loading.

6.3 Limitations

The main limitation of this dissertation is the use of older specimens to gain insight on an injury that mainly occurs in adolescents and young adults.[54] Although results cannot necessarily be generalized to these younger populations, I believe that similar qualitative results would have been found in younger specimens. Quantitative results in ACL strain and number of cycles to ACL failure, however, would most likely differ because of the changes in structural and mechanical properties of the ACL with age.[65] Quantitative results of the microscopic anatomy of the ACL entheses may also differ in the younger populations because fibrocartilaginous entheses are known to be affected by age-related degenerative changes, such as microdamage and an increase in thickness of the calcified fibrocartilage.[62] No evidence exists, however, to suggest that these changes would affect the ACL entheses differently.

Although the *in vitro* landing model used in Chapter 2 and 3 closely replicates the timing and magnitude of the impulsive loads applied to the knee during an *in vivo* single-leg pivot landing, as well as the trans-knee muscle forces, it has several limitations. First, relative strain was measured only in the distal third of the AM fibers of the ACL. It was not possible to attach an additional differential variable reluctance transducer (DVRT) to the PL fibers without compromising the integrity of the knee joint or causing measurement error from the transducer impinging on bone. Given that the PL fibers primarily resist internal tibial rotation,[69] as well as anterior tibial translation near full knee extension,[19,24,26,50] ACL strain may have been underestimated in Chapter 2. The impulsive loads, including internal tibial torque, were applied to the knee specimens in 15° of flexion in the *in vitro* landing model. Second, relative strain was only measured between the barbs of the DVRT at and near the surface of the ACL. The transducer does not allow surface strain measurements elsewhere on the ligament or

measurements throughout the depth of the ligament. Third, knee specimens were tested in isolation, without adjacent segments, such as the foot or trunk, therefore disregarding their role during landings. For example, the ankle joint can absorb energy during landings[52] and the position of the trunk can affect knee loads.[18,31] However, eliminating confounding variables such as trunk position and energy absorbed at the ankle allowed more consistent loading magnitudes within and across knee specimens, and thus the isolation of our variables of interest. Last, although the major knee muscles were represented during the landings, only their tensile resistance to stretch, thus their eccentric behavior, and their monoarticular actions were simulated. This means that the hamstrings tensile force was minimal compared to the quadriceps, which is not the case *in vivo*.[16,40] Nagano et al.[40] reported hamstrings activity to be approximately 25% of that of the quadriceps during a single-leg landing in male and female athletes, a higher ratio than that of the *in vitro* landing model.[44] Also, the hamstrings act isometrically when the knee and hip joint flex in a simulated jump landing with an upright trunk.[42] Given that hamstrings are known to be agonists to the ACL because they limit anterior tibial translation,[32,36,38] the *in vitro* model may have overestimated ACL strain. In fact, Withrow et al.[64] revealed that increasing hamstrings force significantly decreased peak ACL strain in a similar *in vitro* landing model. However, hamstring force was increased to 63% of that of the quadriceps force, which may have overrepresented the hamstrings force produced during *in vivo* landings.

Chapters 2 and 3 of this dissertation addressed only the effect of limited range of internal femoral rotation caused by a sudden kinematic constraint, as someone with FAI will experience when bone-on-bone contact occurs. It does not simulate limited rotation due to soft tissue tension, for example. This type of limitation may reduce the sudden internal tibial deceleration seen in the model with a sudden stop in femoral rotation because the femur would encounter

increasing resistance to internal rotation instead of an immediate high resistance to rotation. Although both *in vitro* models may be realistic, it is unknown why and how hip internal rotation was limited in the athletes having suffered an ACL injury.[4,12,13]

In Chapter 3, an ACL fatigue failure mechanism was investigated with an *in vitro* model, and therefore does not take into account the role of adaptive biological responses. Although no remodeling occurs in a completely ruptured human ACL,[39] it is not known if it occurs in intact or partially injured ACLs. If it does occur, it would be critical to know its rate of remodeling for ACL injury prevention and rehabilitation purposes. We can probably assume that remodeling occurs slowly, over several months, since Type 1 collagen, the basic unit of the ACL,[48] has a slow turnover rate.[60] Consequently, the role played by remodeling and healing is most likely minimal over periods of days or even weeks. Therefore, results obtained from the *in vitro* model presented in Chapter 3 reflect ACL behavior before any such remodeling can occur, and thus cannot be generalized to ACL fatigue occurring over a longer time period.

Although the microscopic anatomy of human tissue can provide useful insights, such information has its limitations. First, the tissue samples only provide a snapshot in time. The enthesis can be described in terms of type and amount of tissue present and shape, but it is nearly impossible to know the “whys” and “hows”. We can only speculate. Due to the nature of cadaver work, the physical activity history of the donors was unknown. This is especially important if the characteristics of an enthesis reflect the forces applied to it.[5,14,15,20] Loads exceeding the enthesis’ remodeling threshold can induce entheseal trauma and micro-trauma, thus producing changes at the enthesis.[62] Second, the tissue samples only provide a snapshot in space. Assumptions are made that the two-dimensional images of the entheses are representative of a three-dimensional

structure. Validating the use of such images with three-dimensional images obtained with a nanofocus computed tomography, for example, would be of interest.

A final limitation is the lack of any tissue material properties for the specimens whose microscopic anatomy was studied in this dissertation. Testing of material properties has to be conducted on fresh or thawed fresh-frozen specimens, but would not yield valid results if conducted on the plastic-embedded specimens prepared for Chapters 4-5. Regional tests of material properties might include nanoindentation tests of hardness,[1,17,23,25] for example. The lack of such tests is unfortunate because their results could have provided insights into the regional differences found in the microscopic anatomy of the ACL entheses. One might expect the entheseal regions that experience large localized strains to have adapted structures and/or material properties to cope with these high strains, in the same way that under Wolff's law,[66] bone that is highly loaded remodels to become stronger by increasing its size and/or density. So, if one examined the arrangement and diameters of the collagen fibrils and fibers through light microscopy or electron microscopy, one might also find evidence of such regional hypertrophy within the entheses. Nonetheless, Chapters 4 and 5 do give a better description of the microscopic anatomy of the ACL entheses than has been available hitherto.

In summary, this dissertation provides important insights into why athletes with a restricted passive range internal rotation at the hip are at higher risk of sustaining an ACL injury. Results obtained from an *in vitro* simulated pivot landing model suggest that limiting hip internal rotation increases peak ACL strain and risk of an ACL fatigue failure by increasing internal tibial rotation and coupled anterior tibial translation. Screening for restrictions in hip internal rotation to prevent ACL ruptures and reruptures, therefore, is recommended. This dissertation also provides insight into the reason the majority of ACL ruptures occur near its femoral enthesis,

with the PL fibers being vulnerable during pivot landings. The analyses of the microscopic anatomy of the ACL entheses suggest that the femoral enthesis is subjected to systematically higher stresses than the tibial enthesis, especially the PL fibers' femoral enthesis during pivot landings.

6.4 References

1. Aifantis KE, Shrivastava S, Odegard GM. (2011) Transverse mechanical properties of collagen fibers from nanoindentation. *J Mater Sci Mater Med*, 22(6): 1375-81.

2. Baek GH, Carlin GJ, Vogrin TM, Woo SL, Harner CD. (1998) Quantitative analysis of collagen fibrils of human cruciate and meniscofemoral ligaments. *Clin Orthop Relat Res*,(357): 205-11.

3. Bedi A, Kelly BT. (2013) Femoroacetabular impingement. *J Bone Joint Surg Am*, 95(1): 82-92.

4. Bedi A, Warren RF, Wojtys EM, Oh YK, Ashton-Miller JA, Oltean H, Kelly BT. (2014) Restriction in hip internal rotation is associated with an increased risk of ACL injury. *Knee Surg Sports Traumatol Arthrosc*, Sept 12. [Epub ahead of print].

5. Benjamin M, Evans EJ, Rao RD, Findlay JA, Pemberton DJ. (1991) Quantitative differences in the histology of the attachment zones of the meniscal horns in the knee joint of man. *J Anat*, 177: 127-34.

6. Boden BP, Dean GS, Feagin JA, Jr., Garrett WE, Jr. (2000) Mechanisms of anterior cruciate ligament injury. *Orthopedics*, 23(6): 573-8.

7. Brandon ML, Haynes PT, Bonamo JR, Flynn MI, Barrett GR, Sherman MF. (2006) The association between posterior-inferior tibial slope and anterior cruciate ligament insufficiency. *Arthroscopy*, 22(8): 894-9.

8. Butler DL, Sheh MY, Stouffer DC, Samaranayake VA, Levy MS. (1990) Surface strain variation in human patellar tendon and knee cruciate ligaments. *J Biomech Eng*, 112(1): 38-45.

9. Canadian Sport For Life, *Play safe: physical literacy and injury prevention guide for leaders*. Retrieved Nov 2014.

10. Durselen L, Claes L, Kiefer H. (1995) The influence of muscle forces and external loads on cruciate ligament strain. *Am J Sports Med*, 23(1): 129-36.

11. Duthon VB, Barea C, Abrassart S, Fasel JH, Fritschy D, Menetrey J. (2006) Anatomy of the anterior cruciate ligament. *Knee Surg Sports Traumatol Arthrosc*, 14(3): 204-13.

12. Ellera Gomes JL, de Castro JV, Becker R. (2008) Decreased hip range of motion and noncontact injuries of the anterior cruciate ligament. *Arthroscopy*, 24(9): 1034-7.

13. Ellera Gomes JL, Palma HM, Ruthner R. (2014) Influence of hip restriction on noncontact ACL rerupture. *Knee Surg Sports Traumatol Arthrosc*, 22(1): 188-91.

14. Evans EJ, Benjamin M, Pemberton DJ. (1990) Fibrocartilage in the attachment zones of the quadriceps tendon and patellar ligament of man. *J Anat*, 171: 155-62.

15. Evans EJ, Benjamin M, Pemberton DJ. (1991) Variations in the amount of calcified tissue at the attachments of the quadriceps tendon and patellar ligament in man. *J Anat*, 174: 145-51.

16. Fagenbaum R, Darling WG. (2003) Jump landing strategies in male and female college athletes and the implications of such strategies for anterior cruciate ligament injury. *Am J Sports Med*, 31(2): 233-40.

17. Ferguson VL, Bushby AJ, Boyde A. (2003) Nanomechanical properties and mineral concentration in articular calcified cartilage and subchondral bone. *J Anat*, 203(2): 191-202.

18. Frank B, Bell DR, Norcross MF, Blackburn JT, Goerger BM, Padua DA. (2013) Trunk and hip biomechanics influence anterior cruciate loading mechanisms in physically active participants. *Am J Sports Med*, 41(11): 2676-83.

19. Gabriel MT, Wong EK, Woo SL, Yagi M, Debski RE. (2004) Distribution of in situ forces in the anterior cruciate ligament in response to rotatory loads. *J Orthop Res*, 22(1): 85-9.

20. Gao J, Messner K. (1996) Quantitative comparison of soft tissue-bone interface at chondral ligament insertions in the rabbit knee joint. *J Anat*, 188 (Pt 2): 367-73.

21. Harner CD, Livesay GA, Kashiwaguchi S, Fujie H, Choi NY, Woo SL. (1995) Comparative study of the size and shape of human anterior and posterior cruciate ligaments. *J Orthop Res*, 13(3): 429-34.

22. Hart JM, Garrison JC, Palmieri-Smith R, Kerrigan DC, Ingersoll CD. (2008) Lower extremity joint moments of collegiate soccer players differ between genders during a forward jump. *J Sport Rehabil*, 17(2): 137-47.

23. Hauch KN, Oyen ML, Odegard GM, Haut Donahue TL. (2009) Nanoindentation of the insertional zones of human meniscal attachments into underlying bone. *J Mech Behav Biomed Mater*, 2(4): 339-47.

24. Hosseini A, Gill TJ, Li G. (2009) In vivo anterior cruciate ligament elongation in response to axial tibial loads. *J Orthop Sci*, 14(3): 298-306.

25. Hu K, Radhakrishnan P, Patel RV, Mao JJ. (2001) Regional structural and viscoelastic properties of fibrocartilage upon dynamic nanoindentation of the articular condyle. *J Struct Biol*, 136(1): 46-52.

26. Jordan SS, DeFrate LE, Nha KW, Papannagari R, Gill TJ, Li G. (2007) The in vivo kinematics of the anteromedial and posterolateral bundles of the anterior cruciate ligament during weightbearing knee flexion. *Am J Sports Med*, 35(4): 547-54.

27. Kim J, DeLancey JO, Ashton-Miller JA. (2011) Why does the pubovisceral muscle fail at its enthesis, and not elsewhere, during the second stage of labor? A computational study. Presented at the *Annual Meeting of the American Society of Biomechanics*. Aug 10-13. Long Beach, CA, USA.

28. Kimura Y, Ishibashi Y, Tsuda E, Yamamoto Y, Tsukada H, Toh S. (2010) Mechanisms for anterior cruciate ligament injuries in badminton. *Br J Sports Med*, 44(15): 1124-7.

29. Koga H, Nakamae A, Shima Y, Iwasa J, Myklebust G, Engebretsen L, Bahr R, Krosshaug T. (2010) Mechanisms for noncontact anterior cruciate ligament injuries: knee joint kinematics in 10 injury situations from female team handball and basketball. *Am J Sports Med*, 38(11): 2218-25.

30. Krosshaug T, Nakamae A, Boden BP, Engebretsen L, Smith G, Slauterbeck JR, Hewett TE, Bahr R. (2007) Mechanisms of anterior cruciate ligament injury in basketball: video analysis of 39 cases. *Am J Sports Med*, 35(3): 359-67.

31. Kulas AS, Hortobagyi T, DeVita P. (2012) Trunk position modulates anterior cruciate ligament forces and strains during a single-leg squat. *Clin Biomech (Bristol, Avon)*, 27(1): 16-21.

32. Li G, Rudy TW, Sakane M, Kanamori A, Ma CB, Woo SL. (1999) The importance of quadriceps and hamstring muscle loading on knee kinematics and in-situ forces in the ACL. *J Biomech*, 32(4): 395-400.

33. Lipps DB, Oh YK, Ashton-Miller JA, Wojtys EM. (2014) Effect of increased quadriceps tensile stiffness on peak anterior cruciate ligament strain during a simulated pivot landing. *J Orthop Res*, 32(3): 423-30.

34. Lipps DB, Wojtys EM, Ashton-Miller JA. (2013) Anterior cruciate ligament fatigue failures in knees subjected to repeated simulated pivot landings. *Am J Sports Med*, 41(5): 1058-66.

35. Ma J. (2012) Experimental and computational characterizations of native ligaments, tendons and engineered 3-D bone-ligament-bone constructs in the knee. PhD dissertation, University of Michigan: Mechanical Engineering. ProQuest/UMI (Publication No. 3531281).

36. MacWilliams BA, Wilson DR, DesJardins JD, Romero J, Chao EY. (1999) Hamstrings cocontraction reduces internal rotation, anterior translation, and anterior cruciate ligament load in weight-bearing flexion. *J Orthop Res*, 17(6): 817-22.

37. Meyer EG, Baumer TG, Slade JM, Smith WE, Haut RC. (2008) Tibiofemoral contact pressures and osteochondral microtrauma during anterior cruciate ligament rupture due to excessive compressive loading and internal torque of the human knee. *Am J Sports Med*, 36(10): 1966-77.

38. More RC, Karras BT, Neiman R, Fritschy D, Woo SL, Daniel DM. (1993) Hamstrings--an anterior cruciate ligament protagonist. An in vitro study. *Am J Sports Med*, 21(2): 231-7.

39. Murray MM, Martin SD, Martin TL, Spector M. (2000) Histological changes in the human anterior cruciate ligament after rupture. *J Bone Joint Surg Am*, 82-A(10): 1387-97.

40. Nagano Y, Ida H, Akai M, Fukubayashi T. (2007) Gender differences in knee kinematics and muscle activity during single limb drop landing. *Knee*, 14(3): 218-23.

41. Nielsen S, Ovesen J, Rasmussen O. (1984) The anterior cruciate ligament of the knee: an experimental study of its importance in rotatory knee instability. *Arch Orthop Trauma Surg*, 103(3): 170-4.

42. Oh YK. (2011) On the mechanisms of non-contact ACL injury during a simulated jump landing: experimental and theoretical analyses. PhD dissertation, University of Michigan: Mechanical Enineering. ProQuest/UMI (Publication No. 3476808).

43. Oh YK, Beaulieu ML, Lipps DB, Wojtys EM, Ashton-Miller JA. (2013) Is the strain concentration at the femoral enthesis a risk factor for anterior cruciate ligament injury? Presented at the *Annual Meeting of the American Society of Biomechanics*. Sept 4-7. Omaha, NE, USA.

44. Oh YK, Kreinbrink JL, Ashton-Miller JA, Wojtys EM. (2011) Effect of ACL transection on internal tibial rotation in an in vitro simulated pivot landing. *J Bone Joint Surg Am*, 93(4): 372-80.

45. Oh YK, Lipps DB, Ashton-Miller JA, Wojtys EM. (2012) What strains the anterior cruciate ligament during a pivot landing? *Am J Sports Med*, 40(3): 574-83.

46. Olsen OE, Myklebust G, Engebretsen L, Bahr R. (2004) Injury mechanisms for anterior cruciate ligament injuries in team handball: a systematic video analysis. *Am J Sports Med*, 32(4): 1002-12.

47. Parry DA, Barnes GR, Craig AS. (1978) A comparison of the size distribution of collagen fibrils in connective tissues as a function of age and a possible relation between fibril size distribution and mechanical properties. *Proc R Soc Lond B Biol Sci*, 203(1152): 305-21.

48. Petersen W, Tillmann B. (1999) Structure and vascularization of the cruciate ligaments of the human knee joint. *Anat Embryol (Berl)*, 200(3): 325-34.

49. Ren Y, Jacobs BJ, Nuber GW, Koh JL, Zhang LQ. (2010) Developing a 6-DOF robot to investigate multi-axis ACL injuries under valgus loading coupled with tibia internal rotation. *Conf Proc IEEE Eng Med Biol Soc*, 2010: 3942-5.

50. Sakane M, Fox RJ, Woo SL, Livesay GA, Li G, Fu FH. (1997) In situ forces in the anterior cruciate ligament and its bundles in response to anterior tibial loads. *J Orthop Res*, 15(2): 285-93.

51. Schlecht SH. (2012) Understanding entheses: bridging the gap between clinical and anthropological perspectives. *Anat Rec (Hoboken)*, 295(8): 1239-51.

52. Self BP, Paine D. (2001) Ankle biomechanics during four landing techniques. *Med Sci Sports Exerc*, 33(8): 1338-44.

53. Senisik S, Özgürbüz C, Ergün M, Yüksel O, Taskiran E, Islegen C, Ertat A. (2011) Posterior tibial slope as a risk factor for anterior cruciate ligament rupture in soccer players. *J Sports Sci Med*, 10(4): 763-767.

54. Shea KG, Pfeiffer R, Wang JH, Curtin M, Apel PJ. (2004) Anterior cruciate ligament injury in pediatric and adolescent soccer players: an analysis of insurance data. *J Pediatr Orthop*, 24(6): 623-8.

55. Shin CS, Chaudhari AM, Andriacchi TP. (2011) Valgus plus internal rotation moments increase ACL strain more than either alone. *Med Sci Sports Exerc*, 43(8): 1484-91.

56. Siebold R, Fu FH. (2008) Assessment and augmentation of symptomatic anteromedial or posterolateral bundle tears of the anterior cruciate ligament. *Arthroscopy*, 24(11): 1289-98.

57. Sonnery-Cottet B, Archbold P, Cucurulo T, Fayard JM, Bortolletto J, Thaunat M, Prost T, Chambat P. (2011) The influence of the tibial slope and the size of the intercondylar notch on rupture of the anterior cruciate ligament. *J Bone Joint Surg Br*, 93(11): 1475-8.

58. Sonnery-Cottet B, Barth J, Graveleau N, Fournier Y, Hager JP, Chambat P. (2009) Arthroscopic identification of isolated tear of the posterolateral bundle of the anterior cruciate ligament. *Arthroscopy*, 25(7): 728-32.

59. Terauchi M, Hatayama K, Yanagisawa S, Saito K, Takagishi K. (2011) Sagittal alignment of the knee and its relationship to noncontact anterior cruciate ligament injuries. *Am J Sports Med*, 39(5): 1090-4.

60. Thorpe CT, Streeter I, Pinchbeck GL, Goodship AE, Clegg PD, Birch HL. (2010) Aspartic acid racemization and collagen degradation markers reveal an accumulation of damage in tendon collagen that is enhanced with aging. *J Biol Chem*, 285(21): 15674-81.

61. Todd MS, Lalliss S, Garcia E, DeBerardino TM, Cameron KL. (2010) The relationship between posterior tibial slope and anterior cruciate ligament injuries. *Am J Sports Med*, 38(1): 63-7.

62. Villotte S, Knüsel CJ. (2013) Understanding entheseal changes: definition and life course changes. *Int J Osteoarchaeol*, 23(2): 135-146.

63. Vyas S, van Eck CF, Vyas N, Fu FH, Otsuka NY. (2011) Increased medial tibial slope in teenage pediatric population with open physes and anterior cruciate ligament injuries. *Knee Surg Sports Traumatol Arthrosc*, 19(3): 372-7.

64. Withrow TJ, Huston LJ, Wojtys EM, Ashton-Miller JA. (2008) Effect of varying hamstring tension on anterior cruciate ligament strain during in vitro impulsive knee flexion and compression loading. *J Bone Joint Surg Am*, 90(4): 815-23.

65. Woo SL, Hollis JM, Adams DJ, Lyon RM, Takai S. (1991) Tensile properties of the human femur-anterior cruciate ligament-tibia complex. The effects of specimen age and orientation. *Am J Sports Med*, 19(3): 217-25.

66. Woo SL, Kuei SC, Amiel D, Gomez MA, Hayes WC, White FC, Akeson WH. (1981) The effect of prolonged physical training on the properties of long bone: a study of Wolff's Law. *J Bone Joint Surg Am*, 63(5): 780-7.

67. Zaffagnini S, Martelli S, Acquaroli F. (2004) Computer investigation of ACL orientation during passive range of motion. *Comput Biol Med*, 34(2): 153-63.

68. Zantop T, Brucker PU, Vidal A, Zelle BA, Fu FH. (2007) Intraarticular rupture pattern of the ACL. *Clin Orthop Relat Res*, 454: 48-53.

69. Zantop T, Herbort M, Raschke MJ, Fu FH, Petersen W. (2007) The role of the anteromedial and posterolateral bundles of the anterior cruciate ligament in anterior tibial translation and internal rotation. *Am J Sports Med*, 35(2): 223-7.

70. Zeng C, Cheng L, Wei J, Gao SG, Yang TB, Luo W, Li YS, Xu M, Lei GH. (2014) The influence of the tibial plateau slopes on injury of the anterior cruciate ligament: a meta-analysis. *Knee Surg Sports Traumatol Arthrosc*, 22(1): 53-65.

CHAPTER 7

CONCLUSIONS

This dissertation aimed at elucidating the noncontact anterior cruciate ligament (ACL) injury mechanism for which ACL loading history, limited range of hip internal rotation, and the microscopic anatomy of the ACL entheses are contributing factors to injury risk. From the results presented in Chapters 2-5, the following conclusions were drawn.

[1] Peak relative strain of the anteromedial bundle of the ACL (AM-ACL) was inversely related to the available range of internal femoral rotation, with strain increasing 1.3% for every 10° decrease in rotation, during an *in vitro* simulated single-leg pivot landing (Chapter 2).

[2] Peak AM-ACL relative strain was 45% larger in the female knee specimens than the male specimens, regardless of the range of internal femoral rotation, during an *in vitro* simulated single-leg pivot landing (Chapter 2).

[3] Knee specimens with limited range of internal femoral rotation had a risk of ACL fatigue failure more than 17 times greater than those with unrestricted rotation, when accounting for sex of donor, during repetitive *in vitro* simulated single-leg pivot landings (Chapter 3).

[4] The female knee specimens had a risk of ACL fatigue failure nearly 27 times higher than the male specimens, when accounting for range of internal femoral rotation, during

repetitive *in vitro* simulated single-leg pivot landings (Chapter 3).

[5] Limiting the available range of internal femoral rotation with a hard stop increased peak ACL strain and risk of ACL fatigue failure by increasing the range of internal tibial rotation and coupled anterior tibial translation during *in vitro* simulated single-leg pivot landings (Chapters 2-3).

[6] The femoral enthesis of the ACL, especially of the posterolateral (PL) fibers, is vulnerable to failure via ligament fatigue during repetitive *in vitro* simulated single-leg pivot landings. All ACLs that failed via a macroscopic tear ruptured at the femoral enthesis, including that of the PL fibers (Chapter 3).

[7] The femoral and tibial entheses of the ACL are fibrocartilaginous entheses. They comprised four distinct zones of tissue: dense fibrous connective tissue, uncalcified fibrocartilage, calcified fibrocartilage, and bone (Chapter 4-5).

[8] The human ACL femoral enthesis had 43% more calcified fibrocartilage, 226% more uncalcified fibrocartilage and a nearly 4-fold more acute ligament entheseal attachment angle than the tibial enthesis. The differences in fibrocartilage quantity were particularly pronounced in the central region of the entheses (Chapter 4).

[9] The quantity of fibrocartilage was relatively uniform in the human ACL tibial enthesis, but rather heterogeneous in the femoral enthesis (Chapters 4-5).

[10] At the human ACL femoral enthesis, systematic regional differences exist in the quantity of fibrocartilage and ligament entheseal attachment angle. There was more calcified and uncalcified fibrocartilage in the inferior region of the origin of the anteromedial (AM)

fibers than that of the PL fibers and the superior regions. These fibers originated from the femur at an angle six times greater than the PL fibers (Chapter 5).

[11] The shape of the femoral entheseal surface varies within an enthesis and between donors, but bilateral similarity exists. Six entheseal surface shapes predominated, with shape being correlated bilaterally (Chapter 5).

CHAPTER 8

RECOMMENDATIONS FOR FUTURE RESEARCH

The long-term goal of this research theme is to prevent ACL injuries to reduce the enormous health and financial burden associated with these injuries.[5,7,11] This dissertation aimed at gaining a better understanding of the pathomechanics of ACL injuries as a step toward bridging the gap between the knowledge derived from research and simple, cost-effective injury prevention tools for clinical practice. Currently, effective preventive strategies continue to elude us. This chapter, therefore, presents recommendations for future research aimed at bridging this gap.

8.1 Restriction in Hip Internal Rotation

In Chapter 2, an inverse relation was revealed between the available range of internal femoral rotation and peak relative strain of the anteromedial bundle of the ACL (AM-ACL) in an *in vitro* landing model. A limitation of this work, however, was that it only addressed the effect of limited rotation because of a sudden stop, and not that due to a more gradual decrease in rotation. Therefore, it simulated a bone-on-bone contact as someone with femoroacetabular impingement may experience, but not a volitional increase in hip muscle tension, for example. It is possible for an athlete to increase muscle tension during the initial contact period of a landing. A muscle can reach 50% of its maximum voluntary tension in approximately 90 ms,[19] which is similar to the time period during which landing forces peak.[13,14] Muscle tensile stiffness, which is proportional to muscle tension,[2] will also increase in concert with muscle tension. It would be of

interest, therefore, to replicate the experimental protocol used in Chapter 2 with gradual decreases in rotation (instead of sudden stops) to determine the effect of limited internal femoral rotation due to an increase in hip soft tissue restraints on peak ACL strain. This would be beneficial because we do not know how and why hip internal rotation was habitually limited in the athletes who suffered an ACL injury.[1,3,4]

Chapters 2-3 explained why athletes with restricted passive range of internal rotation at the hip have a greater risk of rupturing and rerupturing their ACL.[1,3,4] This relation between hip range of motion and injury risk, however, was investigated retrospectively. Future research, therefore, should translate the *in vitro* findings of this dissertation *in vivo* and prospectively confirm that limited hip internal rotation is a risk factor for ACL injury. Such prospective research efforts would allow for quantification of injury risk based on the degree of limited range of hip internal rotation, thus extending the work of Bedi et al.[1] who predicted injury risk with a statistical model. Given that several other contributing factors to ACL injury risk exist, such as a steep posteriorly directed slope of the lateral tibial plateau,[9,15,20,23] a small ACL,[9,10] and high estrogen levels,[8,16,22] further data could be collected to determine the relative importance of limited hip internal rotation and additional factors of interest. Also, injury risk should be quantified separately for males and females, since ACL injury rates are higher among females.[17,21]

To extend the work of Lipps et al.[10] and that presented in Chapter 3 on ACL fatigue failures, it is important to establish the relation between ACL load (or knee load as a surrogate) and number of cycles to ACL injury *in vivo* in the field. However, a reoccurring challenge in ACL injury research, among other areas, is coming up with accurate, noninvasive, but relatively simple methods to quantify joint mechanics outside the laboratory. I challenge the biomechanics,

engineering, and research community as a whole to develop such an innovative tool. One promising avenue might be to use of body-worn miniature wireless inertial measurement units.[12,18] This technology has potential for estimating joint reaction forces,[12] as well as joint kinematics.[18] Eventually, such a tool could allow for continuous monitoring of knee loading magnitude and frequency, as well as other injury risk factors.

8.2 Microscopic Anatomy of the ACL Entheses

In Chapter 3, several types of ACL fatigue failure occurred during *in vitro* repeated pivot landings: (a) complete and partial tears at the femoral enthesis, especially of the posterolateral (PL) fibers; (b) permanent elongations where no macroscopic evidence of rupture was present, but a 3-mm increase in cumulative anterior tibial translation occurred; and (c) tibial avulsions. Hence, failure state was based on macroscopic evidence or ligament behavior. Microscopic damage, however, was not investigated. It would be useful, therefore, to perform a similar study (Chapter 3) and assess damage on a microscopic level, with histological or nanofocus computed tomography techniques, for example. It could provide valuable insight into the ACL fatigue injury mechanism that cannot be obtained with *in vivo* experiments (in humans, at least), despite that such an *in vitro* investigation would not account for the biological responses of the ACL and its entheses. Coupled with the baseline histological data presented in Chapters 4-5, bilateral microscopic differences between tested and untested specimens could be assessed. It also would be useful to assess tested knee specimens for microscopic evidence prior to microscopic failure. Perhaps it would provide additional insight into the development of ACL fatigue failures.

The anatomical studies of Chapters 4-5 did not permit an investigation of the regional and bilateral variation in the viscoelastic material properties of the ACL or its entheses. Clearly, the ultimate tensile strength and ultimate tensile strain of the different regions of the enthesis help

determine under what conditions and where it will fail under a single load or under cyclic loading. Hence, measuring these material properties is an essential step in this line of research. It would also be important to know how age, sex, training, and detraining influence such properties, as well as the time period during which training/detraining changes occur.

Lastly, the histological work of Chapters 4-5 raised several questions regarding the development and remodeling of entheses, and specifically, that of ACL entheses. Future studies, therefore, are warranted to understand how entheses develop and how they respond to various loading types, magnitudes, and frequencies in terms of tissue quantity and shape. This work would have to utilize animal models since the biological responses of entheseal tissue cannot easily be investigated in live humans without using ionizing radiation, which would be unethical, or new forms of high resolution ultrasound imaging. I recommend investigating the potential for ligamentous and entheseal tissue to develop and remodel with training before and after puberty. This work could answer questions such as:

- Can an entheseal region develop and remodel, if loaded repeatedly, to withstand greater stress before damage occurs?
- If so, is its greatest potential for remodeling around puberty?
- Can the mechanical properties (i.e., strain/stress at failure) of the ACL be improved with training?

Revealing a potential for such development and remodeling of the ACL would provide further evidence that the human ACL can be "trained" and hypertrophied *in vivo*[6] as a means to potentially decrease its risk of injury.

8.3 References

1. Bedi A, Warren RF, Wojtys EM, Oh YK, Ashton-Miller JA, Oltean H, Kelly BT. (2014) Restriction in hip internal rotation is associated with an increased risk of ACL injury. *Knee Surg Sports Traumatol Arthrosc*, Sept 12. [Epub ahead of print].

2. Blanpied P, Smidt GL. (1993) The difference in stiffness of the active plantarflexors between young and elderly human females. *J Gerontol*, 48(2): M58-63.

3. Ellera Gomes JL, de Castro JV, Becker R. (2008) Decreased hip range of motion and noncontact injuries of the anterior cruciate ligament. *Arthroscopy*, 24(9): 1034-7.

4. Ellera Gomes JL, Palma HM, Ruthner R. (2014) Influence of hip restriction on noncontact ACL rerupture. *Knee Surg Sports Traumatol Arthrosc*, 22(1): 188-91.

5. Griffin LY, Albohm MJ, Arendt EA, Bahr R, Beynnon BD, Demaio M, Dick RW, Engebretsen L, Garrett WE, Jr., Hannafin JA, Hewett TE, Huston LJ, Ireland ML, Johnson RJ, Lephart S, Mandelbaum BR, Mann BJ, Marks PH, Marshall SW, Myklebust G, Noyes FR, Powers C, Shields C, Jr., Shultz SJ, Silvers H, Slauterbeck J, Taylor DC, Teitz CC, Wojtys EM, Yu B. (2006) Understanding and preventing noncontact anterior cruciate ligament injuries: a review of the Hunt Valley II meeting, January 2005. *Am J Sports Med*, 34(9): 1512-32.

6. Grzelak P, Podgorski M, Stefanczyk L, Krochmalski M, Domzalski M. (2012) Hypertrophied cruciate ligament in high performance weightlifters observed in magnetic resonance imaging. *Int Orthop*, 36(8): 1715-9.

7. Hewett TE, Myer GD, Ford KR. (2006) Anterior cruciate ligament injuries in female athletes: Part 1, mechanisms and risk factors. *Am J Sports Med*, 34(2): 299-311.

8. Lee CY, Liu X, Smith CL, Zhang X, Hsu HC, Wang DY, Luo ZP. (2004) The combined regulation of estrogen and cyclic tension on fibroblast biosynthesis derived from anterior cruciate ligament. *Matrix Biol*, 23(5): 323-9.

9. Lipps DB, Oh YK, Ashton-Miller JA, Wojtys EM. (2012) Morphologic characteristics help explain the gender difference in peak anterior cruciate ligament strain during a simulated pivot landing. *Am J Sports Med*, 40(1): 32-40.

10. Lipps DB, Wojtys EM, Ashton-Miller JA. (2013) Anterior cruciate ligament fatigue failures in knees subjected to repeated simulated pivot landings. *Am J Sports Med*, 41(5): 1058-66.

11. Lohmander LS, Ostenberg A, Englund M, Roos H. (2004) High prevalence of knee osteoarthritis, pain, and functional limitations in female soccer players twelve years after anterior cruciate ligament injury. *Arthritis Rheum*, 50(10): 3145-52.

12. McGinnis RS, Hough J, Perkins NC. (2013) Benchmarking the accuracy of inertial measurement units for estimating joint reactions. Presented at the *ASME 2013 International Mechanical Engineering Congress and Exposition*. Nov 15–21. San Diego, CA, USA.

13. Orishimo KF, Kremenic IJ, Pappas E, Hagins M, Liederbach M. (2009) Comparison of landing biomechanics between male and female professional dancers. *Am J Sports Med*, 37(11): 2187-93.

14. Schmitz RJ, Kulas AS, Perrin DH, Riemann BL, Shultz SJ. (2007) Sex differences in lower extremity biomechanics during single leg landings. *Clin Biomech (Bristol, Avon)*, 22(6): 681-8.

15. Senisik S, Özgürbüz C, Ergün M, Yüksel O, Taskiran E, Islegen C, Ertat A. (2011) Posterior tibial slope as a risk factor for anterior cruciate ligament rupture in soccer players. *J Sports Sci Med*, 10(4): 763-767.

16. Shultz SJ, Wideman L, Montgomery MM, Beasley KN, Nindl BC. (2012) Changes in serum collagen markers, IGF-I, and knee joint laxity across the menstrual cycle. *J Orthop Res*, 30(9): 1405-12.

17. Swenson DM, Collins CL, Best TM, Flanigan DC, Fields SK, Comstock RD. (2013) Epidemiology of knee injuries among US high school athletes, 2005/06-2010/11. *Med Sci Sports Exerc*, 45(3): 462-9.

18. Taylor T, Ko S, Mastrangelo C, Bamberg SJ. (2013) Forward kinematics using IMU on-body sensor network for mobile analysis of human kinematics. *Conf Proc IEEE Eng Med Biol Soc*, 2013: 1230-3.

19. Thelen DG, Schultz AB, Alexander NB, Ashton-Miller JA. (1996) Effects of age on rapid ankle torque development. *J Gerontol A Biol Sci Med Sci*, 51(5): M226-32.

20. Todd MS, Lalliss S, Garcia E, DeBerardino TM, Cameron KL. (2010) The relationship between posterior tibial slope and anterior cruciate ligament injuries. *Am J Sports Med*, 38(1): 63-7.

21. Walden M, Hagglund M, Werner J, Ekstrand J. (2011) The epidemiology of anterior cruciate ligament injury in football (soccer): a review of the literature from a gender-related perspective. *Knee Surg Sports Traumatol Arthrosc*, 19(1): 3-10.

22. Yu WD, Liu SH, Hatch JD, Panossian V, Finerman GA. (1999) Effect of estrogen on cellular metabolism of the human anterior cruciate ligament. *Clin Orthop Relat Res*,(366): 229-38.

23. Zeng C, Cheng L, Wei J, Gao SG, Yang TB, Luo W, Li YS, Xu M, Lei GH. (2014) The influence of the tibial plateau slopes on injury of the anterior cruciate ligament: a meta-analysis. *Knee Surg Sports Traumatol Arthrosc*, 22(1): 53-65.

APPENDICES

APPENDIX A

DETAILED METHODS USED FOR THE LOWER LIMB COMPUTATIONAL MODEL IN CHAPTER 2

A lower limb, comprising three rigid bodies (femur, tibia, foot) interconnected by three torsional springs (representing the elastic resistance of the soft tissues of the hip, knee, ankle) in series, was modeled in Adams (MSC Software, Newport, CA, USA) to better interpret the *in vitro* data. The lower limb model was designed to model the intersegmental transfer of axial momentum occurring during pivot landings. The proximal end of the "femur" rigid body was attached to a fixed pelvic point by means of a torsional spring (k_{Hip}), meanwhile the distal end of the "foot" rigid body was free (Figure 2.5A). The "tibia" rigid body was attached to the "femur" and "foot" bodies by means of torsional springs (k_{Knee} and k_{Ankle}, Figure 2.5A).

The mass and moments of inertia of the "femur", "tibia" and "foot" were obtained from Enoka.[1] Segmental mass was based on a total body mass of 73 kg. The rotational stiffnesses used for the springs (k_{Knee} and k_{Ankle}, Figure 2.5A) representing the knee and ankle were obtained from Schmitz and Shultz. The normalized stiffnesses were converted to absolute values using a body mass of 73 kg and a height of 1.74 m. These values for body mass and height were selected based on the average size of the men from which the segmental data were calculated.[1] All model parameters are presented in Table A.1.

A torque of 10 Nm was applied, peaking at 80 ms, about the longitudinal axis of the foot to create angular momentum. Stiffness of the spring representing the hip (k_{Hip}, Figure 2.5A) was

systematically increased from 0.9 Nm/° to 9.4 Nm/° in 0.6-Nm/° increments, in separate trials. This range of stiffness was selected to replicate the range of femoral rotation found in our experimental data. For each hip stiffness, femoral rotation and tibial rotation and torque (relative to the femur) rotation were calculated.

Table A.1 Lower limb model parameters

Parameter	Value
Hip Torsional Spring	
k_{Hip} (Nm/°)	0.9 – 9.4
preload (N)	0
Femur Rigid Body	
mass (kg)	10.3
I_{xx} (kg·m^2)	0.1995
I_{yy} (kg·m^2)	0.1995
I_{zz} (kg·m^2)	0.1000
Knee Torsional Spring	
k_{Knee} (Nm/°)	1.246
preload (N)	0
Tibia Rigid Body	
mass (kg)	3.2
I_{xx} (kg·m^2)	0.0369
I_{yy} (kg·m^2)	0.0387
I_{zz} (kg·m^2)	0.0063
Ankle Torsional Spring	
k_{Ankle} (Nm/°)	2.491
preload (N)	0
Foot Rigid Body	
mass (kg)	1.0
I_{xx} (kg·m^2)	0.0040
I_{yy} (kg·m^2)	0.0044
I_{zz} (kg·m^2)	0.0010

k: spring stiffness; I: moment of inertia; xx: medial-lateral axis; yy: anterior-posterior axis; zz: longitudinal axis; k: torsional stiffness.

A.1 References

1. Enoka RM, *Neuromechanics of Human Movement*. 4th ed. 2008, Champaign, IL, USA: Human Kinetics. 560.

2. Schmitz RJ, Shultz SJ. (2010) Contribution of knee flexor and extensor strength on sex-specific energy absorption and torsional joint stiffness during drop jumping. *J Athl Train*, 45(5): 445-52.

APPENDIX B

COLLECTION OF HISTOLOGICAL IMAGES OF ALL FEMORAL AND TIBIAL ENTHESES OF 15 HUMAN ANTERIOR CRUCIATE LIGAMENTS

This appendix presents the digital images of all histological tissue sections of the femoral and tibial entheses of the anterior cruciate ligament for all 15 specimens of Chapters 4-5. Parts A-D of each figure are histological images of the femoral enthesis, starting from the most antero-superior section to the most postero-inferior section (Figure B.1). Parts E-H of each figure are histological images of the tibial enthesis, starting from the most medial section to the most lateral section (Figure B.1). All sections were stained with toluidine blue.

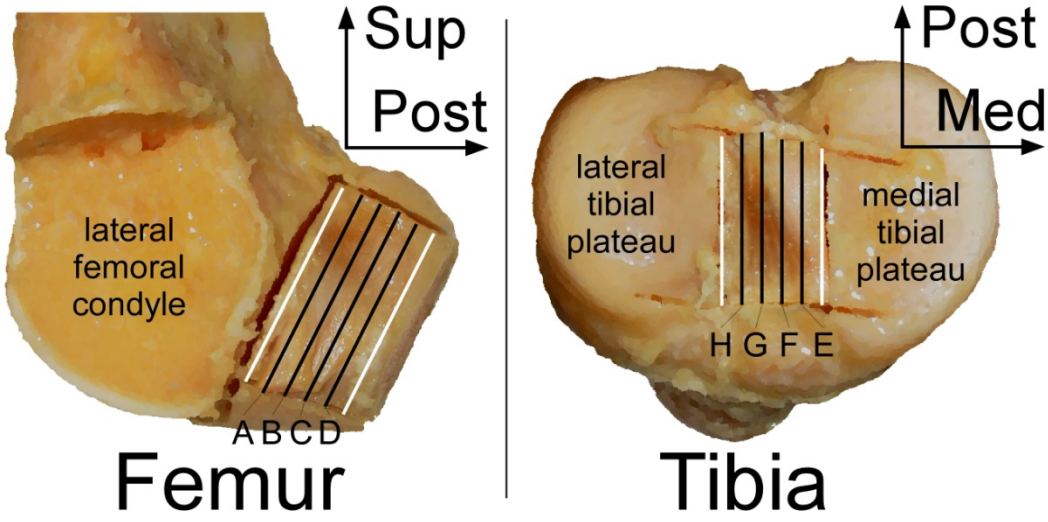

Figure B.1 Location of tissue sections (black lines) whose digital images are presented in this appendix. White lines indicate the edges of the entheses. Letters correspond to the various parts of the following figures. A: 20%; B: 40%; C: 60%; D: 80% of the width of the femoral enthesis. E: 20%; F: 40%; G: 60%; H: 80% of the width of the tibial enthesis.

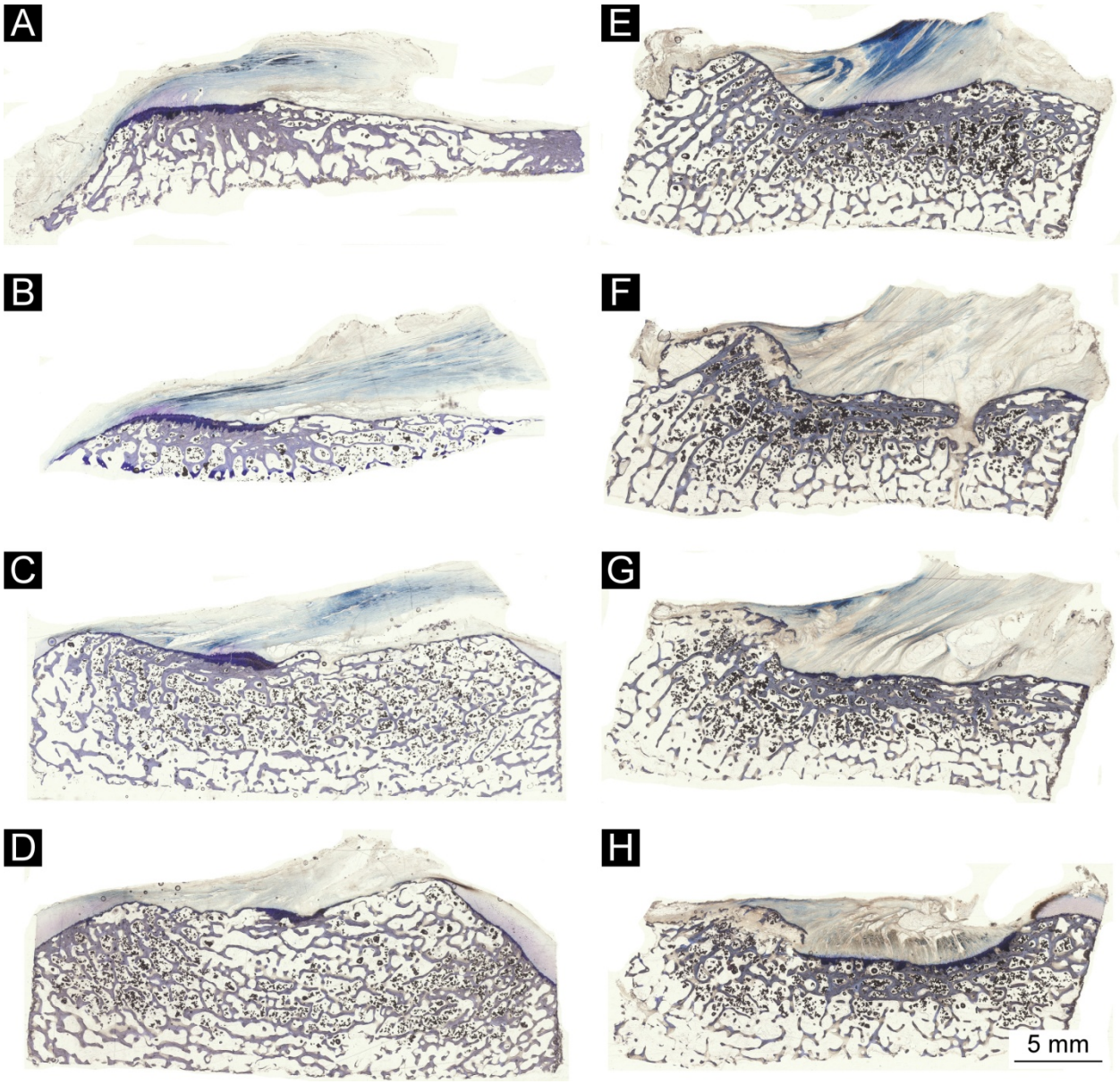

Figure B.2 Histology of the four tissue sections of the left ACL femoral (**A**: 20%; **B**: 40%; **C**: 60%; **D**: 80% of the width of the enthesis) and tibial (**E**: 20%; **F**: 40%; **G**: 60%; **H**: 80% of the width of the enthesis) entheses in specimen #34372.

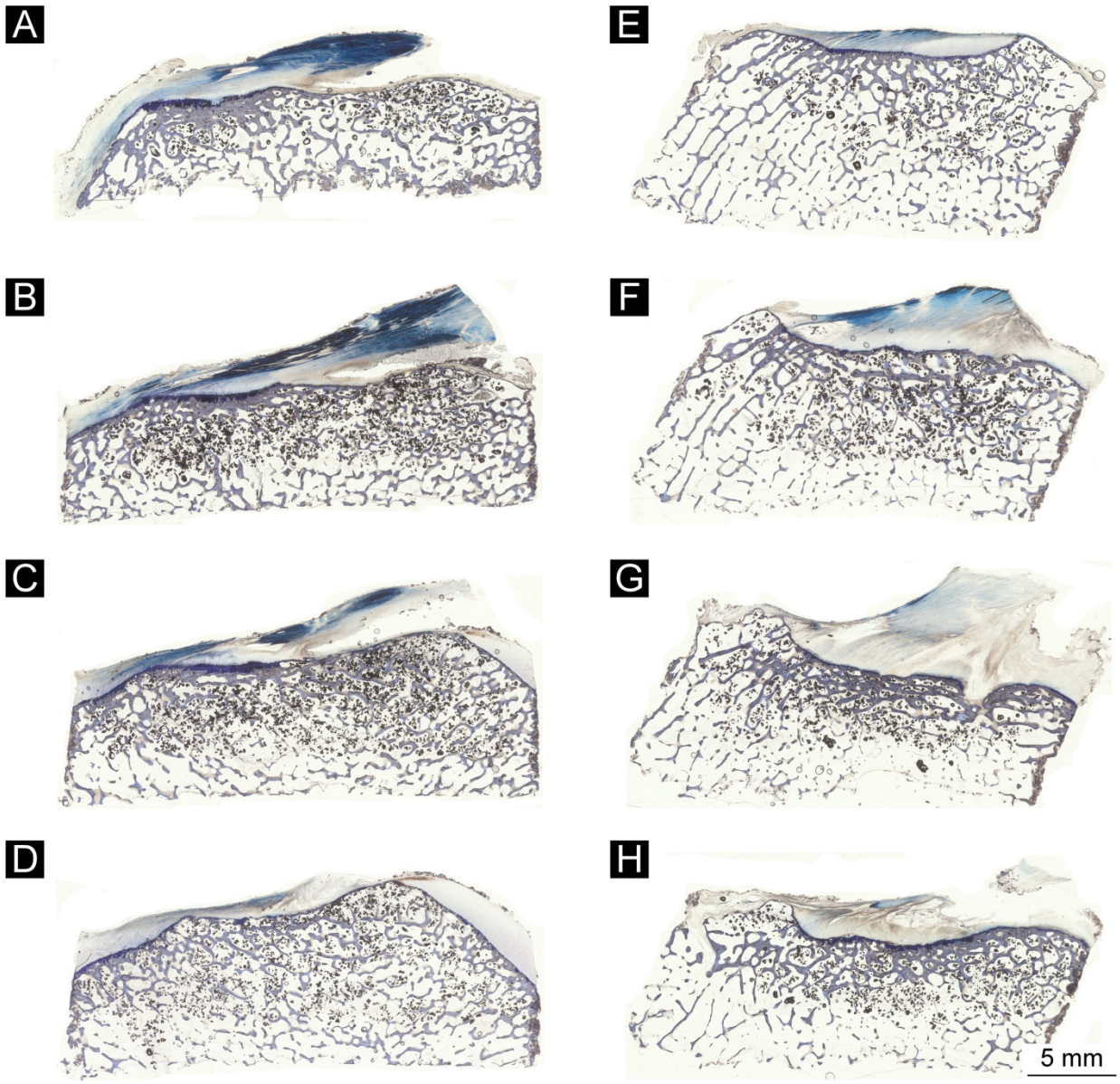

Figure B.3 Histology of the four tissue sections of the left ACL femoral (**A**: 20%; **B**: 40%; **C**: 60%; **D**: 80% of the width of the enthesis) and tibial (**E**: 20%; **F**: 40%; **G**: 60%; **H**: 80% of the width of the enthesis) entheses in specimen #34563.

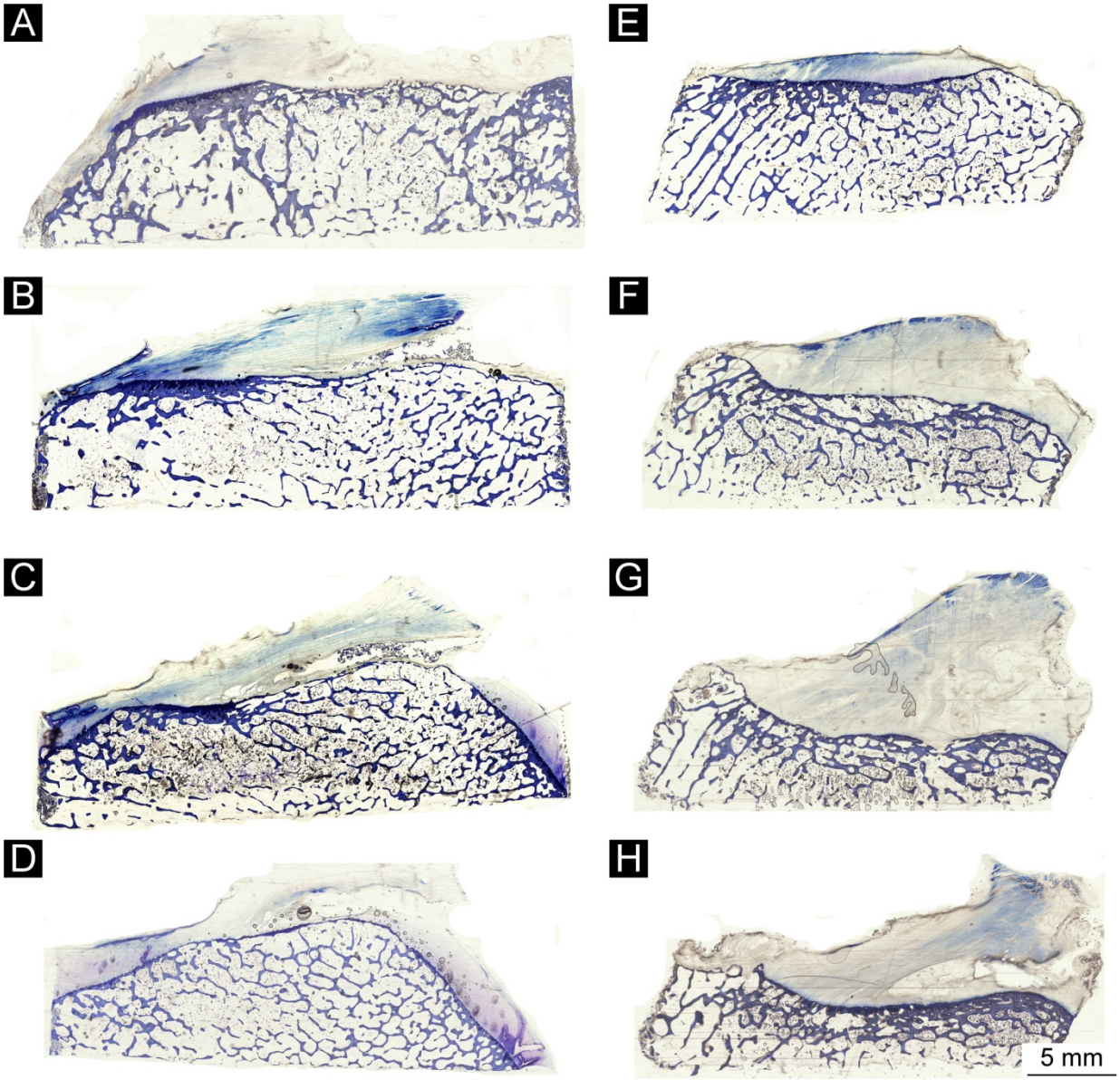

Figure B.4 Histology of the four tissue sections of the right ACL femoral (**A**: 20%; **B**: 40%; **C**: 60%; **D**: 80% of the width of the enthesis) and tibial (**E**: 20%; **F**: 40%; **G**: 60%; **H**: 80% of the width of the enthesis) entheses in specimen #34563.

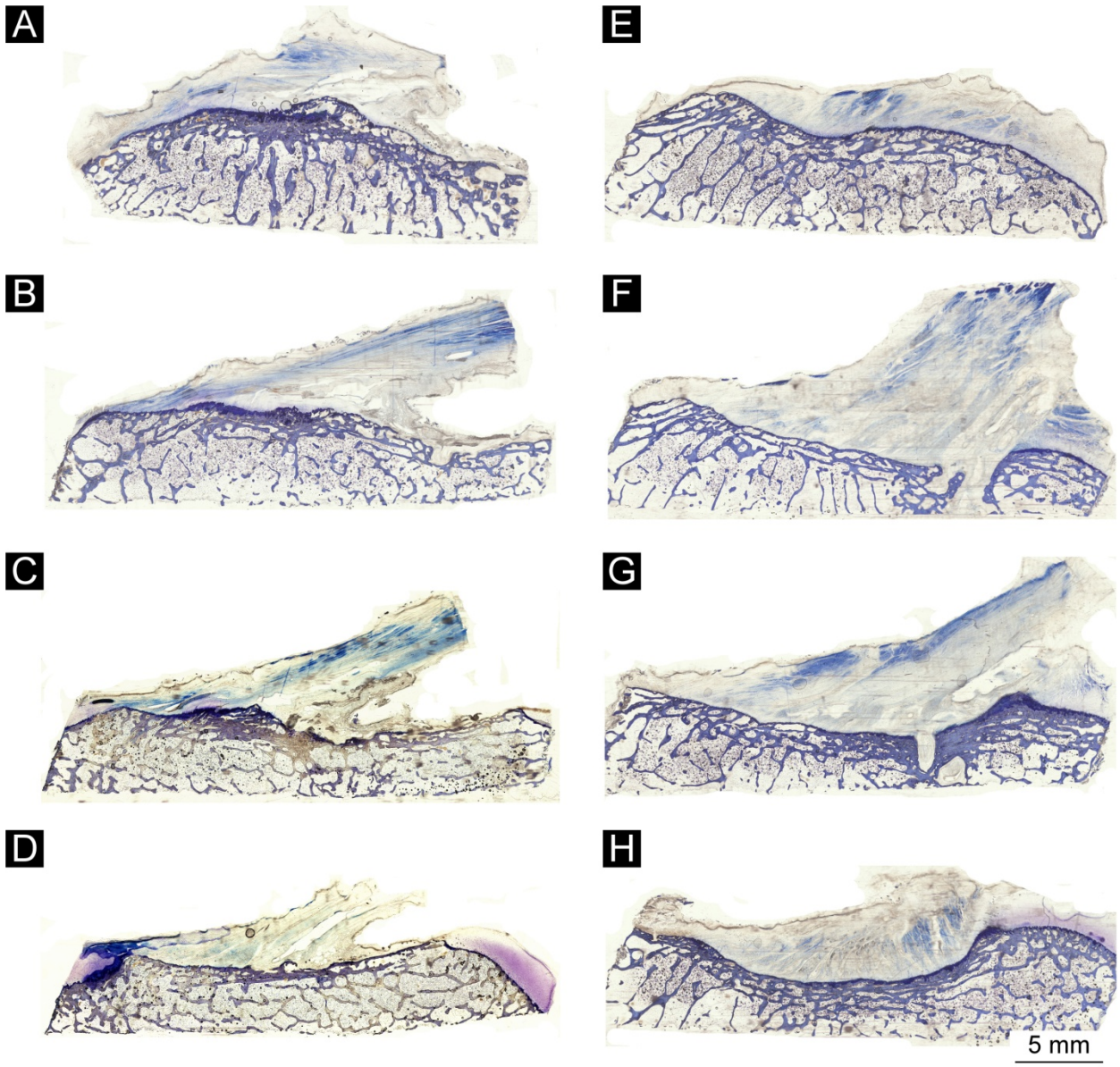

Figure B.5 Histology of the four tissue sections of the left ACL femoral (**A**: 20%; **B**: 40%; **C**: 60%; **D**: 80% of the width of the enthesis) and tibial (**E**: 20%; **F**: 40%; **G**: 60%; **H**: 80% of the width of the enthesis) entheses in specimen #34571.

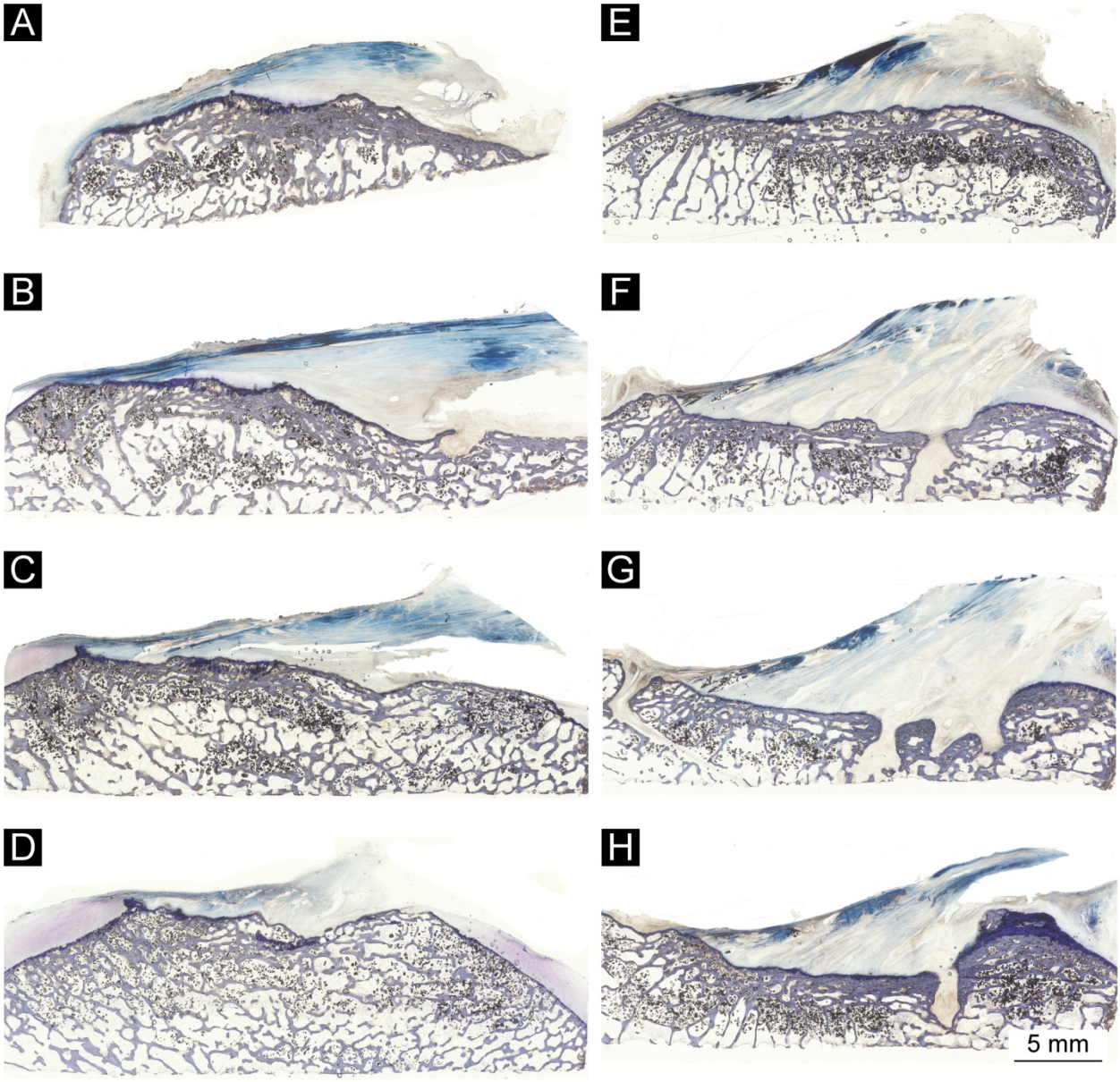

Figure B.6 Histology of the four tissue sections of the right ACL femoral (**A**: 20%; **B**: 40%; **C**: 60%; **D**: 80% of the width of the enthesis) and tibial (**E**: 20%; **F**: 40%; **G**: 60%; **H**: 80% of the width of the enthesis) entheses in specimen #34571.

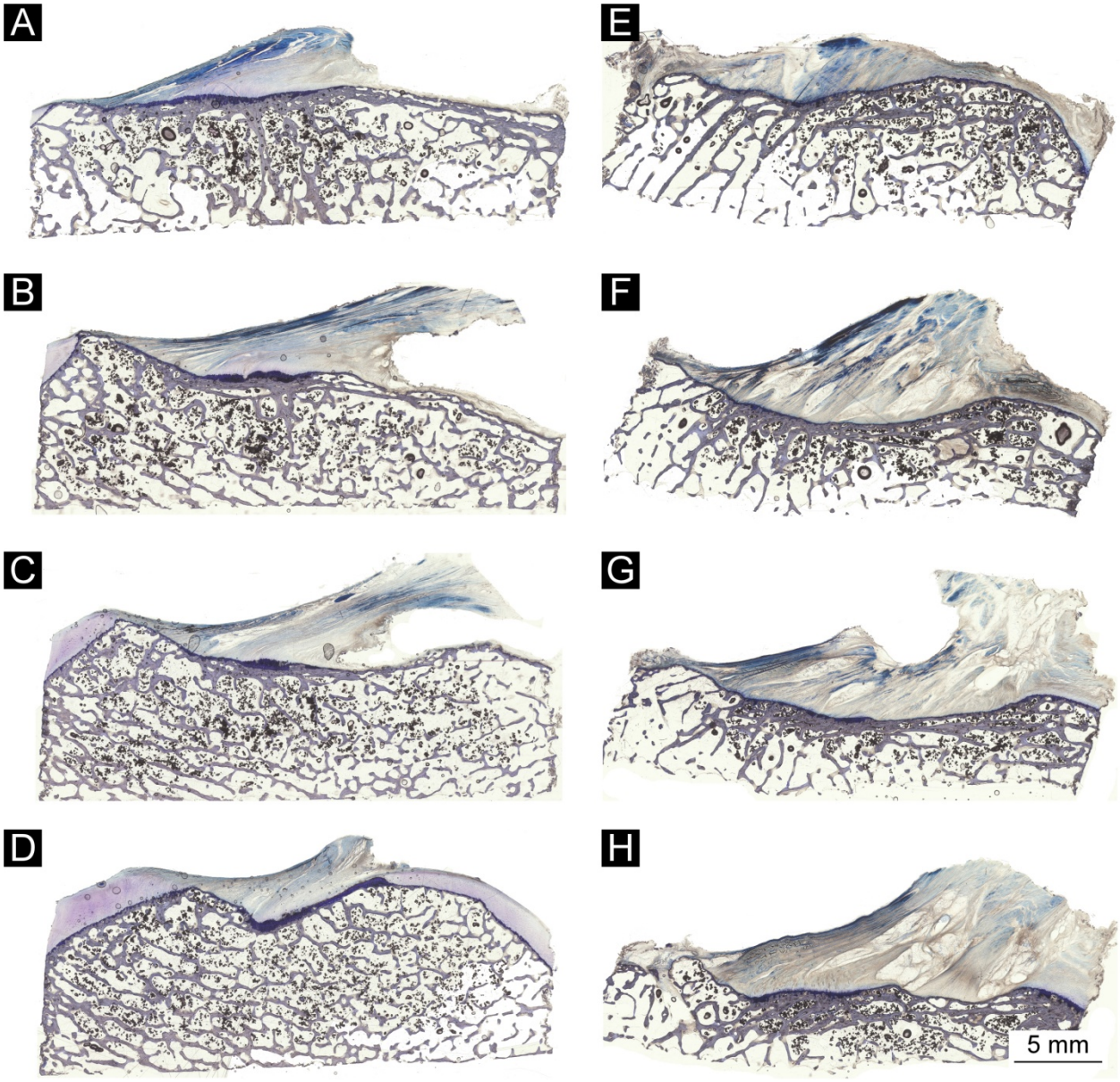

Figure B.7 Histology of the four tissue sections of the left ACL femoral (**A**: 20%; **B**: 40%; **C**: 60%; **D**: 80% of the width of the enthesis) and tibial (**E**: 20%; **F**: 40%; **G**: 60%; **H**: 80% of the width of the enthesis) entheses in specimen #34578.

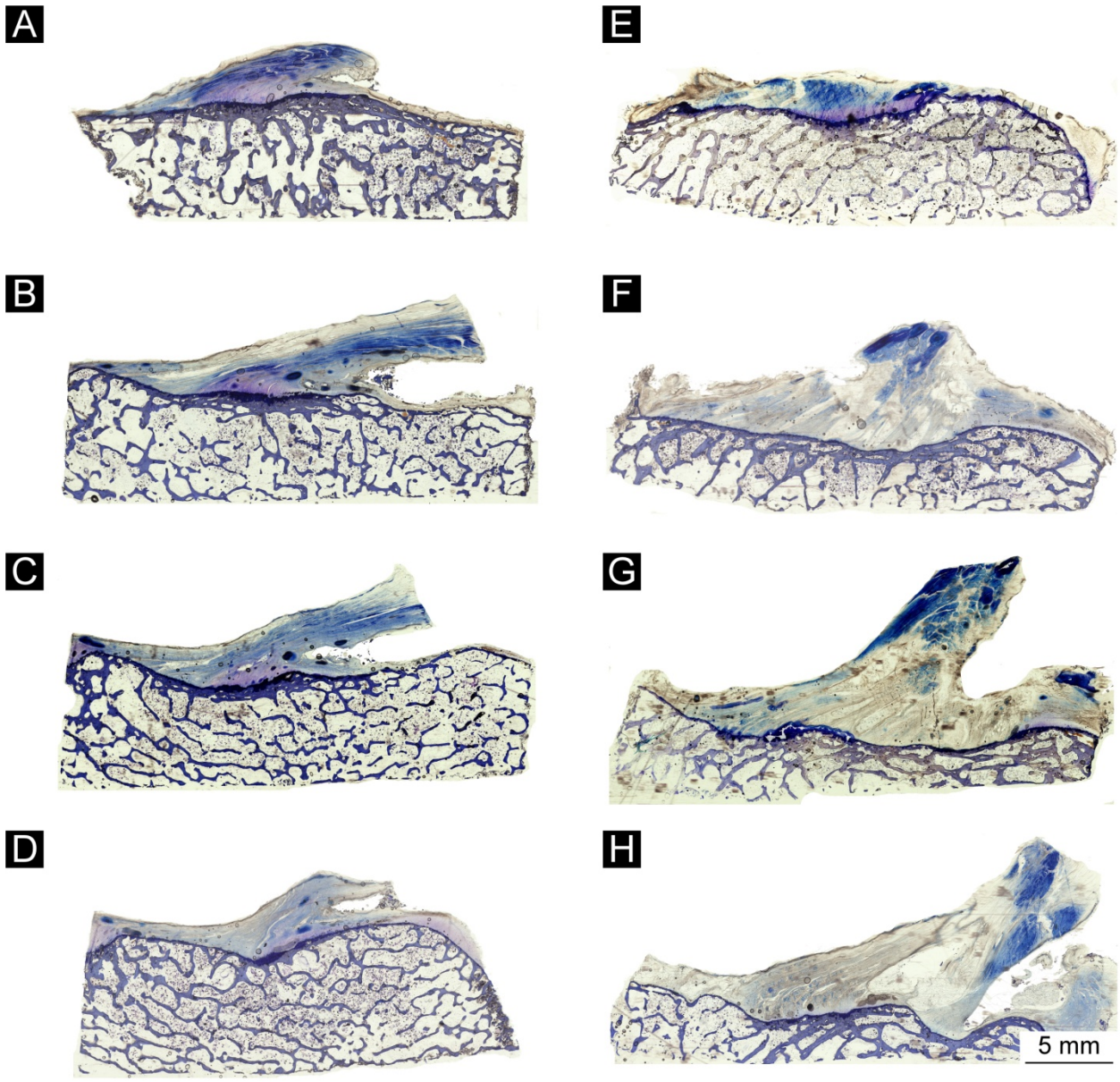

Figure B.8 Histology of the four tissue sections of the right ACL femoral (**A**: 20%; **B**: 40%; **C**: 60%; **D**: 80% of the width of the enthesis) and tibial (**E**: 20%; **F**: 40%; **G**: 60%; **H**: 80% of the width of the enthesis) entheses in specimen #34578.

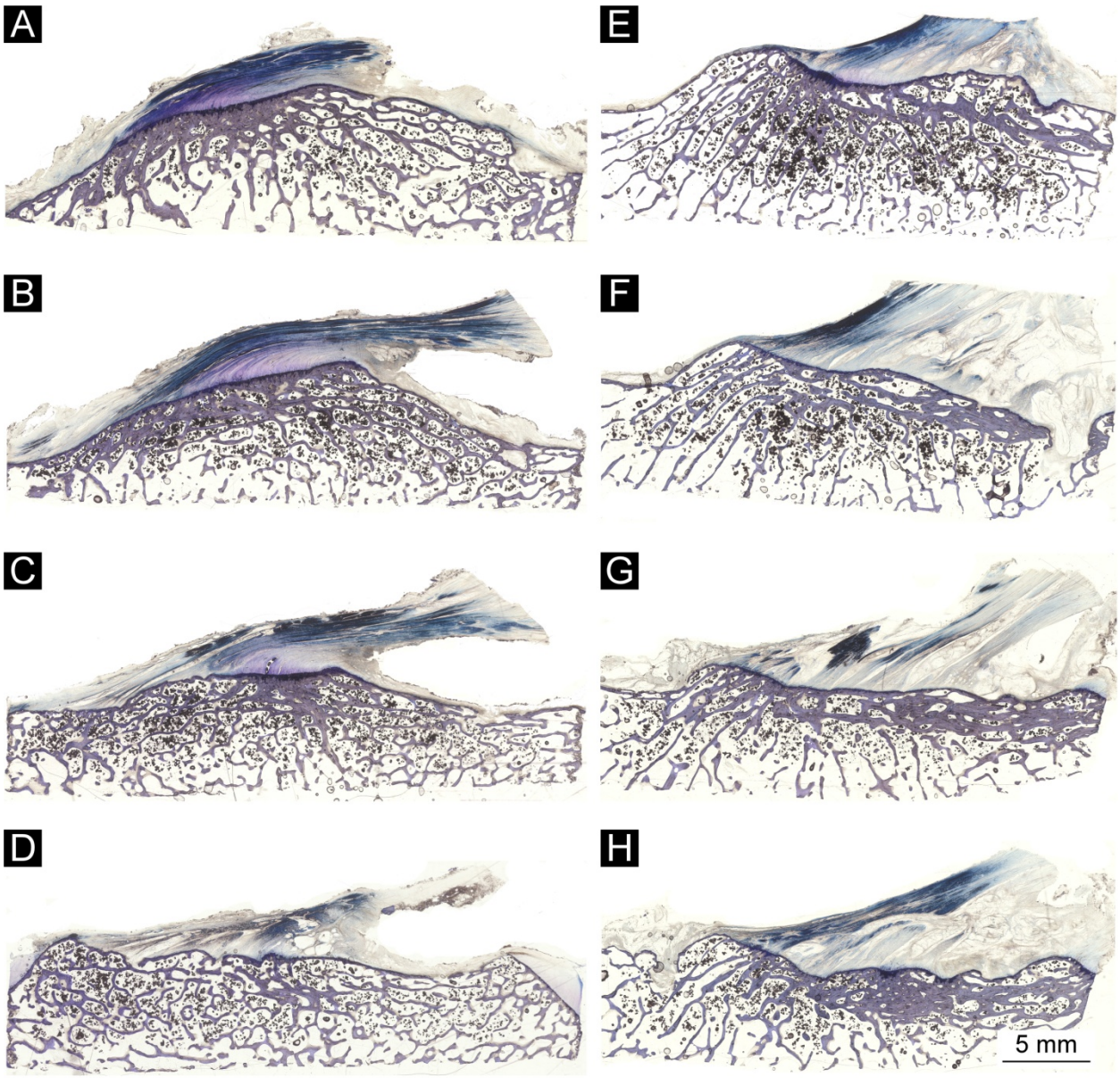

Figure B.9 Histology of the four tissue sections of the left ACL femoral (**A**: 20%; **B**: 40%; **C**: 60%; **D**: 80% of the width of the enthesis) and tibial (**E**: 20%; **F**: 40%; **G**: 60%; **H**: 80% of the width of the enthesis) entheses in specimen #34593.

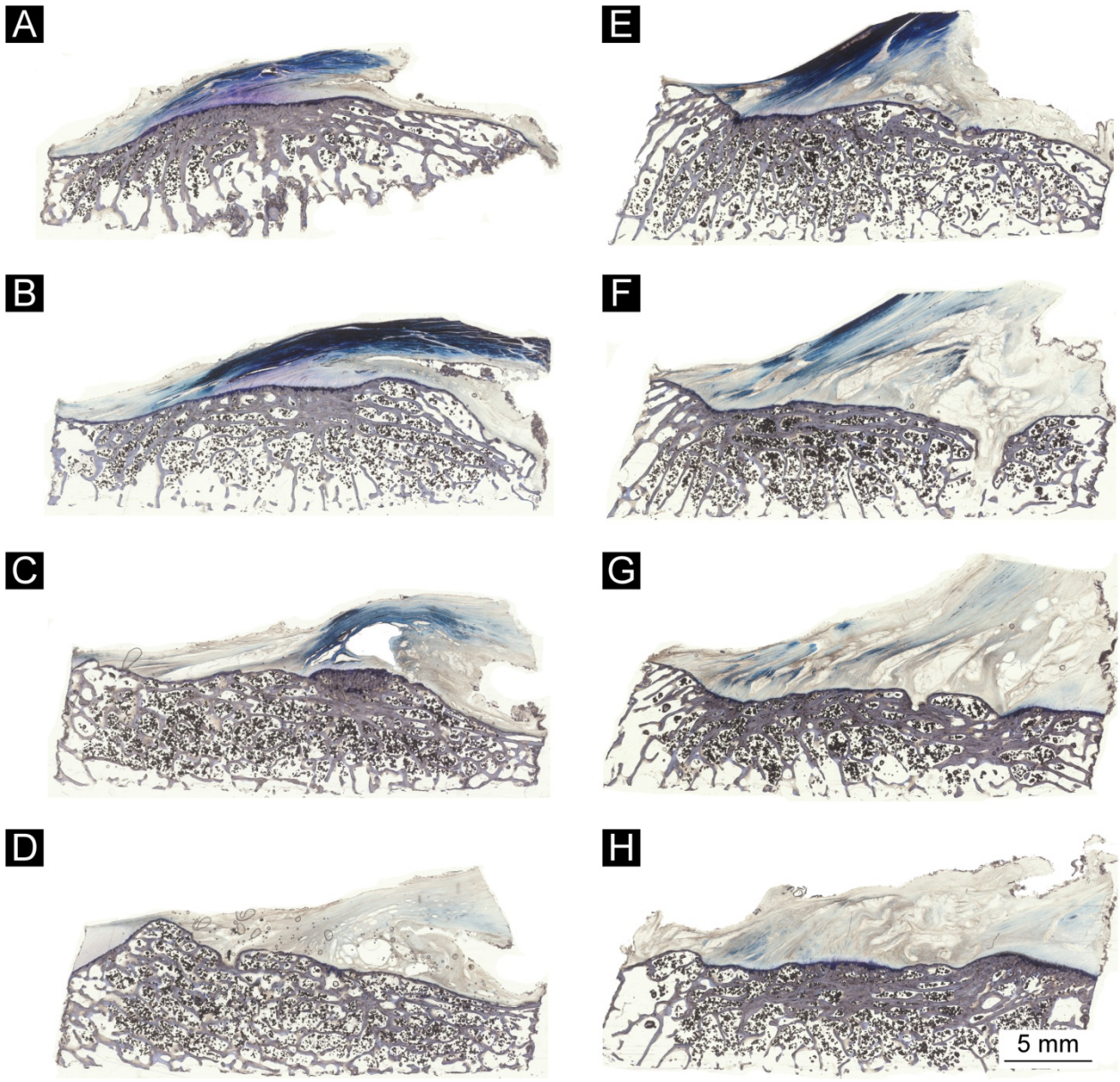

Figure B.10 Histology of the four tissue sections of the right ACL femoral (**A**: 20%; **B**: 40%; **C**: 60%; **D**: 80% of the width of the enthesis) and tibial (**E**: 20%; **F**: 40%; **G**: 60%; **H**: 80% of the width of the enthesis) entheses in specimen #34593.

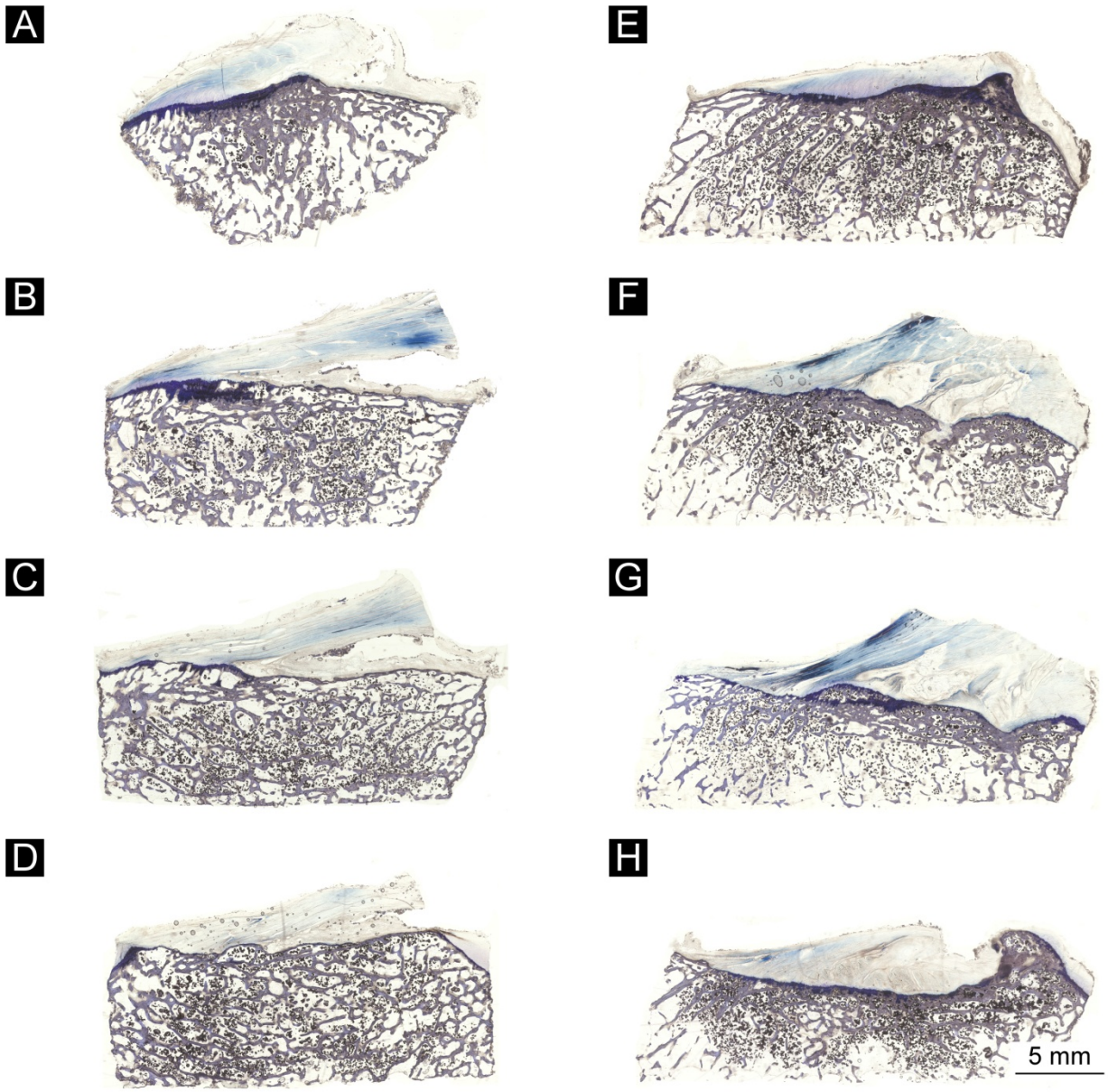

Figure B.11 Histology of the four tissue sections of the left ACL femoral (**A**: 20%; **B**: 40%; **C**: 60%; **D**: 80% of the width of the enthesis) and tibial (**E**: 20%; **F**: 40%; **G**: 60%; **H**: 80% of the width of the enthesis) entheses in specimen #34602.

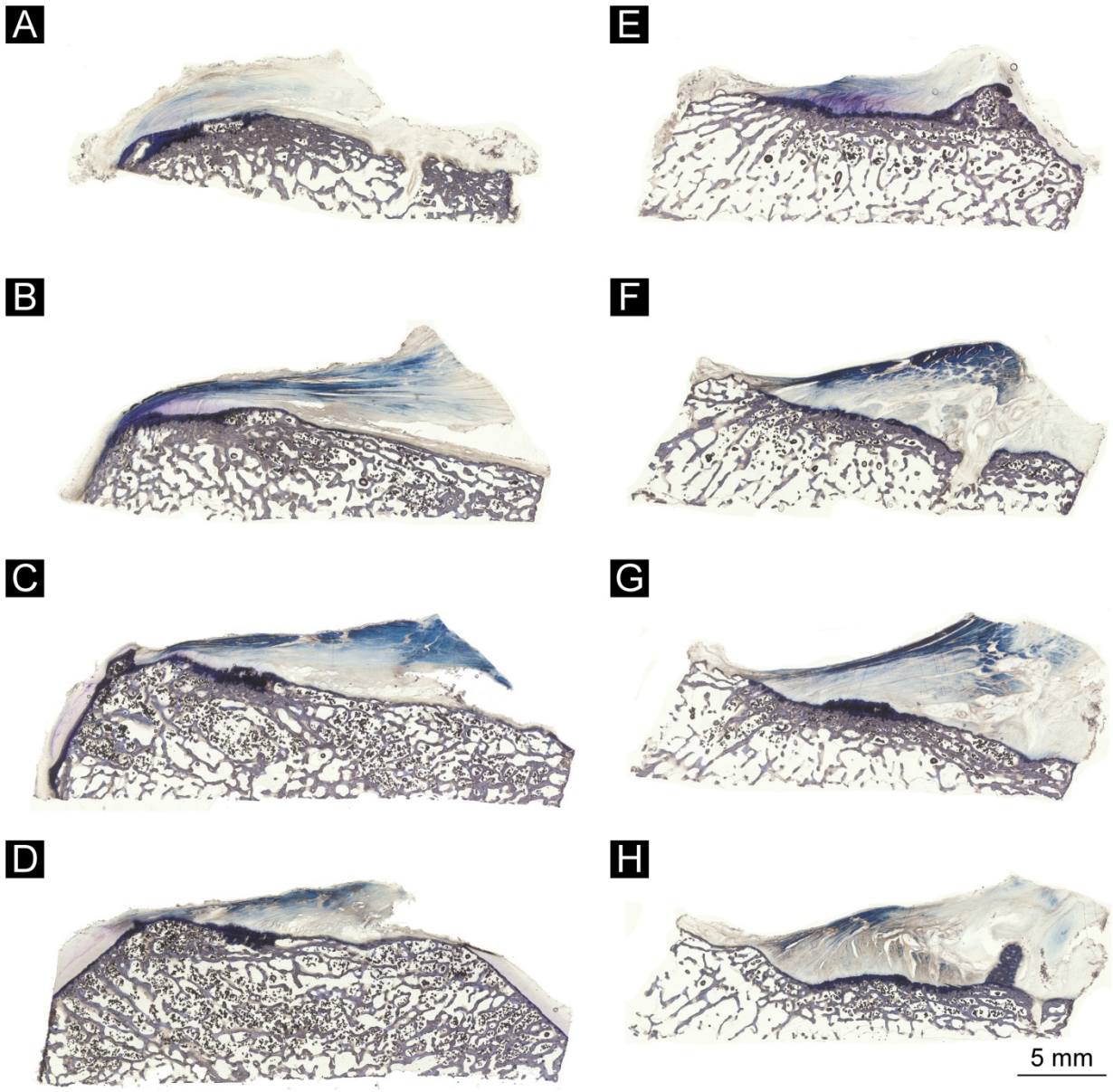

Figure B.12 Histology of the four tissue sections of the right ACL femoral (**A**: 20%; **B**: 40%; **C**: 60%; **D**: 80% of the width of the enthesis) and tibial (**E**: 20%; **F**: 40%; **G**: 60%; **H**: 80% of the width of the enthesis) entheses in specimen #34602.

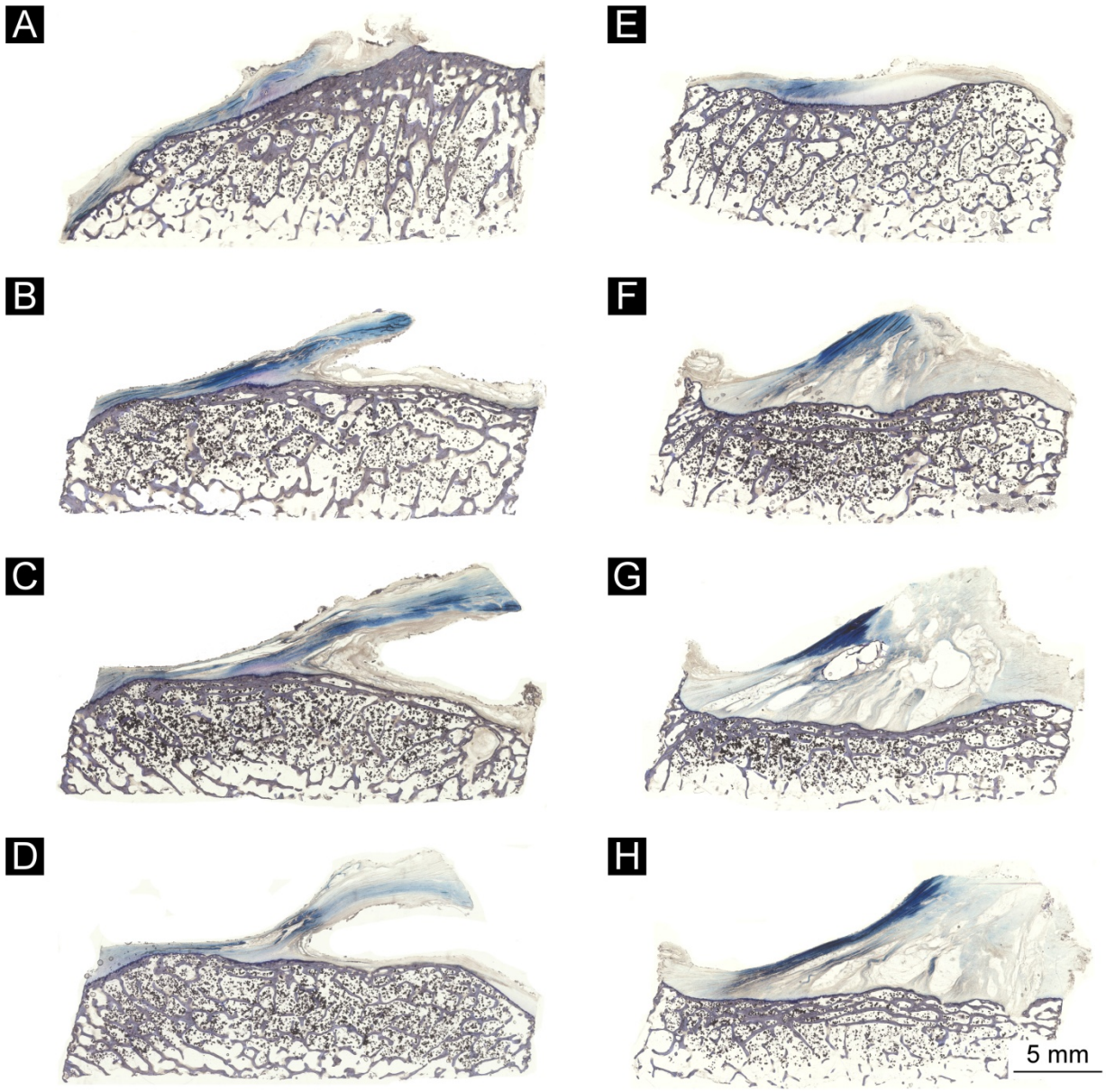

Figure B.13 Histology of the four tissue sections of the left ACL femoral (**A**: 20%; **B**: 40%; **C**: 60%; **D**: 80% of the width of the enthesis) and tibial (**E**: 20%; **F**: 40%; **G**: 60%; **H**: 80% of the width of the enthesis) entheses in specimen #34626.

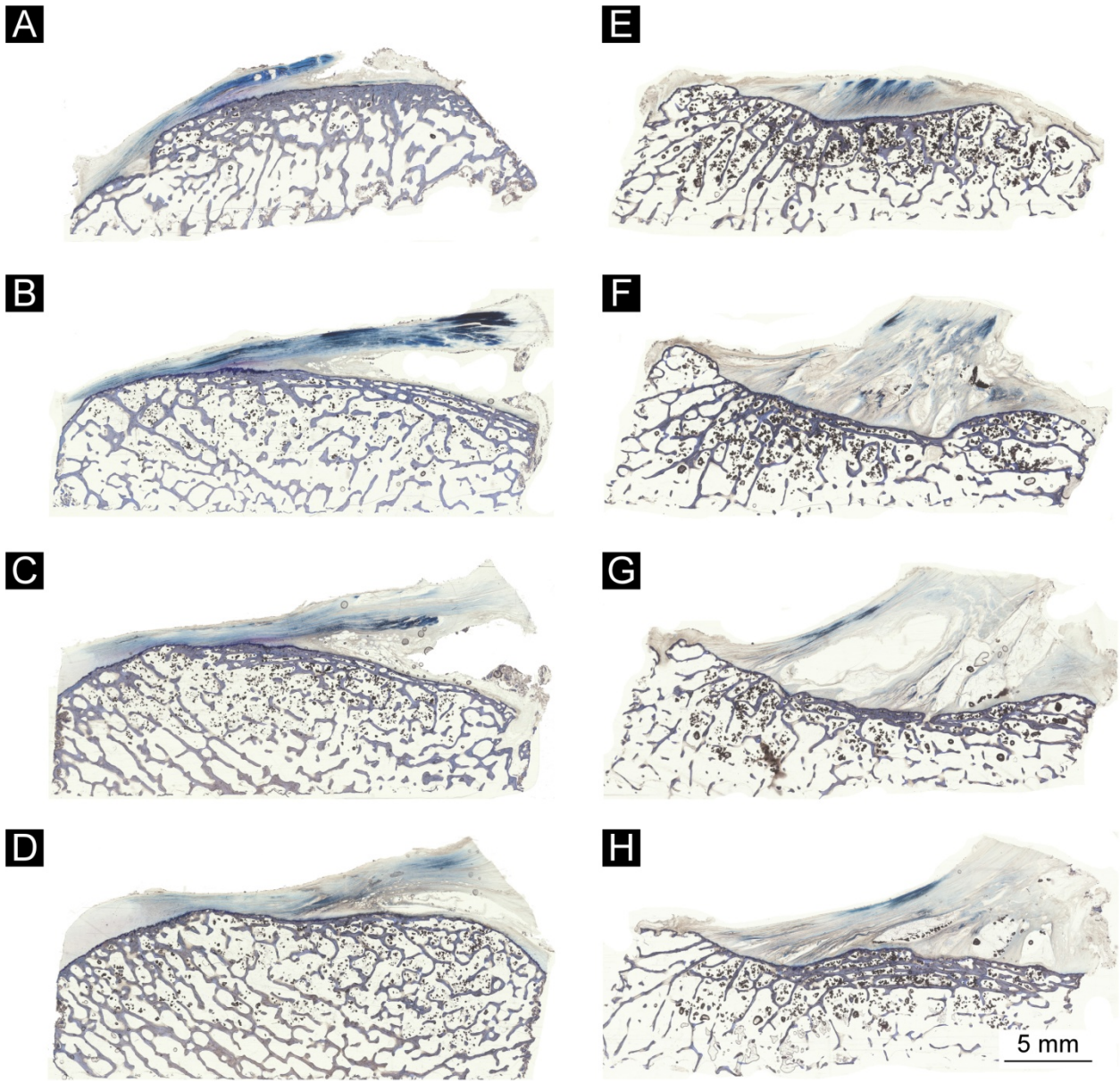

Figure B.14 Histology of the four tissue sections of the right ACL femoral (**A**: 20%; **B**: 40%; **C**: 60%; **D**: 80% of the width of the enthesis) and tibial (**E**: 20%; **F**: 40%; **G**: 60%; **H**: 80% of the width of the enthesis) entheses in specimen #34626.

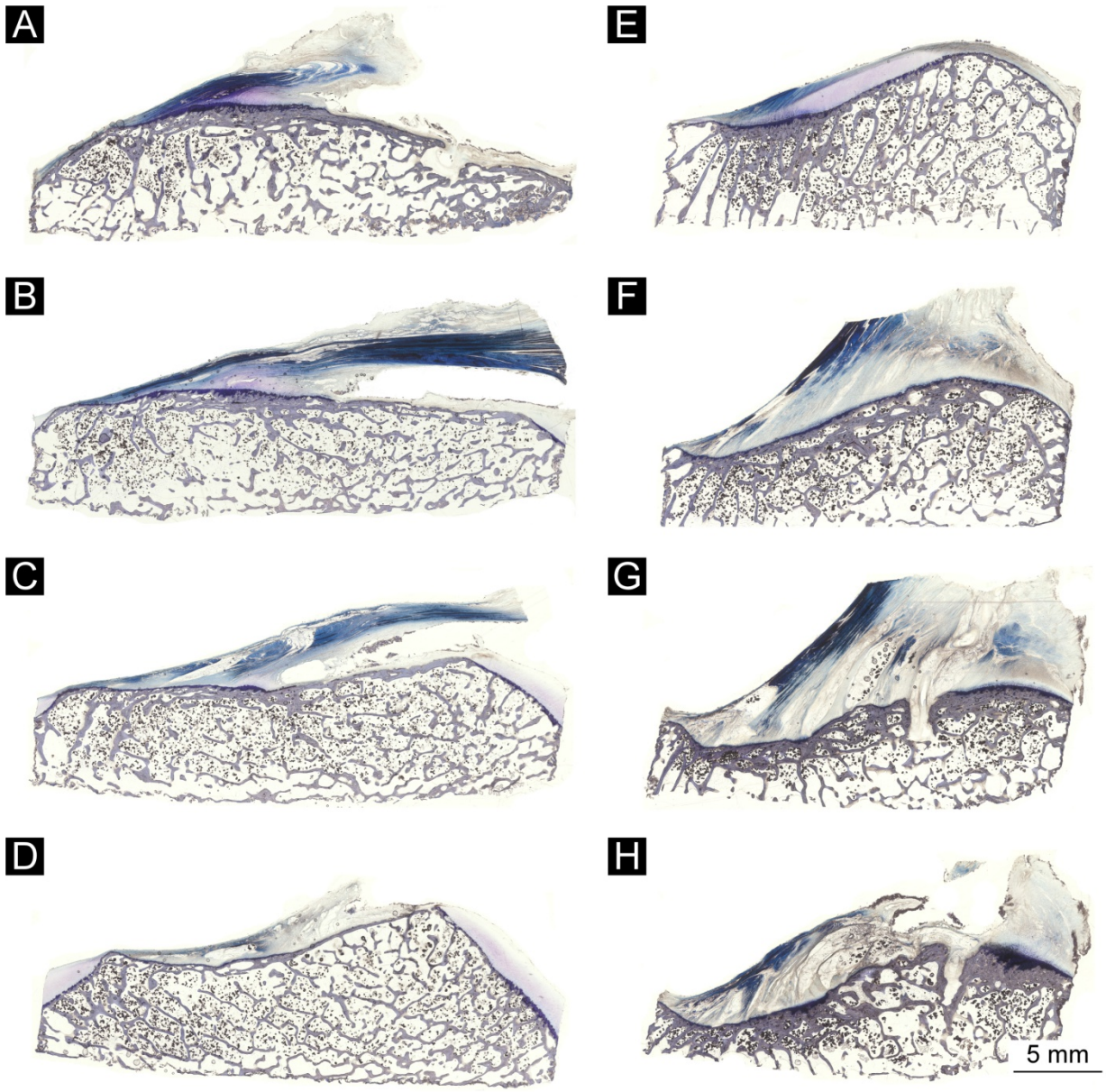

Figure B.15 Histology of the four tissue sections of the left ACL femoral (**A**: 20%; **B**: 40%; **C**: 60%; **D**: 80% of the width of the enthesis) and tibial (**E**: 20%; **F**: 40%; **G**: 60%; **H**: 80% of the width of the enthesis) entheses in specimen #34630.

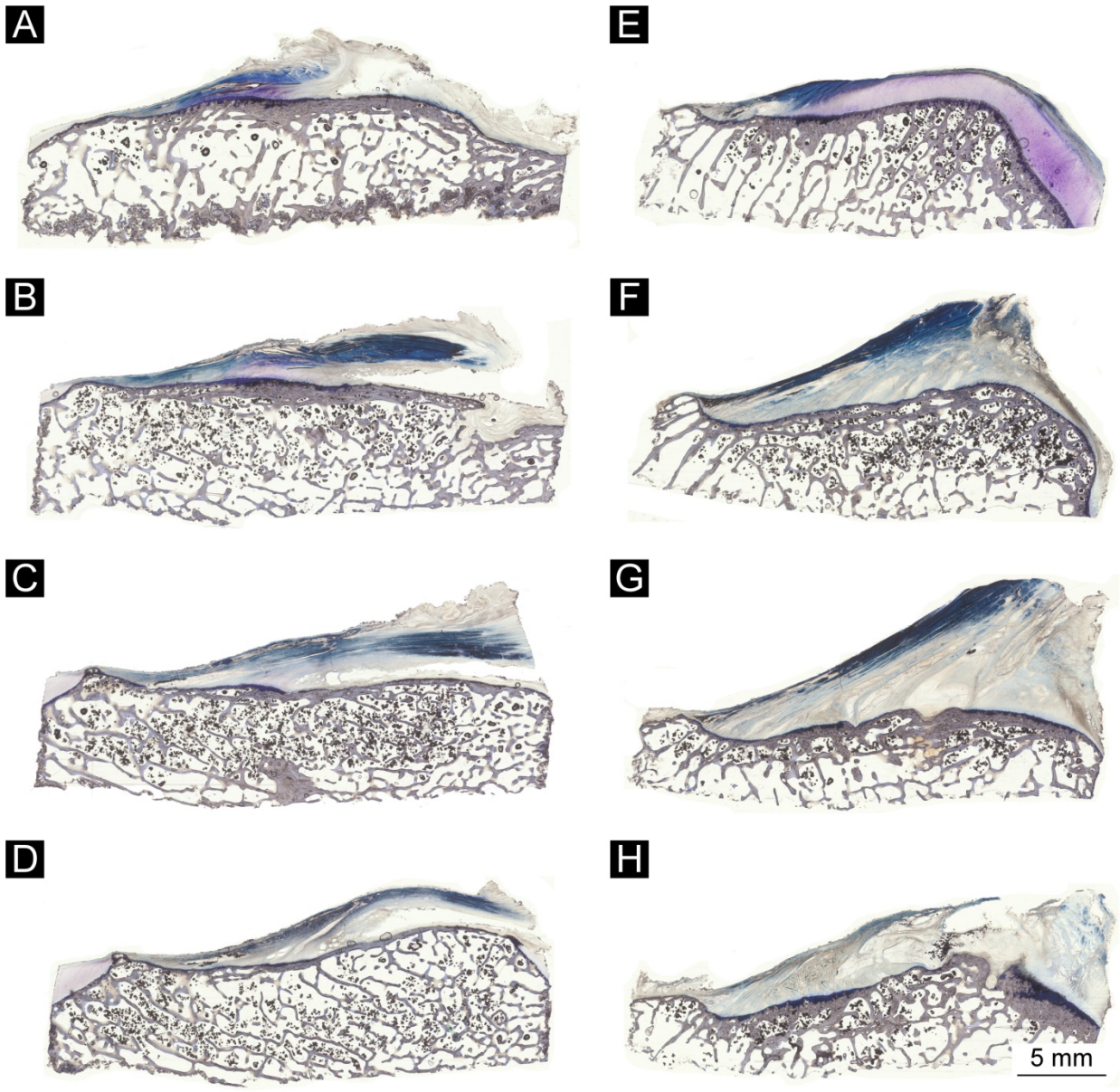

Figure B.16 Histology of the four tissue sections of the right ACL femoral (**A**: 20%; **B**: 40%; **C**: 60%; **D**: 80% of the width of the enthesis) and tibial (**E**: 20%; **F**: 40%; **G**: 60%; **H**: 80% of the width of the enthesis) entheses in specimen #34630.

APPENDIX C

COMPREHENSIVE DATASETS FOR THE DISSERTATION

This appendix presents the complete datasets for Chapters 2-5 of this dissertation. Donor demographics and data for the baseline trials and all internal femoral rotation conditions of Chapter 2 are presenting in Tables C.1-C.7. Donor demographics and data for the last non-pivot trial, first pivot trial, and the last pivot trial (including failure trials for failed specimens) of Chapter 3 are presented in Tables C.8-C.11. Donor demographics of the donors of the knee specimens examined in Chapters 4-5 are presented in Table C.12. Micro-anatomical data for the femoral and tibial ACL entheses of Chapter 4 are presented in Table C.13. Regional data of the microscopic anatomy of the ACL femoral enthesis are presented in Table C.14. The coefficients of the fifth-order polynomial fit to the femoral entheseal surface are presented in Table C.15.

Table C.1 Demographic data of the donors of the knee specimens tested in Chapter 2

Donor ID	Sex	Age (yrs)	Height (m)	Mass (kg)	BMI (kg/m^2)
F20342L	female	45	1.63	54.4	20.6
F20342R	female	45	1.63	54.4	20.6
F20686L	female	50	1.78	63.5	20.1
F20686R	female	50	1.78	63.5	20.1
M21122L	male	57	1.75	86.2	28.1
M21122R	male	57	1.75	86.2	28.1
M30066R	male	58	1.73	68.0	22.8
F34334R	female	55	1.65	45.4	16.6
F34351R	female	65	1.68	56.7	20.2
M34358L	male	60	1.80	88.9	27.3
M34358R	male	60	1.80	88.9	27.3
F34369L	female	72	1.65	60.8	22.3
F34369R	female	72	1.65	60.8	22.3
M34442R	male	61	1.80	68.0	20.9
F34473L	female	49	1.65	72.6	26.6
F34473R	female	49	1.65	72.6	26.6
M34490L	male	71	1.70	77.1	26.6
M34490R	male	71	1.70	77.1	26.6
M60511L	male	52	1.83	86.2	25.8
M60511R	male	52	1.83	86.2	25.8

Table C.2 Chapter 2 dataset: Non-pivot baseline trials (knee compression force and flexion moment) performed before the trials of the main testing sequence

Donor ID	Peak Compression Force (N)	Peak AM-ACL Relative Strain (%)	Range of Knee Flexion (°)	Range of Anterior Tibial Translation (mm)	Peak Quadriceps Force (N)
F20342L	1013	1.52	5.9	2.5	1046
F20342R	1015	3.63	8.0	2.2	1233
F20686L	1289	5.34	5.9	2.3	1238
F20686R	1236	2.08	6.1	2.1	1142
M21122L	1726	2.51	5.7	2.8	1263
M21122R	1555	2.78	5.7	2.9	1458
M30066R	1237	5.76	5.6	1.5	1026
F34334R	940	1.41	5.4	3.0	963
F34351R	1024	6.01	7.5	3.8	981
M34358L	1887	2.96	4.7	1.8	982
M34358R	1590	2.03	5.6	2.5	1228
F34369L	1283	5.31	5.8	2.9	950
F34369R	1161	7.50	6.1	3.0	963
M34442R	1105	4.23	6.3	2.9	1198
F34473L	1155	3.36	7.4	3.4	1010
F34473R	1365	7.02	6.7	2.6	1045
M34490L	1182	4.64	7.1	3.0	1202
M34490R	1386	5.59	5.9	1.7	1146
M60511L	1610	1.07	7.2	1.6	1208
M60511R	1387	0.85	8.3	1.7	1447

Table C.3 Chapter 2 dataset: Pivot trials (knee compression force, flexion moment, and internal tibial torque) with locked internal femoral rotation (block B)

Donor ID	Peak Compression Force (N)	Peak Internal Tibial Torque (Nm)	Range of Internal Femoral Rotation (°)	Femoral Rotational Stiffness (Nm/°)	Peak AM-ACL Relative Strain (%)	Range of Knee Flexion (°)	Range of Anterior Tibial Translation (mm)	Range of Internal Tibial Rotation (°)	Peak Internal Tibial Deceleration (°/s^2)	Peak Quadriceps Force (N)
F20342L	631	22.6	2.5	17.0	10.13	8.9	5.7	15.2	19027	1335
F20342R	603	21.7	2.1	12.1	7.12	10.2	4.2	17.3	20868	1560
F20686L	657	24.3	2.4	10.1	11.08	10.0	5.5	15.4	23078	1515
F20686R	715	24.4	2.4	10.7	4.38	8.1	5.6	16.0	21966	1279
M21122L	1010	33.3	2.9	16.6	4.07	7.7	5.5	13.9	26349	1303
M21122R	981	32.0	3.0	16.0	4.98	7.6	6.1	13.2	24783	1548
M30066R	790	22.8	2.7	12.2	6.50	5.8	3.7	15.5	17812	1102
F34334R	665	22.3	2.5	11.1	4.18	5.4	5.8	17.6	22032	1130
F34351R	632	20.4	2.4	11.0	11.24	8.5	7.5	19.0	18997	1312
M34358L	998	31.5	3.5	15.1	6.21	7.0	6.2	15.5	33129	1068
M34358R	915	29.8	2.8	12.3	4.09	8.1	5.6	13.7	23223	1358
F34369L	713	23.7	2.9	14.8	11.95	8.7	5.9	15.1	20804	1094
F34369R	692	25.1	3.0	12.3	13.98	7.8	5.4	15.3	19402	1311
M34442R	735	25.5	3.0	12.7	9.29	8.1	7.0	16.0	21268	1401
F34473L	574	17.7	2.2	7.9	5.05	10.8	7.2	21.4	20260	1135
F34473R	749	20.6	2.9	11.6	12.14	6.8	6.2	25.5	27414	1353
M34490L	719	23.3	2.7	16.0	14.42	8.8	6.3	14.5	19677	1394
M34490R	731	24.3	2.7	14.7	9.95	9.2	5.0	16.2	21865	1357
M60511L	967	30.3	3.1	13.6	2.14	9.1	3.6	14.6	24731	1556
M60511R	957	29.9	2.6	16.5	3.29	8.7	4.2	14.5	21494	1923

Table C.4 Chapter 2 dataset: Pivot trials (knee compression force, flexion moment, and internal tibial torque) with internal femoral rotation limited by a hard stop to ~7° (block C)

Donor ID	Peak Compression Force (N)	Peak Internal Tibial Torque (Nm)	Range of Internal Femoral Rotation (°)	Femoral Rotational Stiffness (Nm/°)	Peak AM-ACL Relative Strain (%)	Range of Knee Flexion (°)	Range of Anterior Tibial Translation (mm)	Range of Internal Tibial Rotation (°)	Peak Internal Tibial Deceleration (°/s^2)	Peak Quadriceps Force (N)
F20342L	609	22.6	6.8	7.4	10.27	8.3	5.4	15.6	20710	1276
F20342R	632	21.5	5.9	5.8	7.21	9.6	4.6	17.8	19333	1485
F20686L	659	22.8	6.5	7.8	11.17	8.8	5.8	15.8	21156	1380
F20686R	662	23.7	6.1	7.5	4.48	7.7	5.9	16.3	22434	1215
M21122L	988	31.9	6.8	9.6	3.95	7.1	5.7	13.7	26441	1190
M21122R	966	31.5	7.1	9.6	4.90	6.8	6.0	13.2	25642	1425
M30066R	781	24.4	6.5	6.3	6.61	4.2	3.9	15.5	22700	1055
F34334R	614	21.1	6.3	5.9	4.33	5.9	5.8	18.3	22665	1044
F34351R	654	21.4	6.2	5.9	11.38	7.7	7.2	19.2	20837	1240
M34358L	985	31.8	7.5	9.5	6.45	5.7	6.0	15.1	35945	954
M34358R	901	28.8	6.8	8.8	4.14	6.2	5.5	13.8	26819	1259
F34369L	666	23.4	7.0	7.0	11.94	8.5	6.0	15.3	20537	1049
F34369R	634	24.0	7.3	6.4	14.76	8.3	5.4	16.1	19800	1212
M34442R	728	23.4	6.5	7.2	10.32	8.2	6.9	16.5	22443	1335
F34473L	575	18.7	6.2	4.7	5.57	9.6	7.3	21.6	19713	1038
F34473R	753	21.7	7.2	4.7	17.80	6.1	5.7	24.5	26099	1243
M34490L	657	21.9	6.7	7.0	13.41	9.4	6.1	14.8	19658	1265
M34490R	801	26.4	6.1	8.2	10.21	7.3	5.3	16.6	24750	1383
M60511L	905	30.6	7.2	8.8	2.24	8.4	3.4	14.7	25114	1443
M60511R	892	29.7	6.4	9.2	3.32	8.2	4.3	14.7	23822	1872

Table C.5 Chapter 2 dataset: Pivot trials (knee compression force, flexion moment, and internal tibial torque) with internal femoral rotation limited by a hard stop to ~11° (block D)

Donor ID	Peak Compression Force (N)	Peak Internal Tibial Torque (Nm)	Range of Internal Femoral Rotation (°)	Femoral Rotational Stiffness (Nm/°)	Peak AM-ACL Relative Strain (%)	Range of Knee Flexion (°)	Range of Anterior Tibial Translation (mm)	Range of Internal Tibial Rotation (°)	Peak Internal Tibial Deceleration (°/s^2)	Peak Quadriceps Force (N)
F20342L	572	18.5	11.5	2.5	8.32	7.9	5.2	14.6	12421	1195
F20342R	601	17.6	10.5	2.4	6.42	9.2	4.4	16.3	10573	1424
F20686L	644	19.5	11.5	2.2	9.80	7.6	5.0	14.9	13224	1271
F20686R	652	19.0	10.6	3.4	3.87	6.7	5.5	15.3	14434	1120
M21122L	963	26.6	11.2	4.3	3.67	6.6	5.6	12.8	20151	1209
M21122R	953	25.9	11.5	5.2	4.52	6.3	5.5	12.3	20741	1346
M30066R	685	18.9	10.8	1.6	5.64	5.8	3.3	14.6	15214	1013
F34334R	590	18.1	10.9	1.6	4.08	4.6	4.7	16.0	15583	999
F34351R	625	19.4	10.6	2.6	10.74	7.5	6.7	18.2	15615	1200
M34358L	958	27.9	12.1	3.8	6.00	5.4	5.5	13.8	26870	959
M34358R	877	24.1	11.1	3.6	3.76	5.9	4.7	12.7	20418	1264
F34369L	655	21.1	11.5	2.5	10.42	7.4	5.2	14.3	15258	1028
F34369R	666	20.5	11.2	2.6	13.01	6.8	4.5	14.2	14344	1146
M34442R	718	21.8	11.2	3.9	9.56	7.3	6.8	15.7	19493	1287
F34473L	574	17.3	10.2	3.5	5.44	9.5	6.6	20.4	14592	1034
F34473R	710	20.4	11.0	2.3	10.58	5.6	5.5	23.8	19756	1284
M34490L	664	20.9	10.9	4.6	11.00	8.0	5.8	14.0	14509	1266
M34490R	750	22.2	10.5	2.8	9.97	6.6	4.9	15.5	20506	1312
M60511L	874	26.5	11.5	4.0	1.96	8.1	3.2	13.7	18699	1415
M60511R	891	24.0	10.6	4.1	2.87	7.7	4.2	13.9	17256	1773

Table C.6 Chapter 2 dataset: Pivot trials (knee compression force, flexion moment, and internal tibial torque) with unrestricted internal femoral rotation (block E)

Donor ID	Peak Compression Force (N)	Peak Internal Tibial Torque (Nm)	Range of Internal Femoral Rotation (°)	Femoral Rotational Stiffness (Nm/°)	Peak AM-ACL Relative Strain (%)	Range of Knee Flexion (°)	Range of Anterior Tibial Translation (mm)	Range of Internal Tibial Rotation (°)	Peak Internal Tibial Deceleration (°/s^2)	Peak Quadriceps Force (N)
F20342L	558	17.7	14.3	1.8	5.82	7.5	4.7	13.4	10443	1148
F20342R	555	17.3	12.9	2.0	6.20	8.9	4.3	15.7	12374	1362
F20686L	603	18.9	14.1	2.7	9.41	8.4	5.0	13.2	14159	1309
F20686R	686	19.7	14.8	1.2	3.60	5.8	4.5	13.2	13816	1131
M21122L	951	24.3	17.8	3.5	3.11	6.5	4.7	10.9	13968	1151
M21122R	920	24.1	18.6	3.0	3.86	5.9	4.6	10.2	12634	1356
M30066R	707	18.6	14.5	2.2	5.01	5.6	3.3	12.7	10271	1039
F34334R	568	17.6	14.0	0.8	3.64	5.6	4.6	15.0	12855	987
F34351R	562	16.7	13.5	1.3	10.11	7.9	6.4	16.9	11914	1209
M34358L	919	22.5	18.2	3.1	5.16	6.2	4.9	11.9	14636	960
M34358R	888	24.3	16.4	2.2	3.16	5.7	3.9	10.8	13688	1224
F34369L	636	18.0	14.4	2.5	9.94	8.1	5.2	13.1	11125	984
F34369R	591	18.6	15.3	2.1	11.79	7.9	4.4	13.2	11242	1129
M34442R	630	19.4	16.3	1.8	8.57	7.3	6.3	13.6	11431	1272
F34473L	561	15.2	12.6	1.0	5.03	9.7	6.8	19.2	13764	1053
F34473R	610	16.6	14.6	1.3	9.34	6.7	5.3	22.4	18445	1207
M34490L	648	19.4	14.8	2.1	8.91	8.1	5.7	12.9	11045	1254
M34490R	708	21.1	15.1	2.3	9.45	6.8	4.3	13.9	13090	1301
M60511L	881	23.0	17.0	2.5	1.13	7.6	3.1	12.2	12402	1397
M60511R	771	21.8	15.1	3.3	2.35	9.8	3.2	12.9	12404	1598

Table C.7 Chapter 2 dataset: Non-pivot baseline trials (knee compression force and flexion moment) performed after the trials of the main testing sequence

Donor ID	Peak Compression Force (N)	Peak AM-ACL Relative Strain (%)	Range of Knee Flexion (°)	Range of Anterior Tibial Translation (mm)	Peak Quadriceps Force (N)
F20342L	976	2.74	6.5	2.4	1035
F20342R	1002	2.43	7.4	1.6	1198
F20686L	1354	5.58	5.4	2.2	1063
F20686R	1293	1.62	5.2	1.8	1113
M21122L	1704	2.22	6.1	2.3	1117
M21122R	1530	2.41	6.2	2.6	1344
M30066R	1239	5.43	5.4	1.8	1011
F34334R	929	1.45	5.2	2.7	956
F34351R	989	6.74	7.3	4.2	1017
M34358L	1840	3.49	4.5	1.9	942
M34358R	1572	1.67	5.9	2.0	1213
F34369L	1293	5.04	5.5	2.6	968
F34369R	1142	6.64	6.2	3.0	1028
M34442R	1125	4.19	6.2	2.9	1227
F34473L	1169	2.75	7.2	3.7	1026
F34473R	1383	6.21	5.9	2.9	1103
M34490L	1151	4.24	7.5	3.2	1180
M34490R	1426	3.59	5.6	1.8	1152
M60511L	1690	0.88	6.5	1.6	1284
M60511R	1460	1.01	7.3	1.9	1581

Table C.8 Demographic and morphological data of the donors of the knee specimens tested in Chapter 3

Donor ID	Sex	Age (yrs)	Height (m)	Mass (kg)	BMI (kg/m^2)	Knee	Morphologic Data	
							Femoral-ACL Attachment Angle (°)	Tibia Eminence Volume (cm^3)
M01149	Male	33	1.80	77.1	23.7	left	14.3	1.16
						right	17.3	1.24
M01431	Male	59	1.78	81.6	25.8	left	26.4	2.03
						right	23.9	1.98
F02341	Female	35	1.70	50.3	17.4	left	27.3	1.11
						right	30.1	1.39
M02867	Male	56	1.65	65.8	24.1	left	19.4	1.27
						right	30.6	1.54
F10496	Female	36	1.75	68.0	22.2	left	22.3	1.04
						right	19.2	1.03
F20661	Female	44	1.75	54.4	17.7	left	22.8	1.72
						right	25.9	2.11
M21514	Male	24	1.80	63.5	19.5	left	27.5	1.40
						right	26.3	1.69
M22806	Male	22	1.75	74.8	24.4	left	30.7	1.41
						right	25.8	1.12
M30734	Male	56	1.73	58.1	19.5	left	22.7	2.07
						right	23.7	2.02
F34422	Female	40	1.55	41.7	17.4	left	19.6	1.22
						right	29.4	1.04

Table C.8 Demographic and morphological data of the donors of the knee specimens tested in Chapter 3 (continued)

Donor ID	Sex	Age (yrs)	Height (m)	Mass (kg)	BMI (kg/m^2)	Knee	Morphologic Data	
							Femoral-ACL Attachment Angle (°)	Tibia Eminence Volume (cm^3)
M34494	Male	59	1.70	80.3	27.7	left	20.9	1.79
						right	23.6	1.83
F34516	Female	62	1.55	45.4	18.9	left	30.4	1.06
						right	11.9	1.13
F34568	Female	53	1.63	61.2	23.2	left	14.5	0.88
						right	28.5	1.18
F40036	Female	64	1.60	52.2	20.4	left	33.9	1.05
						right	39.7	1.25
M40061	Male	30	1.80	68.9	21.2	left	26.3	1.06
						right	32.2	1.33
F71125	Female	47	1.68	54.4	19.4	left	21.1	1.12
						right	25.2	1.26

Table C.9 Chapter 3 dataset: Kinematic and kinetic data for the last non-pivot trial (knee compression force and flexion moment) of all 32 knee specimens

Donor ID	Knee	Peak Compression Force (N)	Range of Internal Femoral Rotation (°)	Range of Anterior Tibial Translation (mm)	Range of Internal Tibial Rotation (°)	Peak Quadriceps Force (N)
M01149	left	3304	0.9	7.7	12.1	2026
	right	3155	0.3	4.8	5.9	2131
M01431	left	3021	0.0	5.7	7.5	1851
	right	3394	1.2	5.0	7.0	2240
F02341	left	2186	0.0	5.0	6.6	1424
	right	2596	0.0	4.2	5.0	1715
M02867	left	2581	0.4	4.9	5.9	1824
	right	2750	0.1	4.2	6.2	1856
F10496	left	2481	1.1	6.2	6.0	1522
	right	2642	1.6	3.8	5.2	1611
F20661	left	2227	0.0	5.5	4.8	1524
	right	2263	0.0	3.7	4.9	1560
M21514	left	2591	0.0	4.4	5.7	1595
	right	2784	0.0	2.8	4.7	1894
M22806	left	3242	0.5	6.5	10.7	1960
	right	3019	1.3	5.8	11.1	1964
M30734	left	2387	0.0	3.4	3.9	1590
	right	2450	0.0	2.9	2.8	1880
F34422	left	1604	0.7	4.3	6.3	1065
	right	1887	0.5	2.9	3.9	1093

Table C.9 Chapter 3 dataset: Kinematic and kinetic data for the last non-pivot trial (knee compression force and flexion moment) of all 32 knee specimens (continued)

Donor ID	Knee	Peak Compression Force (N)	Range of Internal Femoral Rotation (°)	Range of Anterior Tibial Translation (mm)	Range of Internal Tibial Rotation (°)	Peak Quadriceps Force (N)
M34494	left	2757	0.0	4.9	4.6	1732
	right	3238	0.7	4.1	3.3	2126
F34516	left	2090	0.9	8.3	5.6	1479
	right	1838	0.0	5.2	3.2	1448
F34568	left	2669	0.6	5.4	7.9	1781
	right	2394	0.1	4.2	7.2	1685
F40036	left	2136	0.0	6.1	8.0	1454
	right	2331	0.1	4.4	6.1	1629
M40061	left	2817	0.0	5.7	11.8	1989
	right	2741	0.0	4.6	10.1	1867
F71125	left	2086	0.4	5.5	5.6	1390
	right	2033	0.1	4.1	4.5	1205

Table C.10 Chapter 3 dataset: Kinematic and kinetic data for the first pivot trial (knee compression force, flexion moment, and internal tibial torque) of all 32 knee specimens

Donor ID	Knee	Trial Number	Peak Compression Force (N)	Range of Internal Femoral Rotation (°)	Range of Anterior Tibial Translation (mm)	Range of Internal Tibial Rotation (°)	Peak Quadriceps Force (N)
M01149	left	6	2868	18.3	9.1	21.1	1779
	right	6	3442	4.4	11.0	25.0	1824
M01431	left	6	3263	4.3	8.3	17.9	1877
	right	6	2947	16.2	6.4	16.5	2015
F02341	left	6	2238	13.2	6.8	19.8	1412
	right	6	2802	3.8	7.3	22.2	1894
M02867	left	6	2550	12.7	5.8	14.4	1830
	right	6	3155	4.1	6.2	15.7	2141
F10496	left	7	2834	3.3	8.4	20.8	1747
	right	6	2249	14.8	5.8	20.5	1372
F20661	left	6	2559	3.3	7.7	17.1	1794
	right	6	2377	14.2	5.6	17.6	1652
M21514	left	6	2843	3.2	7.5	14.9	1696
	right	6	2667	15.8	5.0	12.8	1736
M22806	left	6	2965	16.6	8.3	23.5	1778
	right	6	3662	3.5	9.4	26.0	2434
M30734	left	6	2273	14.1	5.4	16.2	1435
	right	6	3053	3.6	6.6	20.3	1911
F34422	left	6	1715	9.5	6.7	15.7	1042
	right	6	1985	3.1	4.9	14.2	1247

Table C.10 Chapter 3 dataset: Kinematic and kinetic data for the first pivot trial (knee compression force, flexion moment, and internal tibial torque) of all 32 knee specimens (continued)

Donor ID	Knee	Trial Number	Peak Compression Force (N)	Range of Internal Femoral Rotation (°)	Range of Anterior Tibial Translation (mm)	Range of Internal Tibial Rotation (°)	Peak Quadriceps Force (N)
M34494	left	6	2876	6.7	8.7	22.0	1711
	right	6	2849	17.7	6.5	19.6	1946
F34516	left	6	2013	10.8	6.7	17.1	1419
	right	6	2067	4.7	10.1	22.8	1490
F34568	left	6	3077	3.9	6.9	19.7	2150
	right	6	2592	13.7	6.8	17.0	1812
F40036	left	6	2241	3.0	8.2	18.2	1593
	right	6	2361	11.9	6.0	18.1	1648
M40061	left	6	3272	3.0	7.3	20.2	2292
	right	6	2756	13.5	5.4	19.2	2047
F71125	left	6	2267	13.2	7.1	15.3	1506
	right	6	2127	3.6	7.8	21.2	1400

Table C.11 Chapter 3 dataset: Kinematic and kinetic data for the last pivot trial (knee compression force, flexion moment, and internal tibial torque), including the trial during which ACL failure occurred in the 8 failed knee specimens

Donor ID	Knee	Failure Type	Trial Number	Range of Anterior Tibial Translation (mm)	Peak Cumulative Anterior Tibial Translation (mm)	Range of Internal Tibial Rotation (°)	Peak Cumulative Internal Tibial Rotation (°)
M01149	left	D	136	8.9	10.4	20.0	23.4
	right	E	127	11.2	13.9	24.7	27.9
M01431	left	E	80	10.0	11.5	17.4	20.6
	right	D	105	7.9	8.2	15.5	19.5
F02341	left	D	110	7.6	9.1	21.6	26.1
	right	A	38	10.2	12.1	23.6	29.0
M02867	left	D	105	5.8	7.1	14.5	16.0
	right	D	105	6.1	7.7	15.1	17.2
F10496	left	D	110	8.7	9.7	19.9	23.4
	right	D	110	6.7	7.6	17.9	22.5
F20661	left	T	14	14.8	15.6	17.6	18.6
	right	D	105	5.6	6.3	17.1	20.5
M21514	left	D	105	7.6	8.1	14.2	16.4
	right	D	105	4.8	5.6	11.1	14.1
M22806	left	D	105	8.1	8.7	23.1	26.0
	right	D	105	10.3	10.9	24.6	28.9
M30734	left	D	105	5.5	6.5	16.0	19.7
	right	D	105	5.7	7.1	18.4	22.6

A: tibial avulsion; D: did not fail; E permanent elongation; P: partial ACL tear; T: complete ACL tear

Table C.11 Chapter 3 dataset: Kinematic and kinetic data for the last pivot trial (knee compression force, flexion moment, and internal tibial torque), including the trial during which ACL failure occurred in the 8 failed knee specimens (continued)

Donor ID	Knee	Failure Type	Trial Number	Range of Anterior Tibial Translation (mm)	Peak Cumulative Anterior Tibial Translation (mm)	Range of Internal Tibial Rotation (°)	Peak Cumulative Internal Tibial Rotation (°)
F34422	left	D	105	6.5	7.9	14.5	18.1
	right	D	105	4.9	5.8	12.9	15.6
M34494	left	P	45	11.1	12.1	21.1	23.8
	right	D	105	6.8	7.8	20.9	21.6
F34516	left	D	10	8.1	8.8	18.1	20.1
	right	P	7	12.1	13.0	22.0	24.4
F34568	left	D	105	7.7	8.9	19.5	23.1
	right	D	105	6.1	7.8	16.2	18.4
F40036	left	A	6	8.2	8.2	18.2	18.2
	right	A	10	6.0	6.5	18.6	19.5
M40061	left	D	105	7.5	8.4	19.4	22.9
	right	D	105	4.9	5.6	18.1	21.0
F71125	left	D	105	7.0	8.0	14.8	18.4
	right	D	105	8.9	10.0	22.2	24.9

A: tibial avulsion; D: did not fail; E permanent elongation; P: partial ACL tear; T: complete ACL tear

Table C.12 Demographic data of the donors of the knee specimens examined in Chapters 4-5

Donor ID	Sex	Age (yrs)	Height (m)	Mass (kg)	BMI (kg/m^2)
F34372L	female	48	1.73	71.7	24.0
F34563L	female	53	1.65	45.8	16.8
F34563R	female	53	1.65	45.8	16.8
M34571L	female	54	1.73	58.1	19.5
M34571R	female	54	1.73	58.1	19.5
M34578L	female	47	1.75	72.6	23.6
M34578R	female	47	1.75	72.6	23.6
M34593L	female	57	1.91	99.8	27.5
M34593R	female	57	1.91	99.8	27.5
F34602L	female	69	1.60	68.5	26.7
F34602R	female	69	1.60	68.5	26.7
M34626L	female	48	1.63	65.8	24.9
M34626R	female	48	1.63	65.8	24.9
F34630L	female	41	1.65	81.6	30.0
F34630R	female	41	1.65	81.6	30.0

Table C.13 Chapter 4 dataset: Microscopic anatomy of the ACL femoral and tibial entheses

		Relative Area of Calcified Fibrocartilage ($\mu m^2/\mu m$)			Depth of Uncalcified Fibrocartilage (μm)			Ligament Entheseal Attachment Angle (°)
Donor ID	**Enthesis**	**Entire Enthesis**	**Middle 50%**	**Outer 50%**	**Entire Enthesis**	**Middle 50%**	**Outer 50%**	**Entire Enthesis**
F34372L	femoral	229	272	186	76	118	32	9.7
	tibial	137	175	104	31	38	23	40.9
F34563L	femoral	160	228	102	107	135	79	8.6
	tibial	123	155	94	31	37	26	26.7
F34563R	femoral	166	241	92	180	202	155	-3.9
	tibial	83	103	64	180	202	155	33.0
M34571L	femoral	135	207	64	129	217	40	20.2
	tibial	110	90	127	75	87	63	46.8
M34571R	femoral	243	299	189	167	225	111	10.2
	tibial	117	122	112	41	52	29	33.3
M34578L	femoral	220	306	135	317	546	90	27.2
	tibial	114	137	92	25	37	13	45.7
M34578R	femoral	156	229	84	311	564	67	18.7
	tibial	83	76	90	51	78	26	48.2
M34593L	femoral	155	180	133	183	269	98	2.3
	tibial	128	122	134	43	76	11	38.9
M34593R	femoral	132	129	134	97	165	27	10.7
	tibial	130	151	110	44	77	11	38.3
F34602L	femoral	340	389	292	201	309	99	12.9
	tibial	242	282	203	89	138	41	31.0

Table C.13 Chapter 4 dataset: Microscopic anatomy of the ACL femoral and tibial entheses (continued)

		Relative Area of Calcified Fibrocartilage ($\mu m^2/\mu m$)			Depth of Uncalcified Fibrocartilage (μm)			Ligament Entheseal Attachment Angle (°)
Donor ID	**Enthesis**	**Entire Enthesis**	**Middle 50%**	**Outer 50%**	**Entire Enthesis**	**Middle 50%**	**Outer 50%**	**Entire Enthesis**
F34602R	femoral	423	525	327	283	436	126	6.2
	tibial	319	386	254	66	124	15	37.4
M34626L	femoral	80	90	71	186	264	111	12.3
	tibial	70	66	72	72	66	76	38.7
M34626R	femoral	97	110	85	135	154	116	0.5
	tibial	80	86	73	6	11	1	47.4
F34630L	femoral	119	162	79	173	172	174	9.0
	tibial	112	123	100	43	66	19	34.5
F34630R	femoral	151	188	113	140	138	141	5.0
	tibial	113	134	90	28	37	18	35.0

Table C.14 Chapter 5 dataset: Regional microscopic anatomy of the ACL femoral enthesis

	Relative Area of Calcified Fibrocartilage ($\mu m^2/\mu m$)				Depth of Uncalcified Fibrocartilage (μm)				Ligament Entheseal Attachment Angle (°)	
Donor ID	**Antero-Superior Region**	**Antero-Inferior Region**	**Postero-Superior Region**	**Postero-Inferior Region**	**Antero-Superior Region**	**Antero-Inferior Region**	**Postero-Superior Region**	**Postero-Inferior Region**	**Anterior Sections**	**Posterior Sections**
F34372L	156	389	102	294	121	95	11	81	-4.5	23.8
F34563L	131	222	137	157	87	163	128	46	-1.5	18.6
F34563R	165	280	138	92	128	467	114	2	-8.1	0.4
M34571L	179	172	109	80	200	239	64	12	11.0	29.3
M34571R	241	233	250	248	104	378	70	107	2.8	17.6
M34578L	165	227	188	306	80	718	166	305	22.6	31.8
M34578R	130	202	103	190	212	540	125	373	11.8	25.5
M34593L	155	198	79	191	82	441	0	212	-7.5	12.1
M34593R	122	161	85	160	72	287	2	27	3.0	18.4
F34602L	421	640	140	157	302	336	35	137	9.4	16.4
F34602R	576	291	354	453	383	293	159	294	-3.3	15.7
M34626L	53	94	87	87	67	357	83	226	7.4	17.2
M34626R	75	126	97	91	34	321	37	154	-6.1	7.0
F34630L	107	229	80	67	47	573	6	83	1.3	16.7
F34630R	134	265	101	104	39	361	12	142	4.4	5.6

Table C.15 Chapter 5 dataset: Coefficients of fifth-order polynomial fit to femoral entheseal surface

	Coefficients of Fifth-Order Polynomial					
Donor ID	**0**	**1**	**2**	**3**	**4**	**5**
F34563L	498.3×10^{-17}	-595.0×10^{-13}	23.0×10^{-8}	-26.3×10^{-5}	-285.9×10^{-3}	958.9
F34563R	-2.8×10^{-17}	5.3×10^{-13}	-1.4×10^{-8}	11.8×10^{-5}	-471.3×10^{-3}	981.8
M34571L	303.9×10^{-17}	-440.6×10^{-13}	22.6×10^{-8}	-44.0×10^{-5}	234.3×10^{-3}	409.4
M34571R	441.0×10^{-17}	-609.1×10^{-13}	30.4×10^{-8}	-64.3×10^{-5}	511.5×10^{-3}	282.3
M34578L	-303.0×10^{-17}	451.8×10^{-13}	-22.6×10^{-8}	36.7×10^{-5}	103.7×10^{-3}	238.4
M34578R	-183.5×10^{-17}	384.8×10^{-13}	-22.7×10^{-8}	41.7×10^{-5}	-1.1×10^{-3}	329.8
M34593L	313.3×10^{-17}	-367.3×10^{-13}	16.3×10^{-8}	-30.1×10^{-5}	-1.3×10^{-3}	809.5
M34593R	234.8×10^{-17}	-332.8×10^{-13}	19.5×10^{-8}	-54.1×10^{-5}	530.9×10^{-3}	500.5
F34602L	1219.5×10^{-17}	-1393.8×10^{-13}	53.1×10^{-8}	-71.3×10^{-5}	23.5×10^{-3}	741.0
F34602R	75.3×10^{-17}	58.5×10^{-13}	-12.7×10^{-8}	56.4×10^{-5}	-870.1×10^{-3}	656.4
M34626L	-58.1×10^{-17}	235.5×10^{-13}	-21.3×10^{-8}	76.5×10^{-5}	-1233.1×10^{-3}	1036.2
M34626R	363.5×10^{-17}	-392.5×10^{-13}	11.4×10^{-8}	7.3×10^{-5}	-745.9×10^{-3}	1008.6
F34630L	-392.5×10^{-17}	442.3×10^{-13}	-16.8×10^{-8}	27.4×10^{-5}	-379.8×10^{-3}	832.5
F34630R	-860.5×10^{-17}	841.8×10^{-13}	-21.3×10^{-8}	-10.6×10^{-5}	$6.68.9\times10^{-3}$	371.0